NASA CR-135030
FCR-0165

DEVELOPMENT OF ADVANCED FUEL CELL SYSTEM

(Phase IV)

by

A. P. Meyer
W. F. Bell

31 January 1976

UNITED TECHNOLOGIES CORPORATION
Power Systems Division

(NASA-CR-135030) DEVELOPMENT OF ADVANCED FUEL CELL SYSTEM (PHASE 4) Final Report, 20 Feb. - 31 Dec. 1975 (United Technologies Corp.) 98 p HC $5.00 CSCL 10A G3/44

N76-23686

Unclas
25388

Prepared for

NATIONAL AERONAUTICS AND SPACE ADMINISTRATION

NASA Lewis Research Center
Contract NAS3-15339
Dr. L. H. Thaller, Project Manager

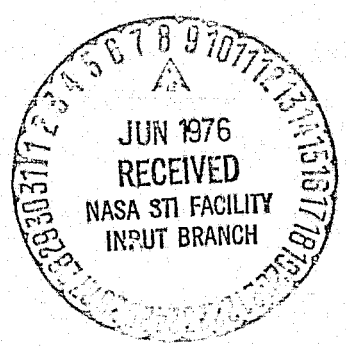

FCR-0165

FINAL REPORT

DEVELOPMENT OF ADVANCED FUEL CELL SYSTEM

(Phase IV)

by

A. P. Meyer
W. F. Bell

31 January 1976

UNITED TECHNOLOGIES CORPORATION
Power Systems Division – Fuel Cell Operations
Box 109, Governors Highway
South Windsor, Connecticut 06074

Prepared for

NATIONAL AERONAUTICS AND SPACE ADMINISTRATION

CONTRACT NAS3-15339

NASA Lewis Research Center
Cleveland, Ohio
Dr. L. H. Thaller, Project Manager
Power Procurement Section

FOREWORD

This report describes the several research and development tasks performed during Phase IV of an advanced fuel cell technology program.

The work was performed under a NASA Contract NAS3-15339 from 20 February 1975 through 31 December 1975. The NASA Program Manager for this contract was Dr. Lawrence H. Thaller. The contributions of Dr. Thaller and other members of the Direct Energy Conversion Laboratory staff at the NASA Lewis Research Center are gratefully acknowledged.

Principal Power Systems Division personnel who directed the tasks performed in this program were:

A. P. Meyer
W. F. Bell

CONTENTS

CONTENTS (Cont.)

ILLUSTRATIONS

ILLUSTRATIONS (CONT'D)

ILLUSTRATIONS (CONT'D)

TABLES

ABSTRACT

A multiple-task research and development program was performed to improve the weight, life, and performance characteristics of hydrogen-oxygen alkaline fuel cells for advanced power systems. During Phase IV covered by this report, the lowest stabilized degradation rate observed in all the testing completed during four phases of the program, 1 μv/hour, was demonstrated. This test continues after 5000 hours of operation. The cell incorporates a PPF anode, a 90Au/10Pt cathode, a hybrid frame, and a Fybex matrix. These elements were developed under this program to extend cell life. The result demonstrated during Phase III, at the laboratory level, that the 80Au/20Pt cathode is as stable as a 90Au/10Pt cathode of twice the precious metal loading, was confirmed in full-scale cells during Phase IV. A hybrid frame two-cell plaque with dedicated flow fields and manifolds for all fluids was demonstrated to prevent the cell-to-cell electrolyte transfer that limited the endurance of multicell plaques during Phase I. At the conclusion of Phase IV, more than 90,900 hours of testing had been completed and twelve different cell designs had been evaluated. A technology base has been established which is ready for evaluation at the powerplant level.

I SUMMARY

This document reports the activity and results of Phase IV of a long-range research program to improve the life and performance and reduce the weight of alkaline fuel cells. The specific tasks are focused on meeting technology goals defined by the Engineering Model System (EMS), an advanced long-life, lightweight powerplant concept. The program is evolutionary in nature. Work has been carried out at the laboratory level, in subscale cells, and in full-scale cell assemblies. As fundamental improvements are defined in the laboratory; e.g., better catalysts and materials, they are committed to evaluation in the working environment of subscale fuel cells. If their merit is demonstrated at this level, they are committed to the full-scale cell tests for a final evaluation. The work completed during this phase of the program built on the accomplishments of the earlier phases. Each of the tasks and the results achieved are summarized below and are reported in detail in the sections which follow.

A. Materials Research

1.0 Electrodes

Task Description

This task focused on investigation and evaluation of electrode catalysts and structures. The overall task objective was to attain higher performance, lower catalyst loading, and improved long-term stability.

Results

During Phase IV, evaluation of the 80Au-20Pt cathode catalyst was continued. Results of laboratory testing during Phase III had shown that the endurance qualities of the 80Au-20Pt cathode were equal to those of "standard" 90Au-10Pt cathodes. Because of their higher specific area, the 80Au-20Pt alloy electrodes approached the activity levels of standard cathodes with only half the precious metal loading. Full size electrodes of this type were fabricated and tested in Cell Nos. 40 and 41 and in Two-Cell Plaque No. 1. Over 10,000 load hours were accumulated in these tests. A comparison of the cathode activity of Cell Nos. 40 and 41 with that of two representative 90Au-10Pt cathode cells is made in Figure 1. The initial activity of the 80Au-20Pt catalyst cells is slightly lower than the 90Au-10Pt cathodes, but with time the activity levels approach each other. Additional testing may show the 80Au-20Pt catalyst to be more stable than 90Au-10Pt catalyst and it may be preferred for extended operation. These tests conducted on full-scale strip cells with electrodes made using shop fabrication procedures showed that the change from laboratory manufacture to shop manufacture had no deleterious effect on their characteristics.

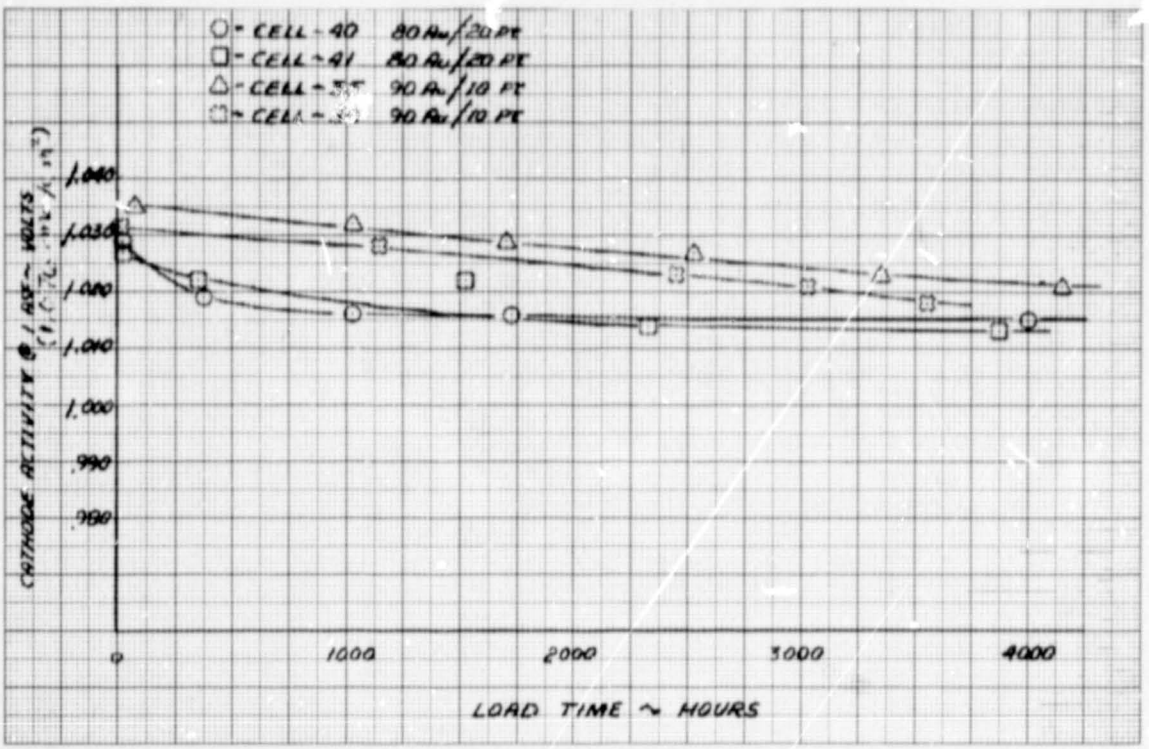

Figure 1 – Cathode Endurance Comparison

2.0 Matrices

Test Description

In the Phase III program, silicon-containing deposits on the anode were identified as a primary cause of anode flooding and increasing anode diffusion over long operating periods. The deposits were the product of corrosion of asbestos matrices. Fybex matrices, which contain no silicates, were tested in two 2 in. x 2 in. (5.08 cm x 5.08 cm) at 190° (87.8°C) and 250°F (121.1°C) for over 2300 hours. In both cases the decay attributable to anode diffusion was lower than that experienced in asbestos matrix cells.

Results

During Phase IV, Fybex matrices were evaluated in full-scale cells. Cell Nos. 42, 43, and 44 were fabricated with filtered Fybex matrices. These cells accumulated a total of over 7000 hours of load time during the contract period. Figure 2 shows a comparison of the anode diffusion losses of two long-term asbestos-matrix cells, Nos. 30 and 35, and Cell Nos. 42 and 44. Consequently, replacement of asbestos as a matrix material can significantly reduce the degradation rate of cells over long periods of time. Fybex itself is not a good candidate for future cells since it is no longer commercially available. However, there are several other materials, including zirconia and ceria, which may be suitable replacements for asbestos. These materials should be evaluated in future work.

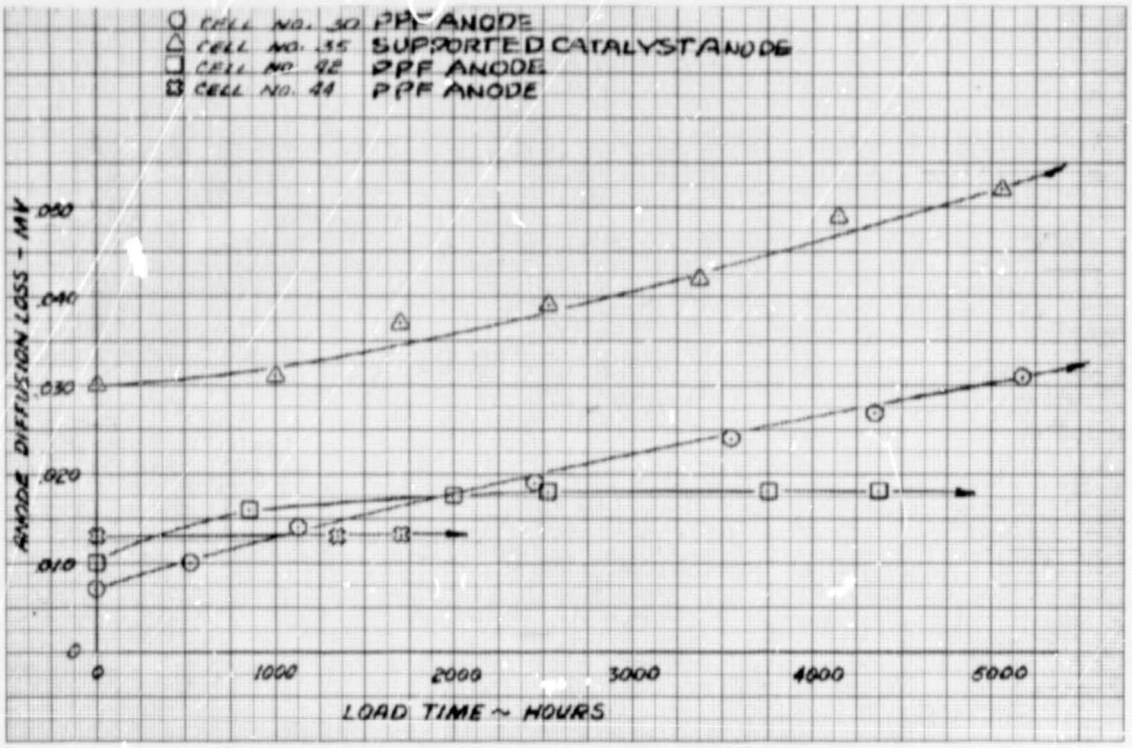

Figure 2 – Anode Diffusion Loss Comparison

B. Unitization Research

Task Description

Phase I plaque testing revealed electrolyte transfer from cell-to-cell could occur through the gas housings which are common to the plaque's six cells. To overcome this problem, development of a plaque design in which each cell had dedicated gas cavities and manifolds was undertaken.

Results

A two-cell plaque design was defined and developed in which all subassemblies, the unitized electrode assembly, the gas flow field frames, and the passive water removal assembly are bonded into an integral unit. Each cell is completely sealed from its neighbor. A set of subassemblies ready for bonding is shown in Figure 3.

Both gas cross-pressure tests prior to operation and operating tests showed that effective sealing of the cells one from another had been achieved. In a test in which one cell was filled with potassium hydroxide electrolyte and the other with sodium hydroxide, analysis of the electrolytes after testing showed only small quantities of sodium in the potassium hydroxide. This small quantity of sodium had no effect on the operation of either cell. This design is suitable for construction of multicell plaques in the future.

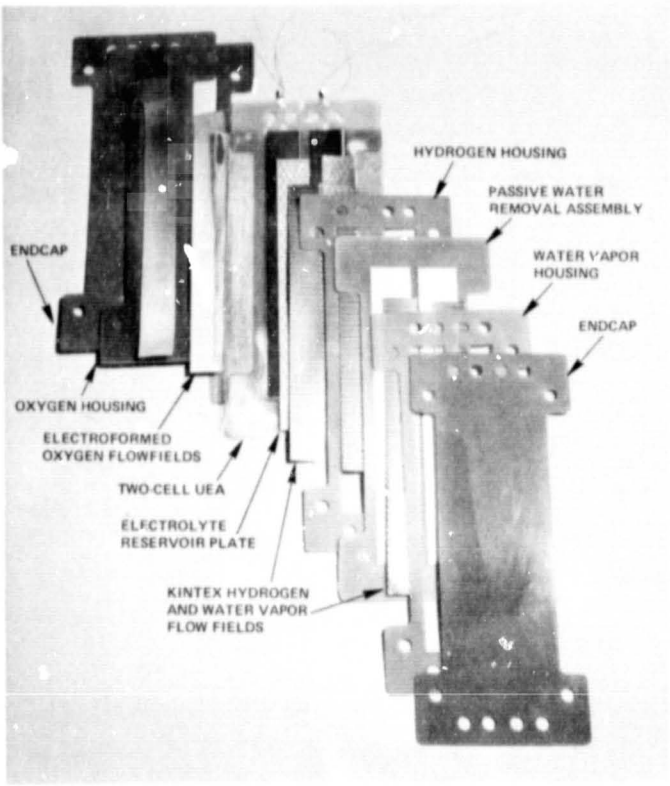

Figure 3 – Components of a Two-Cell Plaque Assembly (WCN-3666)

A second unitization task was fabrication of the first hybrid frame unitized electrode assemblies with a particulate matrix. The processes used were developed based on the methods with which reconstituted asbestos matrices are unitized. The primary difference was the addition of an extra laminate layer about the edge and which penetrates slightly into the matrix. This modification ensures a positive high-cross-pressure seal at the matrix-frame bond even if the particulate matrices do not absorb the frame resin during the heat-bonding step in fabrication. Three cells, Nos. 42, 43 and 44, were fabricated using this method and were successfully tested. No problems with cross leakage at the matrix frame occurred.

C. Cell and Plaque Testing

Task Description

The single cell and plaque tasks provide the means for evaluating the performance and endurance characteristics of evolutionary EMS fuel cell designs. The investigations performed in this area are: evaluation of alternative cell designs, testing to determine the compatibility of alternative cell frame materials and construction techniques in the actual cell environment, and development of cell fabrication procedures to translate the most compatible materials available into practical cell configurations.

Results

Four different NASA-approved single cell designs and two different NASA-approved two cell plaque configurations were evaluated by test during Phase IV. More than 90,900 hours of cell testing have now been accomplished under the program. The longest cell test at 100 ASF (107.6 ma/cm^2) is 10,020 hours in duration and the longest test at 200 ASF (215.2 ma/cm^2) is 6680 hours in duration. These long term tests were accomplished in earlier phases of the program.

During this phase, the lowest performance degradation rate demonstrated at any time in this program was exhibited by Cell No. 42. The overall average degradation rate is less than 5μ V/hour, with a rate of approximately 1μ V/hour after the first 1000 hours of test. This cell incorporates a 90Au/10Pt cathode, a Fybex matrix and a hybrid frame. Each of these components was specifically developed during the program to extend cell endurance capability. Figure 4 presents a comparison of the degradation rate of Cell Nos. 42 and 44, both of this configuration, with that of Cell Nos. 30 and 35 which had previously been among the cells with the lowest degradation rate. The low degradation rate is attributed primarily to the Fybex matrix which does not increasing anode diffusion loss in tests of long duration.

Testing of two two-cell plaques demonstrated a sealed, fully-bonded plaque design will prevent the cell-to-cell electrolyte transfer that limited the endurance of multicell plaque tests during Phase I. This design fabricated in a hybrid-frame unitized plaque assembly was evaluated with both standard PPF and 90Au/10Pt electrodes and the advanced supported catalyst anode and 80Au/20Pt cathode. This configuration is a suitable basis for the design and construction of an advanced powerplant power section. Although the electrolyte transfer problem has been overcome, both plaques exhibited higher than normal decay rate in both cells, loss of dry-side tolerance in Cell No. 1 and initially higher decay rate and increasing internal resistance in Cell No. 1. Specific causes for these effects were not identified and will require investigation in future programs.

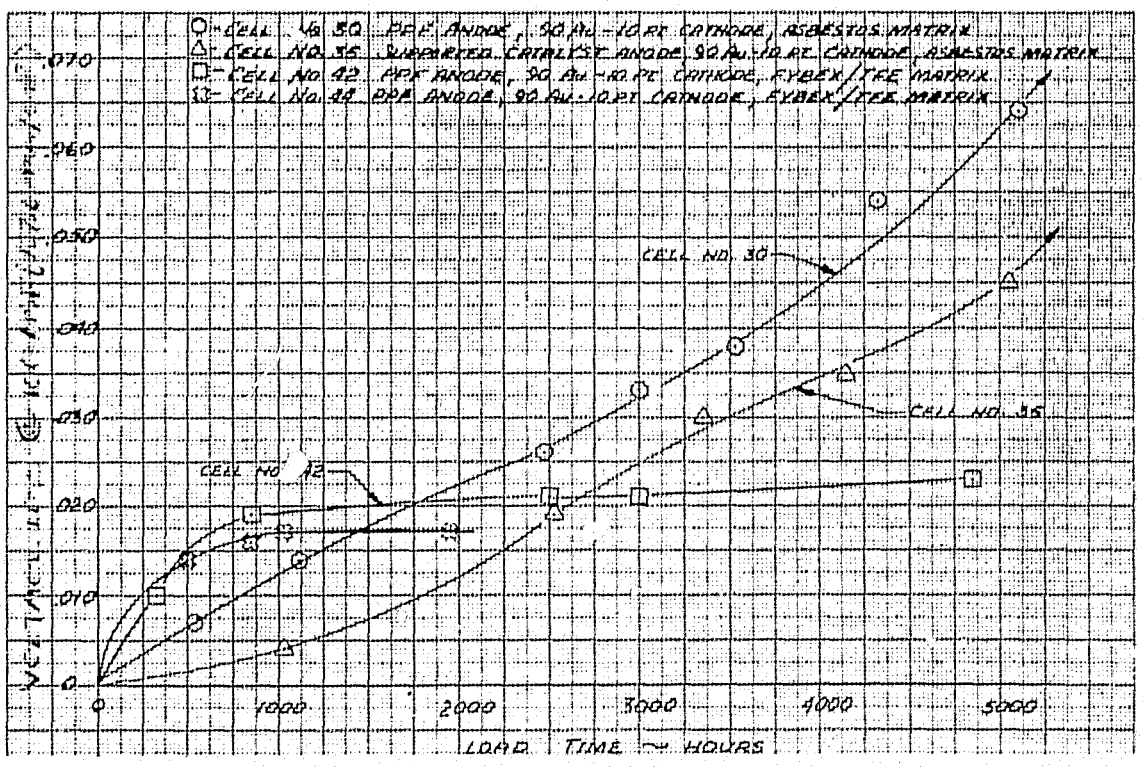

Figure 4 — Single Cell Voltage Loss Comparison

II. INTRODUCTION

The Lewis Research Center of the National Aeronautics and Space Administration is conducting a fuel cell system technology advancement program oriented toward advanced space applications. The emphasis in this program is on applied fuel cell research and development to build a new technology base from which advanced fuel cell systems can be developed. The work is being guided by an advanced fuel cell system, the specifications for which require a system weight of 20 lb/kW and an operating life of 10,000 hours.

The technology being developed has broad applicability for space and undersea power systems touching as it does on the fundamentals of fuel cell science and art (electrode catalysts and structures, matrix materials, compatibility of structural materials, lightweight cell components, and fabrication techniques).

The several work areas of the program and the emphasis in each were planned to meet the objectives stated by NASA LeRC; the key elements of these objectives are:

> "Goals – The NASA Lewis Research Center is embarking on an advanced fuel cell program . . . The overall goal is to advance the technology to provide a low cost, long life fuel cell system to meet Shuttle requirements . . .
>
> Phasing – A multiphase development program is anticipated. The first phases cover two aspects of the total program.
>
> 1) The initiation of an on-going technology program to achieve necessary improvements in the fuel cells and ancillary components.
>
> 2) A preliminary design for an Engineering Model System that will incorporate the best current ideas for meeting the program goals."

The program consists of contractor performed work and complementary work performed at the Lewis Research Center. Phases I, II, III and IV of the program have been completed. In each phase several interrelated program tasks have been performed aimed at meeting requirements of the next generation of fuel cell systems, as well as providing supporting technology for on-going, mission-oriented fuel cell system programs. In programs that are specifically mission-oriented, very often scheduling constraints require that technology shortcomings be circumvented by design rather than being addressed directly. Advanced technology programs, on the other hand, permit more effort to be applied to solving basic problems. The potential benefits of such a program are two-fold. First, a superior system can emerge at a technological level where a potential user can compare it to an existing inventory system. Second, and of equal importance, technology generated during such a program can be utilized by on-going mission-oriented programs.

This report describes the several research and development tasks performed by PSD during the fourth phase of this advanced fuel cell program. The program tasks performed were:

A. Materials Research

B. Unitization Research

C. Stack Component Fabrication

D. Cell and Plaque Testing

A summary of the results achieved during Phase IV is presented in Section I, Summary. The following sections present detailed discussions of the work performed in the individual task areas.

III. MATERIALS RESEARCH

A. Electrodes

The original objective of the Phase I electrode technology advancement effort was to improve the performance and stability of the alkaline electrolyte fuel cell, principally by the development of new cathode catalyst. As the work progressed, data were generated which indicated that structural development of both electrodes would improve stability of cells operating at powerplant conditions. Several catalysts, including gold alloyed with either platinum, nickel, rhodium and copper, showed potential for improving the performance and stability of cathodes. Higher sinter temperature structures and supported catalysts showed potential for improving anodes. These alloys and structures were further evaluated and developed during Phases II, III and IV. During Phase IV, tests of full-size cells incorporating these candidate electrode materials that had begun in Phase III were continued. Post-test analyses of the electrodes from these cells, conducted at the conclusion of their tests, were carried out under this task. Special diagnostic evaluations of electrodes were also made in support of the tests of Cells Nos. 42 and 43, and the two-cell plaque development started in Phase IV.

1.0 Post-Test Evaluation of Full-Size Electrodes

As part of the Phase IV program, full-scale 0.1146-ft^2 (106-cm^2) cells were endurance tested to evaluate catalyst compositions and electrode structures for suitability at design conditions. The endurance tests are described in Section IV of this report. Post-test analyese of two of these cells are described in this section. The evaluations included half-cell testing of electrode sections and chemical and microstructural analyses, including X-ray examination techniques, to determine crystallite size.

Cell No. 40 — A post-test analysis was made of Cell No. 40, which had an 80 Au-20 Pt catalyst cathode and a supported platinum anode and had been tested for 4160 hours at 100 ASF, (107.6 ma/cm^2) 180°F (82.2°C). The half-cell (H/C) performance test result for the 80 Au-20 Pt cell catalyst cathode in Cell No. 40 is shown in Figure 5 along with the result of a half-cell performance test of an early 80 Au-20 Pt cathode tested for 4000 hours in a laboratory-size cell, MO219. The cathode in Cell No. 40 had 20 mV less activation loss than the cathode in Cell MO219, but had higher diffusion losses at current densities above 100 ma/cm^2. The specific cause of the cathodes high diffusion loss could not be identified, but it did occur just after a refill at 4000 hours into the test. It may be that the increase in diffusion loss was caused during this process. However, the full-scale cathode's activation level was higher than that of the laboratory cell even after the 4000 hours of test and up until the refill its diffusion losses were estimated to be consistent with the laboratory cell. Therefore it was concluded that in scaling up the fabrication processes from laboratory to shop manufacture the 80 Au-20 Pt cathode was not adversely affected.

The cathode activation and diffusion losses for Cell Nos. 30 and 40 are shown in Figure 6. Cell No. 30 is used as a standard of comparison because it ran for 10,000 hours with a 90 Au-10 Pt cathode and PPF anode at the same conditions as Cell No. 40 and exhibited a decay rate among the lowest in the LeRC program. Cell No. 40's cathode activation level was initially lower than that of Cell No. 30, but was more stable with time even though its cathode catalyst loading was half that of Cell No. 30 (10 mg/cm^2 versus 20 mg/cm^2). This confirmed the same

early conclusion reported at the end of Phase III, based only on 90 Au-Pt and 80 Au-20 Pt laboratory cells. Cell No. 40's cathode diffusion loss was comparable to that of Cell No. 30 until it was refilled after 4000 hours of operation. Subsequent to refill its cathode diffusion loss rose abruptly as has been noted above. Another 80 Au-20 Pt cathode, operated for more than 8000 hours, showed diffusion loss characteristics for its entire operating period similar to the characteristic of Cell No. 40 before refill.

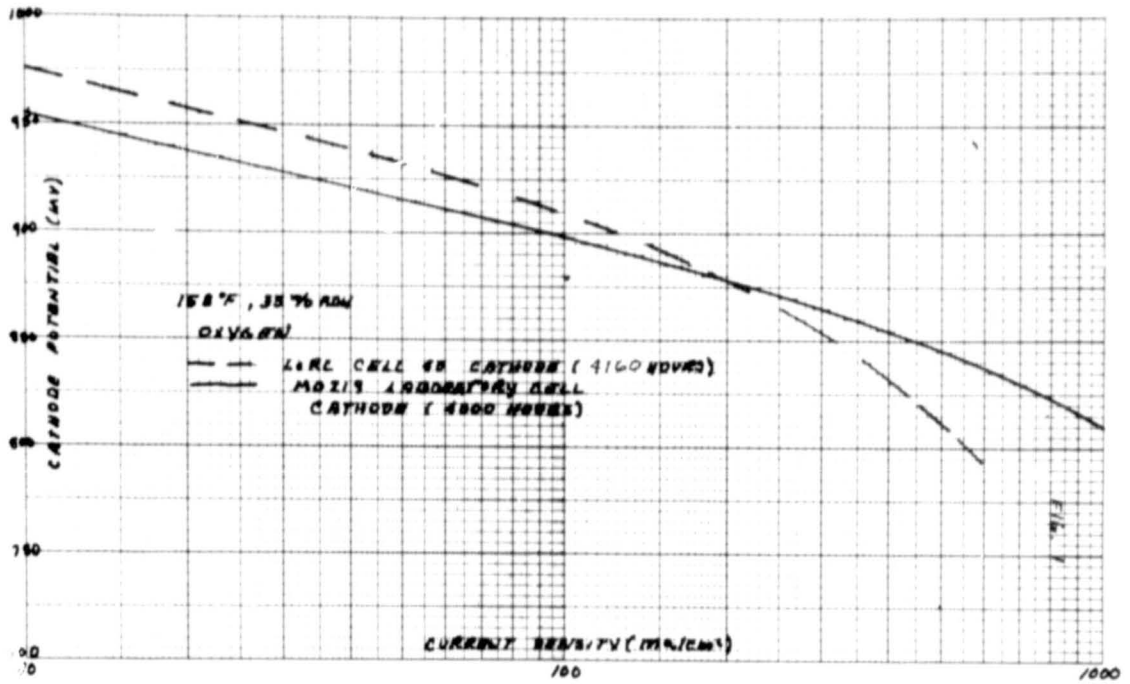

Figure 5 — Cell No. 40 — Post-Test Half Cell Cathode Evaluation

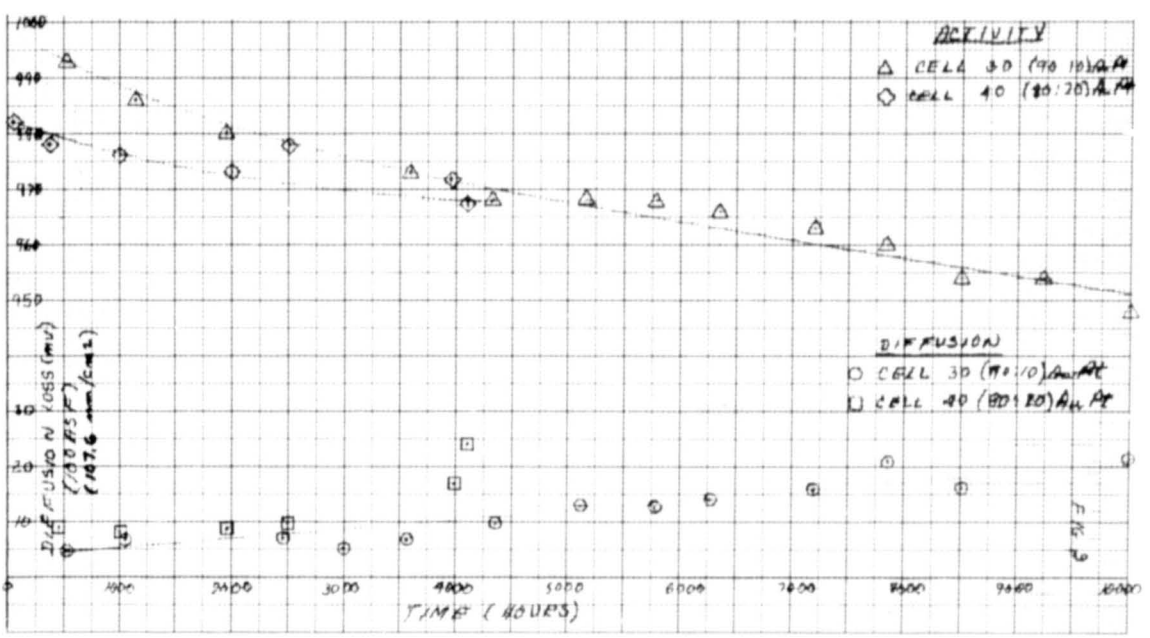

Figure 6 — Cathode Activation and Diffusion Losses for Cell Nos. 30 and 40

Table I shows the measured migration of platinum from the cathode to the anode and the increase in anode and cathode catalyst crystallite size for Cell No. 40. The post test H/C result on the supported Pt anode from Cell No. 40 showed the anode to be flooded and silicon was found on the gas side of the anode. The silicon, a product of asbestos matrix corrosion, migrates through the anodes and deposits as a wettable layer on the gas side of the anode resulting in flooding and diffusion losses. Whether the flooding was caused solely by the silicon from the asbestos matrix or by a combination of silicon and electrode structure deterioration cannot be determined from the available data. However, the level of anode diffusion is higher than in asbestos matrix cells with PPF anodes operated for comparable times. PPF anodes have a higher Teflon content and are sintered at a higher temperature than these electrodes. In addition, there is a basic difference in the catalyst distribution between a supported anode and a PPF anode. The difference is illustrated in Figure 7. If the gas side of both electrodes is flooded, because of silicon migration, the PPF anode has more catalyst present at the gas liquid interface than the supported anode. This could result in lower diffusion losses for PPF anode by one-half, based on the difference in thickness, loading, and surface area between the two anode types.

TABLE I

CELL NO. 40 CHEMICAL AND XRD ANALYSIS

CHEMICAL ANALYSIS

	CATALYST PLATINUM CONTENT	
	INITIAL mg/cm^2	FINAL mg/cm^2
Cathode	2.0	0.45
Anode	0.5	1.14

XRD CRYSTALLITE SIZE

	Initial Crystallite Size (Å)	Final Crystallite Size (Å)
Cathode	60±15	265±10
Anode	(≤30)	85±15

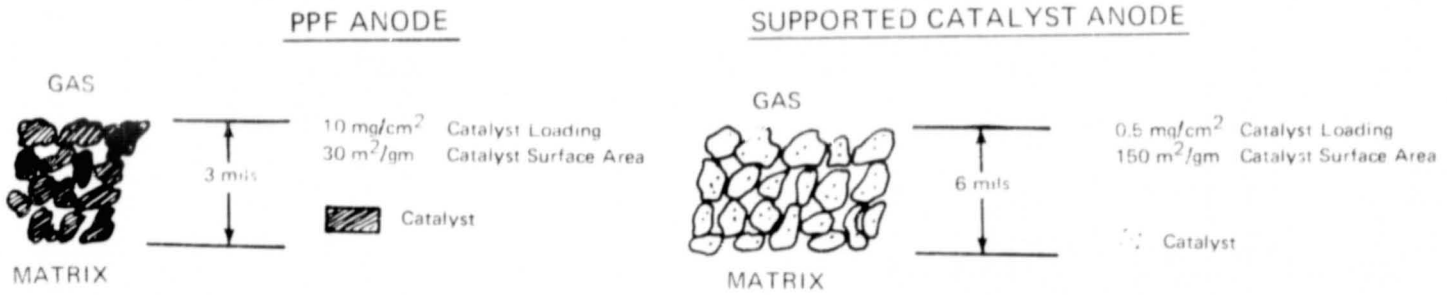

Figure 7 – Anode Cross Section

The anode diffusion losses for Cell No. 30 and Cell No. 40 are shown in Figure 8. The supported catalyst anode in Cell No 40 had higher initial diffusion losses than the PPF anode which is related to the initial hydrophobicity of the supported structure. A refill at 350 hours lowered the diffusion losses somewhat, but not to the level of anode in Cell No. 30. Between 3000 and 4000 hours the electrode became flooded resulting in markedly higher losses.

To render the supported anodes more fillable, a pretreatment of the electrodes with sulfuric acid was instituted; this pretreatment decreased the initially high diffusion losses. Future tests of supported catalyst anodes with matrices containing no silicon should permit further determination of the losses due to the silicon and those due to the structure itself.

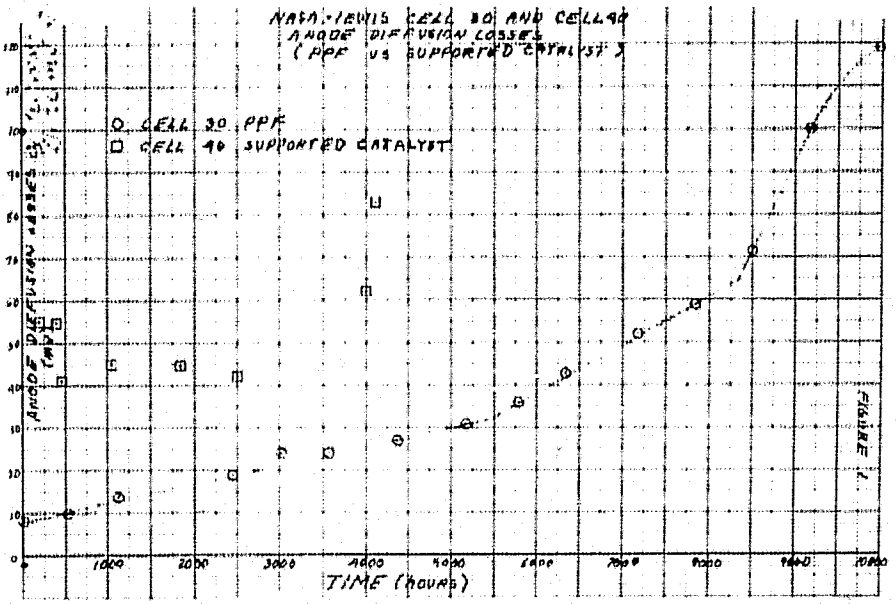

Figure 8 — Anode Diffusion Losses for Cell Nos. 30 and 40

Cell No. 43 — Following the shutdown of Cell No. 43, post-test analyses of the electrodes were initiated. This cell contained a PPF anode, a 90 Au-10 Pt cathode, and a Fybex matrix. It accumulated 911 hours of which 541 hours of operation were at 250°F (121.1°C), 28 psia, (19.3 n/cm^2).

Visual examination of the anode revealed wetting of the gas side. Half-cell diagnostics under hydrogen confirmed severe flooding as evidenced by a decrease in limiting current to 250 ASF, (269 ma/cm^2).

Washing the electrode with water produced little improvement and half-cell testing of the washed electrode under oxygen showed a greatly diminished catalyst activity relative to a fresh anode.

Resintering the anode caused a substantial improvement in performance. The polarization on hydrogen at 500 ma/cm^2 was reduced to 28 mV, the deviation from Tafel line on oxygen at 500 ma/cm^2 was reduced from 125 to 10 mV and the catalyst activity doubled. The

most probable explanation for this behavior is that there was some organic contaminant on the surface of both the Teflon and the platinum which volatized or burned off during resintering. The most probable contaminant is residue from the wetting agent used in fabricating the Fybex matrix.

Half-cell testing of the cathode indicated that its catalyst activity was about half the original value. This is probably attributable to recrystallization resulting from operation at 250°F (121.1°C).

Resintering the cathode did not improve its activity, but raised the limiting current on air from about 300 to 600 ASF (323 to 646 ma/cm^2). This suggests that the catalyst agglomerates shrank away from the Teflon during recrystallization and that resintering restored the catalyst-Teflon interface.

2.0 Electrode Diagnostic Evaluations

These laboratory evaluations were conducted in support of the tests of single cells and two-cell plaques discussed in Section VI, Cell and Plaque Testing. They were used to help isolate causes of abnormal operation in full-scale test articles.

The first series of laboratory evaluations were conducted to determine the cause of the low performance experienced in Cell Nos. 42 and 43. These cells contained standard PPF and 90Au-10Pt electrodes with Fybex matrices applied to the electrodes by a filtration process. A poison or contaminant, introduced into the electrodes during the matrix application process, was suspected as a primary cause of their low performance. Half-cell tests of anodes had shown no detrimental effect of Fybex application. Consequently a series of laboratory half-cell tests, listed in Table II, were run on Fybex-coated cathode samples to isolate the poisoning agent. Various sintering and leaching techniques were used in attempts to eliminate the poison. The results of these tests showed that the Triton wetting agent used in the matrix slurry was apparently responsible for much of the loss since cathode samples with this agent leached out performed significantly better than those in which the Triton remained, see Figure 9. A final cathode sample in which no Triton was used in the matrix slurry was also found to perform well. As a result of these tests, a new cell using a Fybex matrix with no wetting agent was fabricated and tested as Cell No. 44.

The second laboratory evaluation was conducted in support of the testing of Two-Cell Plaque No. 2. A PPF anode from the same batch as that in Two-Cell Plaque No. 2 was analyzed to determine if a substandard anode might be contributing to the abnormal operation of Cell No. 1 in the plaque. The results showed no unusual performance or wettability characteristics of the anode. Therefore it was concluded that the performance and tolerance problems exhibited in the two-cell plaques is due to phenomena other than poor anodes.

B. Matrices

During the Phase I program, NASA LeRC and P&WA began evaluation of potassium titanate as an alkaline fuel cell matrix material. The material evaluated was manufactured by E. I. Dupont deNemours & Company under the trade name Fybex. Early tests at the LeRC and

TABLE II

ELECTRODE CONTAMINATION INVESTIGATION
(90 Au-10 Pt Cathodes)

TEST NO.	MATRIX	ACTIVITY (V @ 10 ma/cm^2)	TAFEL (mV/Decade)
1	Before Fybex Application	1.008	48
2	Before Fybex Application	1.005	48
3	After Fybex with Triton Leached	0.991	48
4	Fybex — Infra-red Sintered	1.004	45
5	Fybex — Infra-red Sintered	0.993	46
6	Fybex — 350°F (176.6°C) Air Sinter — 530°F (276.7°C) N_2 Sinter	0.995	50
7	Before Fybex Application (new electrode sample)	1.013	41
8	After Fybex — no Triton	1.008	44

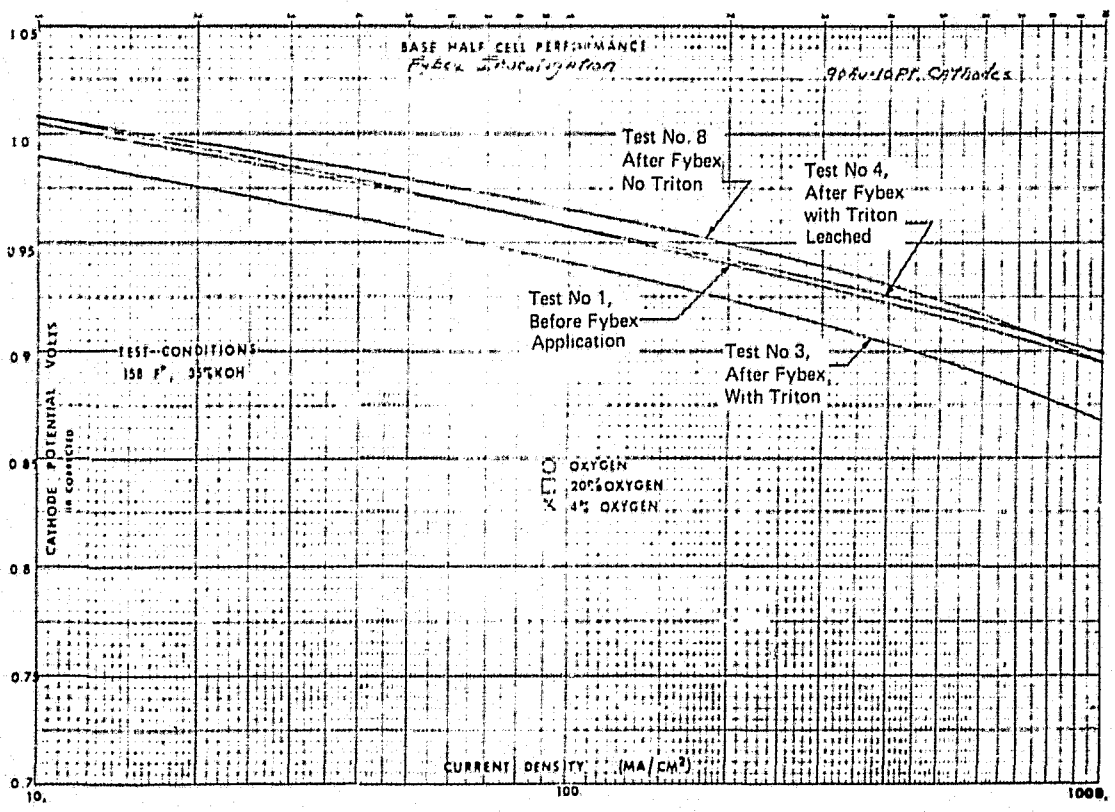

Figure 9 — Results of Electrode Contamination Investigation

P&WA showed Fybex to be compatible with KOH and to exhibit good bubble pressures up to 20 psid (13.8 n/cm^2).

Phase II efforts focused on developing methods for fabricating Fybex matrices with improved mechanical properties. These efforts were thwarted, however, by changes made by the supplier, Dupont, in the process for manufacturing the raw material. These changes altered the Zeta potential of the Fybex fibers and in turn the mechanical properties P&WA could achieve in fabricating a matrix. To solve this problem two approaches were considered: (1) specially process the Fybex to reobtain the Zeta potentials of the original pilot lots of material, or (2) develop procedures for fabricating matrices which are unaffected by the change in Zeta potential. The latter approach was explored during the Phase III program and a filtration process was developed that permitted fabrication of a matrix directly on electrodes. Tests of 2-in. x 2-in. (5.08-cm x 5.08-cm) laboratory cells verified that this process produced matrices worthy of evaluation in full-size cells. In Phase IV this process was used to fabricate Fybex matrices for full-size cells which have demonstrated the lowest degradation rates of any cells in the test series under this program.

However, initial attempts to use this process in Phase IV resulted in non-uniform matrix thickness with buildup at the edges of the electrode active area. This was due to higher porosity at the edges of the catalyst layer than at the center of the electrode which allowed an excess amount of slurry to flow through the edges. To counteract this effect the edges were impregnated with a thin epoxy or polysulfone "frame" to seal large pores. Electrodes made with these "frames" were substantially improved with much of the edge buildup eliminated. A similar, although less severe, problem on the anodes caused by local points of higher porosity resulted in small mounds of Fybex scattered over the active area. Rolling the matrix after filtering minimized this problem. Following the resolution of these problems, Fybex was successfully filtered on electrodes for Cell Nos. 42 and 43. Both cells were subsequently bubble checked and tested successfully. Performance of Cell Nos. 42 and 43 was lower than expected. As noted above, this performance loss was attributed to contamination of the electrodes caused by poisons introduced during matrix application. Consequently, several electrode samples were coated with Fybex in the manner used for Cell Nos. 42 and 43 and a set of electrodes coated with a Fybex layer containing no wetting agent was prepared. The "standard" Fybex slurry uses TFE-3170 which contains a small amount of Triton wetting agent; TFE-42 which contains no wetting agent was substituted in the new slurry. No problems were encountered with the fabrication of these matrices and a set of electrodes for Cell No. 44, which has performed well, was made with this procedure. This procedure will be the basis for any particulate matrices that are fabricated in the future of Fybex or other materials such as ceria or zirconia.

Because particulate matrices applied to electrodes by filtration are delicate, damage during subsequent cell fabrication steps is possible. To achieve a more rugged matrix that could be handled with less care, development of a fiber-reinforced matrix was investigated. Trials were conducted with a mixture of Fybex and asbestos as a possible alternate to the pure Fybex-TFE matrix. A mixture of 80 percent Fybex and 20 percent asbestos, chosen as a starting point, resulted in a good sheet material. A non-operating cell unitized with this matrix exhibited excellent bubble pressure, 35 psia (24.1 n/cm^2).

Although use of asbestos as a reinforcing material is not desirable because of its corrosion characteristics, this concept of fiber reinforcement was proven to have merit and composites with other more-corrosion-resistant fibers, such as polybenzimadazole (PBI) could be pursued in the future.

During the Phase IV program Mssrs. R. W. Vine and S. T. Narsavage, who were responsible for much of the matrix development work throughout this program, presented a paper entitled, "Porous Matrix Structures for Alkaline Electrolyte Fuel Cells" at the Spring Meeting of the Electrochemical Society Inc. in Toronto Canada, May 11-16, 1975. This paper provides a concise overview of both the experimental and analytical work conducted under this program. It is included in this report as Appendix A.

IV. Stack Component Fabrication

During Phase III five new test articles were fabricated; three single cells and two two-cell plaques. The single cells were all of the type, described above and were fabricated according to the method described. The two-cell plaques were fabricated in the same manner. However, the specific internal details of the plaques did vary. These differences are described in detail in Section VI, Cell and Plaque Testing.

V. Unitization Research

The EMS weight and life goals impose stringent requirements on cell fabrication technology. To minimize weight, thin cells which must be fabricated to close tolerances are required. A cell frame thickness variation of a few thousandths of an inch, which would be acceptable in conventional thicker cells, would represent a significant percentage of a total cell dimension for lightweight cells. This could result in degraded cell performance because of poor contact between cell components and sealing of adjacent subassemblies could be unreliable. The reactant differential pressure (bubble pressure) capability of the matrix-to-frame joint in the water transport plate and the fuel cell subassemblies must be reliable. The materials used to make this joint and to form the cell frame must be highly resistant to attack by reactants, water, and electrolyte. Finally, assembly and bonding processes must be compatible with normal manufacturing equipment and must result in reasonable costs.

Much of the unitization work in Phases I and II involved identifying materials compatible with the fuel cell environment and learning to fabricate these materials into cells with acceptable dimensional and bubble pressure characteristics. The most compatible of these materials could not be fabricated into cell frames using adhesive bonded joints. To permit their use, thermal laminating was explored as a method for bonding and fabricating them into cell frames. A major problem was encountered using this fabrication method. The temperatures needed for laminating caused a differential thermal expansion between the cell electrodes and frame. The result was that the dimensional characteristics of these cells were poor because of screen wrinkling. Materials which could be laminated at lower temperatures were less compatible with the fuel cell environment.

At the end of Phase II, a cell design was conceived which overcame these corrosion and fabrication problems. This was a hybrid frame composed of polysulfone and epoxy/glass-fiber. In this method polysulfone, which had demonstrated excellent compatibility with the fuel cell environment, was used as a frame around the asbestos matrix, as shown in Figure 10. The epoxy/glass-fiber was used to form a frame that surrounds the polysulfone. The function of the polysulfone is to minimize contact between the electrolyte and the epoxy/glass-fiber. The amount of polysulfone is minimized because of the large thermal expansion coefficient difference between it and the electrode screens. Epoxy/glass-fiber counteracts the polysulfone expansion problems and acts as a stiffener.

During Phase III this method was used exclusively for fabrication of single cell assemblies and was shown to have corrosion resistance superior to that of epoxy/glass-fiber frames. The main thrust of the Phase IV unitization effort was to: (1) Adapt this frame design to the special requirements for unitization of filtered particulate (Fybex) matrices, and (2) develop a hybrid frame for two-cell plaques incorporating positve sealing of electrolyte within each cell.

A. Unitization of Cells with Particulate Matrices

Unitization of cells with particulate (Fybex) matrices filtered on to the elctrodes was accomplished using a modification of the process used with sheet matrices such as reconstituted asbestos. As shown in Figure 10, the polysulfone laminate layers are positioned about a sheet matrix so that when they are heat-bonded together they form a channel about the periphery of the matrix. During the bonding process the polysulfone flows and penetrates the matrix providing a joint with high cross-pressure integrity. With a particulate matrix, which is more delicate and not as resistant to compression as the fiberous asbestos matrix, penetration of the polysulfone into the matrix during bonding was not certain. To assure a high cross-pressure joint an additional laminate layer (0.0015 in. thick (0.038 mm)) was incorporated into the layup prior to bonding. This layer extended into and between the layers of matrix applied to each electrode before bonding occurred. The final unitized assembly after bonding is shown in Figure 11. Although this additional layer may not be necessary, it precluded any cross-leakage developing in these first Fybex-matrix cells.

B. Unitization of Two-Cell Plaques

Testing of multicell plaque assemblies, which incorporated reactant housings and manifolds common to all the cells of one plaque, had a limited endurance capability due to transfer of electrolyte from cells of high potential to cells of lower potential in the plaque. Study of the transfer mechanism revealed that electrolyte bridges between the individual cells within the reactant gas housings were essential to the process. To prevent this transfer mechanism, a plaque design which isolated each cell from its neighbor with dedicated reactant housings and manifolds for each cell was proposed. This design eliminated any possibility of an electrolyte bridge between cells, but was a more difficult design to fabricate than the design with common reactant passages. Therefore the first objective of this subtask was to fabricate this new plaque design. A two-cell plaque was chosen for development, rather than the six-cell plaque fabricated earlier in the program, because it was judged by NASA-LeRC to better meet near-term applications requirements than the larger plaque. An additional objective was to execute it as a hybrid-frame design. All previous plaques had been of the simpler

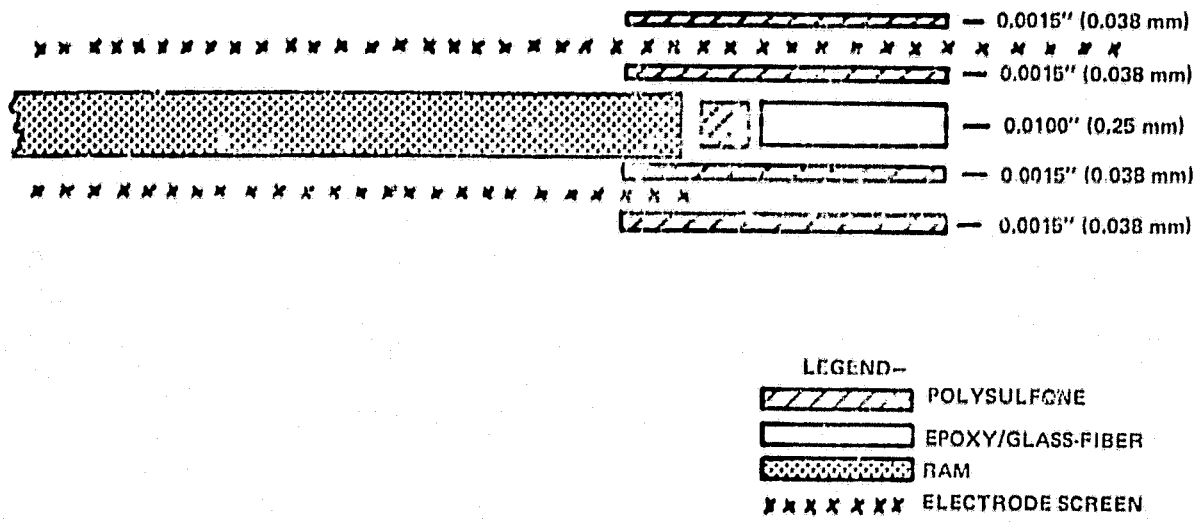

Figure 10 — Hybrid - Polysulfone - Epoxy/Glass-Fiber Frame Design

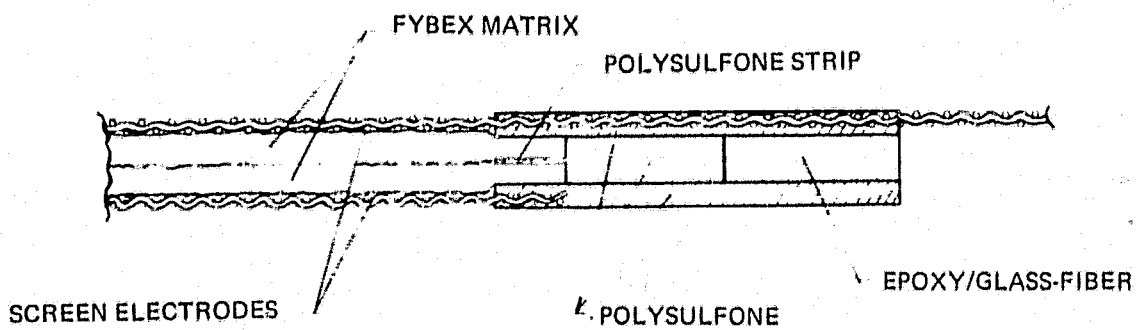

Figure 11 — Unitized Frame Construction For Particulate Matrices

epoxy/glass-fiber design. The first step was to develop a hybrid intercell joint the most critical part of the plaque assembly. The details of a finished intercell joint are shown in Figure 12. The figure shows the cathode of one cell is electrically connected to the anode of the adjoining cell. This is accomplished by fabricating the two electrodes on a common substrate that is threaded through the various layers of polysulfone and glass fiber, which form the frame and intercell spacer, before bonding. The assembly is then press cured at a particular set of temperature and pressure conditions. Temperature and pressure are selected to ensure that sufficient flow of polysulfone is attained to achieve complete interlaminate bonding, and high cross-pressure joints without causing electrical shorting of electrode screens.

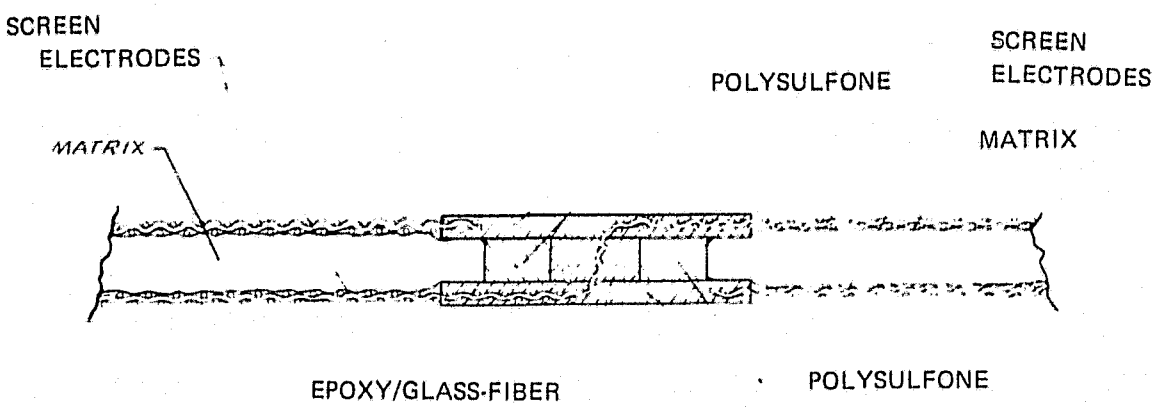

Figure 12 — Intercell Joint

The passive water removal unit assemblies for these two-cell plaques were fabricated using standard epoxy/glass-fiber procedures. A minor change in the two-cell plaque water transport plate design was made. The porous Teflon electrolyte barrier was bonded into and made an integral part of the PWR. Previously it had simply been laid atop the PWR as it was assembled into an operating cell or plaque assembly. A cross section of this arrangement is shown in Figure 13. A completed two-cell plaque and a passive water removal unit are shown in Figure 14.

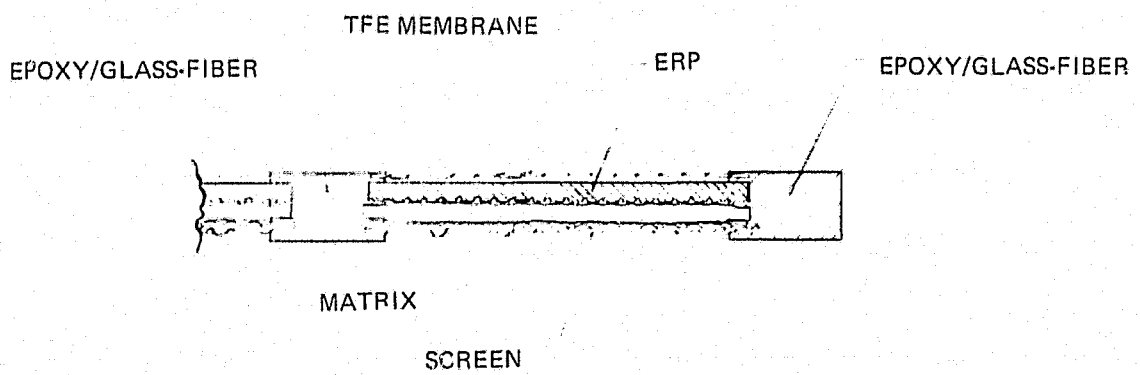

Figure 13 — Cross Section of Improved Passive Water Removal Unit

The second objective was to develop a plaque-PWR-gas housing assembly which isolated one cell from the other completely to provide a sure electrolyte barrier between cells. The approach was to develop a completely bonded assembly which virtually encapsulated each cell in its own reactant housings. Figure 15 shows the cross section of all the elements which are bonded into final assembly. Each of the components located between bond layers is first fabricated separately and is then bonded in sequence to the UEA (Unitized Electrode Assembly). Figure 16 shows the individual components before bonding has begun. The Kintex flow field material was first introduced into the LeRC cell program in this design. It is an expanded metal material which has the desirable properties of low-cost, low-weight, and low-pressure-drop in the directions of flow both parallel and perpendicular to its primary plane. Figure 17 shows the material in detail with the directions in which hydrogen and water vapor flow through it when it is used in the anode space. It is available in many specific geometries presently used for compact heat exchanger fabrication and can be obtained in special geometries if required.

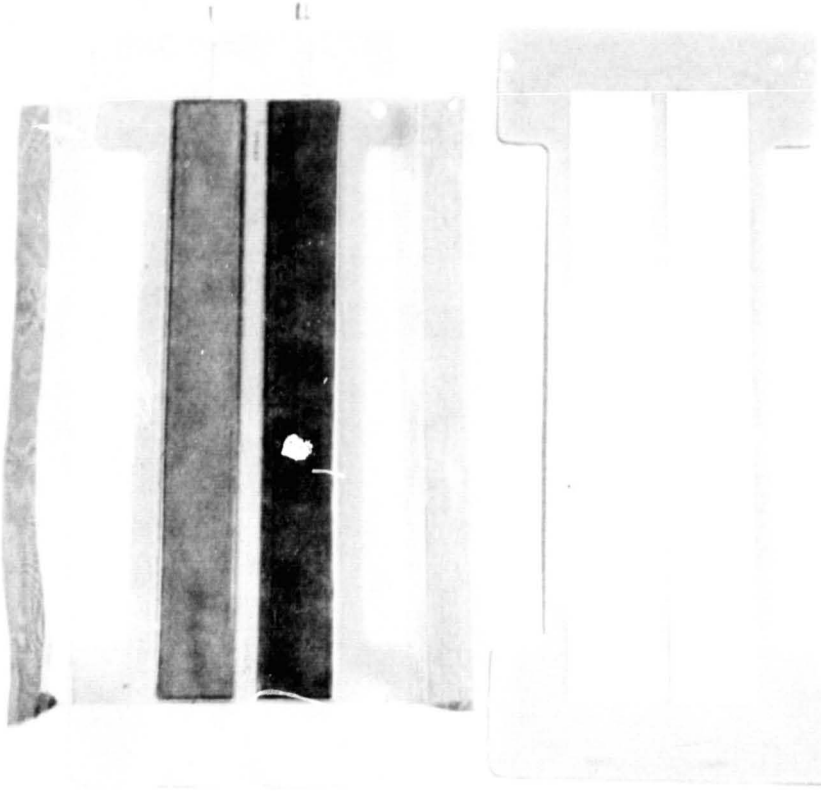

Figure 14 — Two-Cell Plaque and Passive Water Removal Unit (WCN-3664)

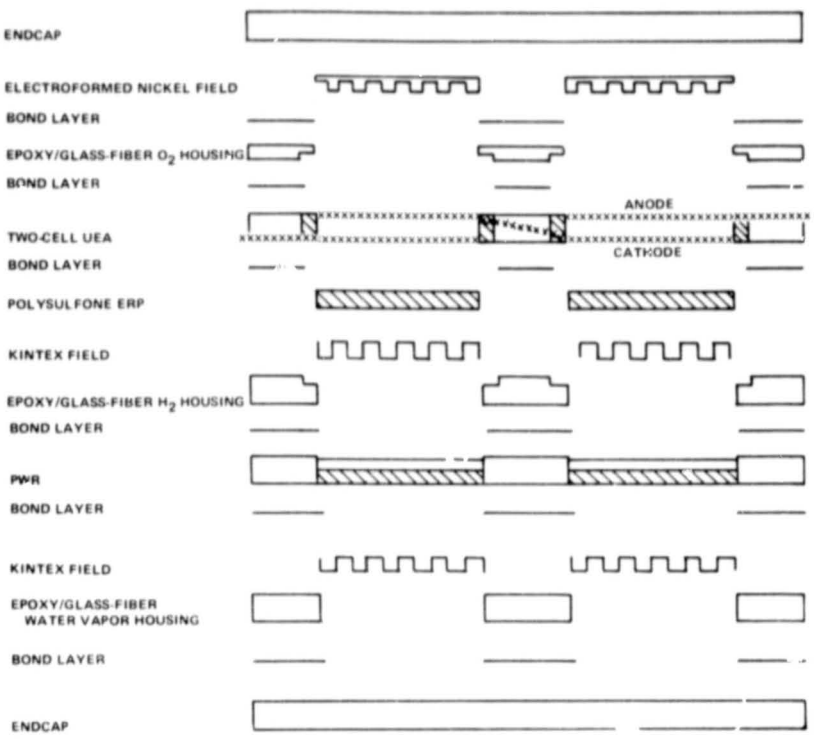

Figure 15 — Two-Cell Plaque Assembly Cross Section

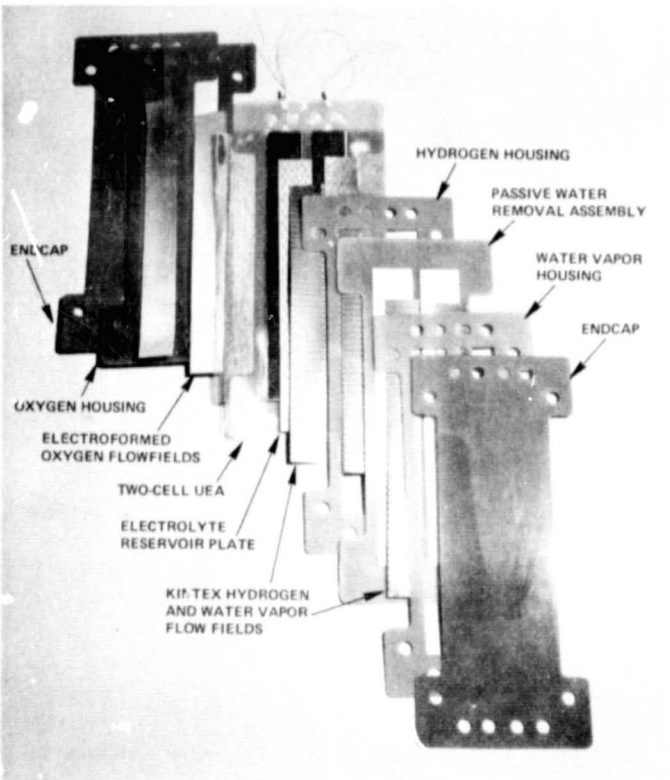

Figure 16 — Components of a Two-Cell Plaque Assembly (WCN-3664)

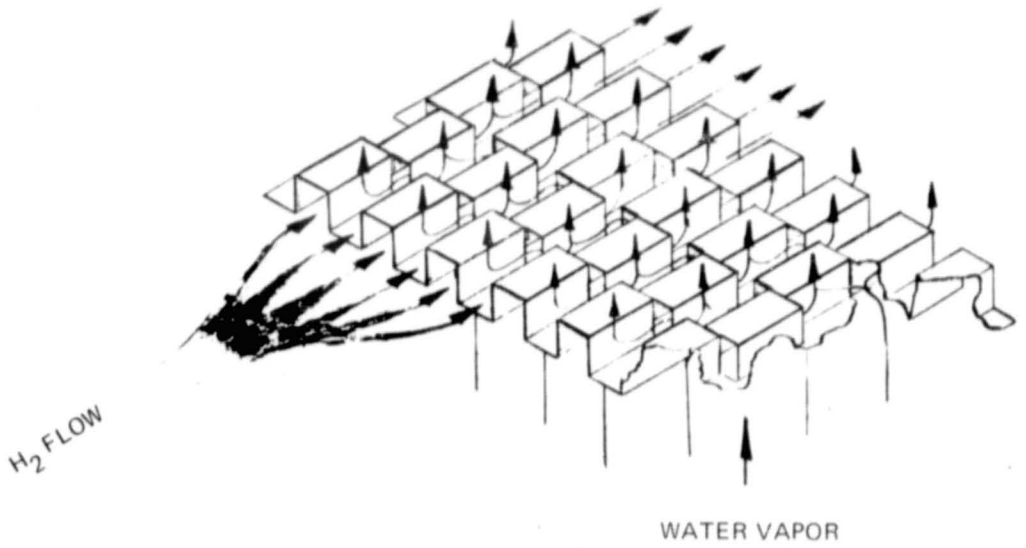

Figure 17 – Kintex Flow Field Material

During fabrication trials it was found that electrode screen wrinkling occurred during the bonding of the UEA to the adjacent frames using polysulfone bond layers. The wrinkling was caused by polysulfone extrusion during the bonding process which also resulted in oxygen port plugging and electrode shorting. To alleviate this problem, frames adjacent to the unitized electrode assembly were undercut, as shown in Figure 18, to reduce the pressure on, and the flow of the polysulfone in, the region adjacent to the active area. In addition, polysulfone bonding trials indicated that complete bonding could be attained at lower temperatures and pressures than used initially, thus further reducing flow of the polysulfone. After incorporating these changes in the final assembly process, successful bonds were obtained and the unit showed no port plugging or electrical shorting. A typical completed assembly is shown in Figure 19.

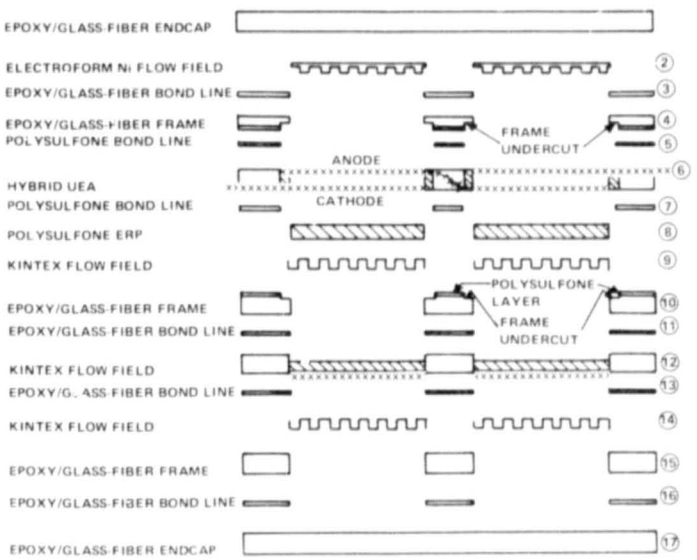

Figure 18 – Two-Cell Plaque Layup Cross Section

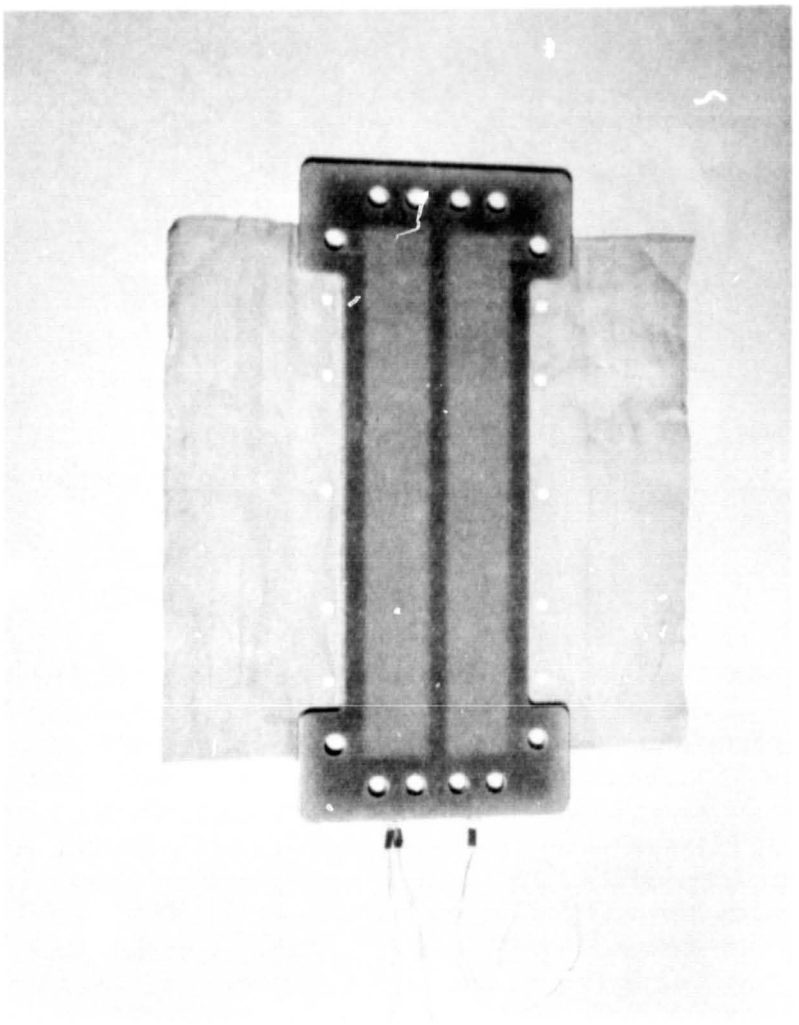

Figure 19 – Bonded Two-Cell Plaque Assembly (WCN-3649)

VI Cell and Plaque Testing

Single Cell and Plaque Testing received the major emphasis in the technology advancement effort performed during Phase IV. This task served as the focal point for integrating the results of the design analysis and the results of the materials development tasks. The NASA goals for operating life, weight, and system operational features call for a significant advance in fuel cell power section state-of-the-art. These goals have led to the preliminary EMS design which established the following cell requirements:

- Minimum thickness component parts and flow fields for low weight
- Plastic structural materials for low weight
- Highly compatible materials for long life
- Passive water removal
- Evaporative cooling

  } Required by the system, and their use favors long life

- Edge current collection, as a consequence of the above items

Single cells and individual plaques are the smallest building blocks for evaluation of these requirements. Although a single cell does not duplicate the intercell seal geometry of a plaque, and neither requires evaporative cooling for temperature control, they are the most cost effective approach for investigation of all the other EMS power section features.

B. Test Facilities and Test Procedures

The test facilities used for single cell and plaque testing are shown in Figures 20 and 21. These stands were originally used for work performed under contract NAS3-13229 and were adapted for passive water removal cell testing during the present contract. A schematic of the test stands is shown in Figure 22.

Reactants of fuel cell grade or better are supplied to the test stands. To eliminate test variables associated with reactant impurities, the hydrogen is further purified in a palladium-silver separator bank which reduces any contamination below detectable limits. Oxygen is purified using a Mine Safety Appliance catalytic oxidizer. Any hydrocarbons in the oxygen stream are oxidized to carbon dioxide and are removed by sodium-hydroxide scrubber columns. This system is shown in Figure 23. The carbon dioxide level downstream of the scrubber is continuously monitored by a LIRA gas analyzer. These readings indicate that the oxidizer is removing 8 to 12 ppm (equivalent) methane from the oxygen stream and that the carbon dioxide level entering the fuel cells is less than 0.5 ppm.

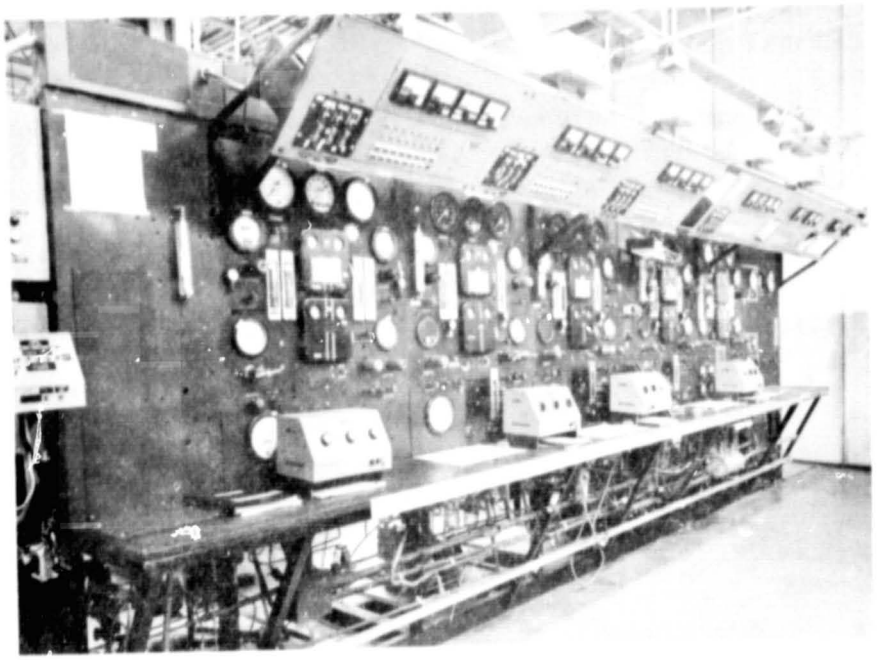

Figure 20 — Single Cell Test Facility (Front)

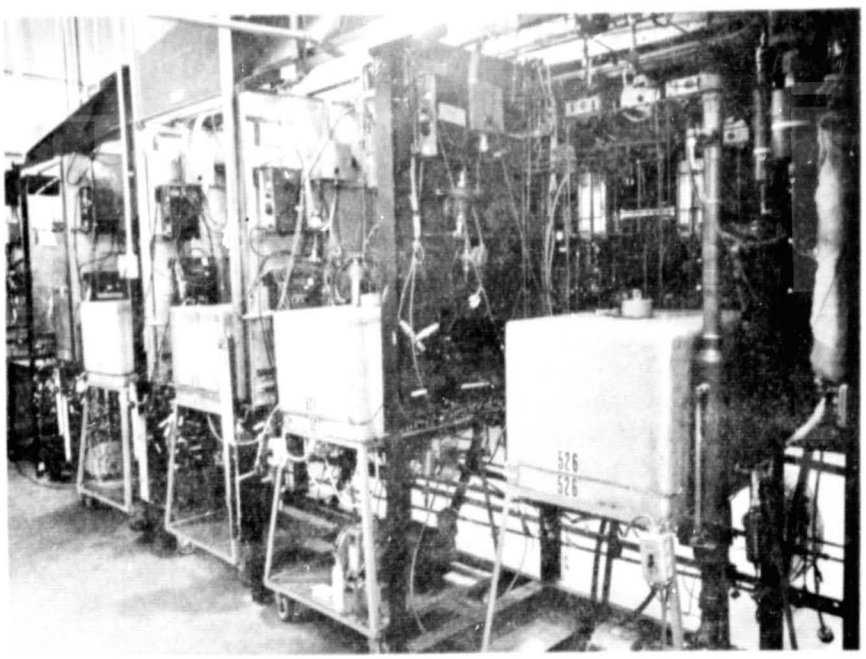

Figure 21 — Single Cell Test Facility (Rear)

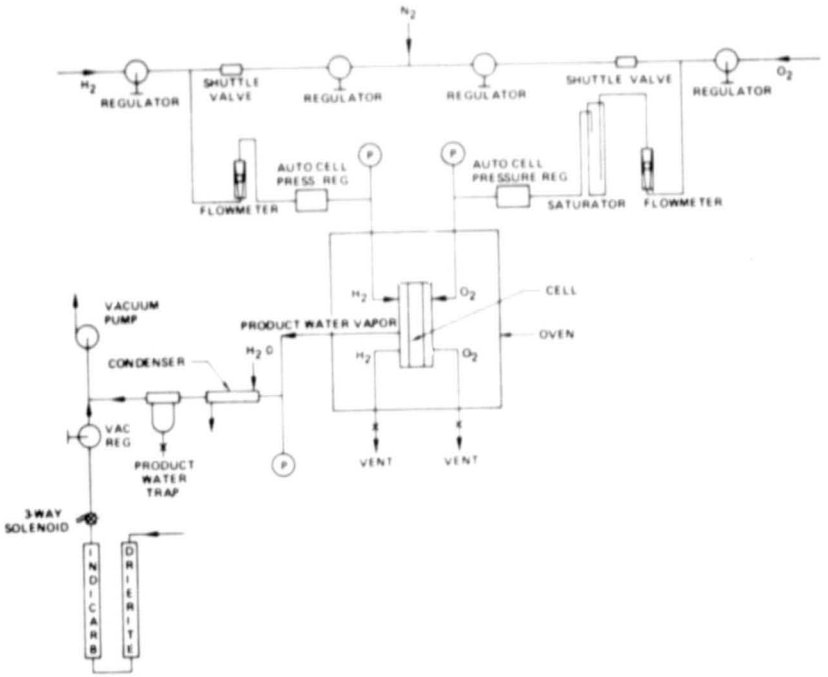

Figure 22 — Single Cell Test Stand Schematic

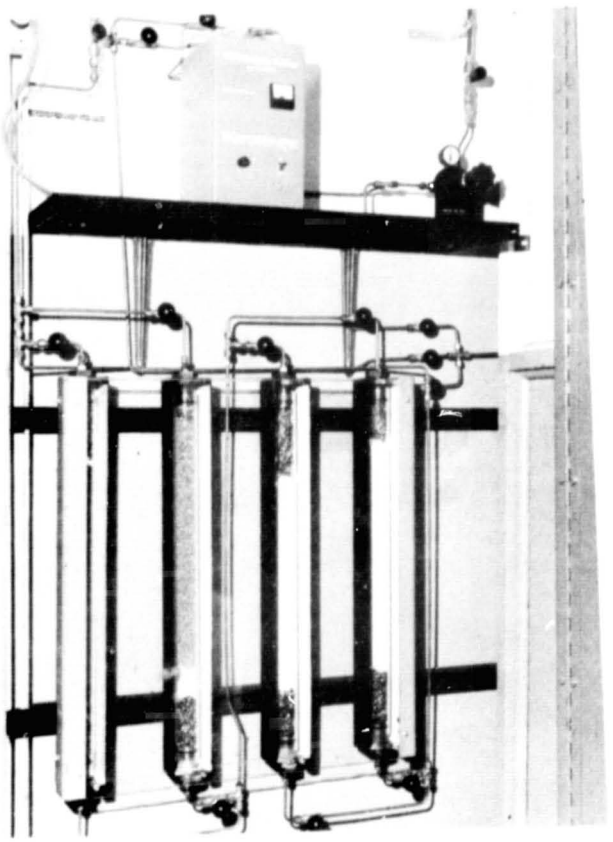

Figure 23 — Catalytic Oxidizer and Schrubber System

Temperature control of the test articles is provided by an insulated oven which is maintained within ±2°F (1.1°C) by a thermoelectric solid-state temperature controller. The relatively massive single cell and plaque endplates, in combination with the isothermal oven, maintain a uniform cell temperature. Cell temperature instrumentation showed that the simple oven temperature control method is effective in maintaining cell temperatures uniform within ±1.5°F (0.83°C) over a range of current densities to 300 ASF (322.8 ma/cm^2).

The product water removal system also duplicates the EMS design. A conventional Duo-Seal® vacuum pump is used to provide a sub-atmospheric pressure sink for product water vapor. The pH of the product water is regularly monitored. Trap water samples are checked once a day, using a Beckman Zeromatic®pH meter.

Performance data is measured and recorded by PSD's Automatic Data Acquisition and Reduction (ADAR) System. The following parameters are recorded once every hour and are stored on magnetic tape:

Parameter	Accuracy
Cell Voltage, volts	± 0.002 v
Cell Current, amps	± 0.02 a
Oven Temperature	± 3°F (1.7°C)
Oxygen End Plate Temperature	± 3°F (1.7°C)
Endplate Temperatures	± 3°F (1.7°C)
Barometric Pressure	± 0.03%

The ADAR system was designed to minimize experimental error and to reduce the amount of manual data handling. In addition to providing periodic scanning of the above parameters and transcribing them to engineering units, the ADAR system keeps an accurate log of total load hours. A typical ADAR printout for the NASA-LeRC Advanced Development Fuel Cells is shown in Figure 24.

```
STAND: X-527      , LERC CELL 42

RIG: 38901-42   DATE: 12/11/75   TIME: 11 3   LHRS:  4176

 LOAD      TOTAL
10.524 .    .888

CELL VOLTAGES:
      1
  0  .888

TEMPERATURES
  02 SAT EXIT **  128.

  PLUS END PLATE: 1=  178.  2=  179.  3=  180.
  NEG. END PLATE: 1=  130.  2=  181.  3=  181.  4=  180.
  OVEN WALL:      1=  178.

BAROMETRIC PRESS.= 14.685

X-527  RECORD STORED IN DATA BASE!
```

Figure 24 — Typical ADAR Printout

The heart of the ADAR system is a Hewlett-Packard Model 2100S digital computer. Other major components in the system, also from Hewlett-Packard, are a Model 2911 Guarded Cross-bar Scanner and Model 2402 Digital Voltmeter to scan and measure the test signals and a Model 2754 Teleprinter to print out the data.

All of the above data can also be read out directly at each station on conventional test stand instrumentation. Presssure and flows are controlled and monitored by appropriate regulators, gages, flowmeters, and valves, as shown in Figure 20.

The ADAR system is used only for automatic data acquisition. Automatic control is provided by appropriate test stand instrumentation, with provisions for automatic shutdown of any test article when pre-established limits are exceeded. For the NASA-LeRC program, these protective controls are:

Parameter	Limit
Voltage	Low (adjustable)
Current	High or Low (adjustable)
Temperature	High or Low (adjustable)
Vacuum Pressure	High or Low

Should an automatic shutdown occur the ADAR system immediately scans the test parameters. This record is later used to pinpoint the cause of shutdown. These automated control and protective features have resulted in very reliable single cell operation. Over 90,900 hours of fuel cell load were attained on 39 different fuel cells with only one stand-related failure. Some automatic shutdowns occurred because cell conditions exceeded the protective limits described above. In all of these cases, the cells were not damaged and normal testing could continue.

Single cell and plaque testing was primarily devoted to endurance tests. However, various diagnostic procedures were performed on all of the test articles to document any decay mechanisms and to determine design and off-design performance characteristics of the various cell configurations.

Typical test conditions for the programs were:

Cell Current Density	100 or 200 ASF (107.6 or 215.2 ma/cm^2)
Cell Temperature	180°F (82.2°C)
Product Water Vacuum	22 inch Hg (7.4 n/cm^2)
Hydrogen Pressure	16 psia (11.0 n/cm^2)
Hydrogen Flow	Consumption, plus 3 minute purge every 4 hours
Hydrogen Inlet Dewpoint	Dry
Oxygen Pressure	16 psia (11.0 n/cm^2)
Oxygen Flow	2 x consumption
Oxygen Inlet Dewpoint	130°F (54.4°C)
Average Electrolyte Concentration	34 percent KOH

Diagnostic techniques which were regularly employed included the following:

Performance Calibrations: Voltage-current characteristics were generated to 500 ASF (538 ma/cm^2), which is somewhat above the EMS peak power operating conditions. Recorded periodically, the performance calibration changes with time are valuable tools in determining the type and extent of any decay mechanisims. This is especially true of the semi-log representation of the performance data on an IR free basis which are commonly described as Tafel plo

Tafel Plots: The Tafel region refers to the low current density portion of a performance calibration. In this region, anode and ohmic polarizations are minimal or correctable so the cell voltage is essentially cathode-activation-limited performance. The Tafel region extends from approximately 1 ASF (1.076 ma/cm^2) to a level where diffusion losses become significant, 10 to 100 ASF (10.8 to 107.6 ma/cm^2), which is a function of operating temperature and pressure. In the Tafel region, the semi-log voltage-current curve should be a straight line, with a slope characteristic of the catalyst/reactant combination and a level proportional to the cathode activation.

Departures from this slope are an indication of parasitic loads, either internal cell shorting or gas crossover. Thus, the Tafel slope is a diagnostic tool useful in assessing the life expectancy of an operating cell. Changes in the levels of Tafel data are also a useful tool, since they indicate changes in the activity of the catalyst, either through changes in the number of active catalytic sites or structural modifications (e.g., recrystallization), changing the effect catalyst active area.

The so-called Tafel plot is also a useful diagnostic tool at current densities above the Tafel region. At these current densities, typical of operating cells, internal resistance (IR) corrections are required. When the cell performance is thus corrected, changes in the shape of the curves can be interpreted as changes in the diffusion characteristics of the electrodes. In this region, transport limitations are encountered if the electrode structure is not adequate for delivery of reactants or removal of product water. For example, diffusion problems can be related to microscopic flooding of the Teflon pores in a wet proofed electrode, or to increased concentration gradients in a heavily carbonated cell. While the semi-log performance plots alone do not distinguish such possible causes or even anode from cathode losses, they are valuable tools, in conjunction with previous experience and post-test analysis, in evaluating any performance decay trends.

Internal Resistance (IR): Internal resistance or ohmic polarization losses are unavoidable in any cell. However, these losses can be minimized by matrices with high porosity and correct assembly to ensure proper cell compression. In the strip cell with edge current collection there are also resistance losses in the electrode substrates and edge frames which are measured together with the conventional ohmic loss. IR measurements are taken periodically to ensure that the initial assembly is correct and that the correct cell compression is being maintained.

IR measurements are taken by the current interruption technique. Typically, a 100 ASF (107.6 ma/cm^2) load is interrupted and the resulting step change in voltage is measured on a Tektronic Type 545 oscilloscope. Since other polarizations have a long response time, the step change is a direct measure of internal cell resistance.

Dilute Oxygen Diagnostic Test: Although the Tafel and IR tests give good indication of relative cathode-matrix-anode losses at low current densities, they cannot be used to distinguish cathode and anode losses in the diffusion regime, the area of operational interest. The dilute oxygen technique permits identification of anode and cathode losses in the diffusion regime by running performance sweeps on 20% oxygen/80% nitrogen and on pure oxygen. It is based on the fact that cathode performance is proportional to the partial pressure of oxygen. A graphical procedure based on this relationship, illustrated in Figure 25, allows determination of individual electrode performance.

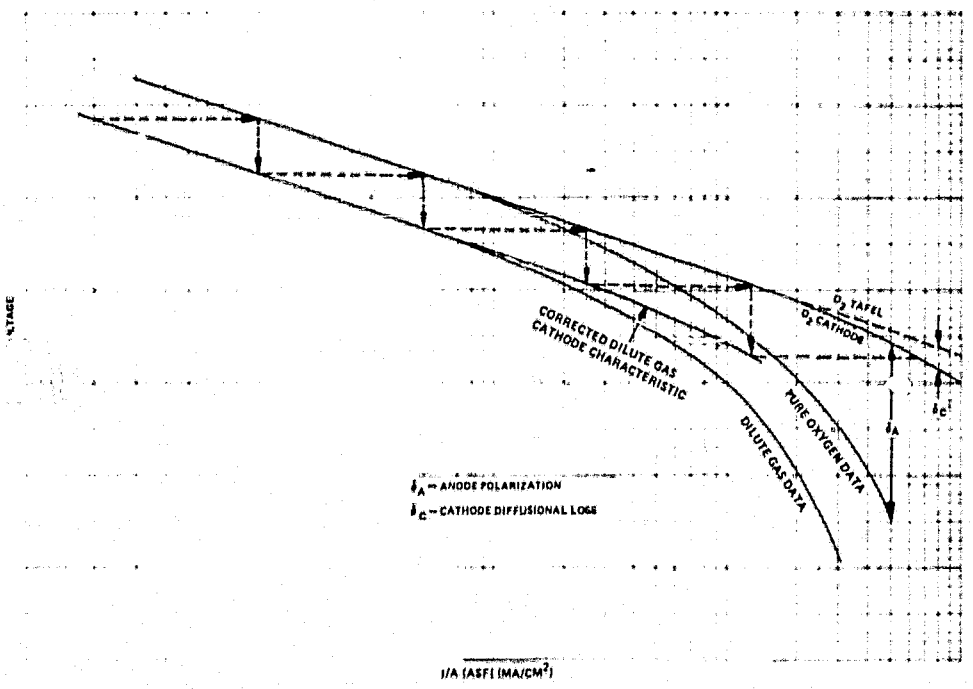

Figure 25 — Dilute Gas Diagnostic Method

A point in the activation region is selected on the dilute gas (20% O_2) data curve and the current is multiplied by 5, the ratio of oxygen partial pressures. The corrected point is plotted and compared to the O_2 data curve; if the point falls on the O_2 curve, no anode polarization has occurred. When a deviation occurs between the corrected point and the actual O_2 curve, the deviation is attributed to anode polarization. A correction is then made up to the 20 percent O_2 curve corresponding to this amount of anode polarization and the procedure is repeated.

When the true O_2 polarization curve is obtained, the difference between this curve and the generated O_2 data is anode loss. The deviation of the corrected cathode performance curve from the O_2 Tafel line is normally attributed to diffusional loss.

This approach does not separate anode losses into such categories as poisoning, flooding, concentration polarization and undescribed resistance but it does show clearly which electrode has the major effect on cell performance.

Off-Design Tolerance: If a cell is improperly filled, or if the contact between the ERP and cell is inadequate, the off-design tolerance characteristics of the cell will depart from the theoretical value. Off-design tolerance data can be generated in various ways. In the passive water removal cells, the most convenient and most severe method is to vary product water vacuum. Since the vacuum is changed almost instantaneously, the cell is subjected to a very rapid transient, taxing the transport properties of the ERP much more severely than off-design tolerance conditions imposed by slowly changing dewpoints on saturated gases.

Post-Test Analysis: All cells are subjected to post-test analysis. This includes visual (and microscopic) examination of components for observable changes in physical properties, structural defects or peculiar deposits. Because of the importance of low corrosion rates, all of the single cells in this program were carefully analyzed for carbonate conversion. Selected cells were also sectioned for laboratory tests, including floating half-cell tests of individual electrodes and measurement of catalyst activity and platinum migration.

C. Summary of Single Cell Testing

The overall goals of the single cell test program were to perform short term performance tests, with suitable diagnostics, to determine the following performance characteristics:

- Voltage vs. current density (performance calibration)
- Response to different operating conditions (off-design tolerance)
- Electrolyte retention
- Define endurance limiting phenomena and develop methods for extending cell life.

Two types of testing can be performed in the Single Cell Program. Research and Technology (R&T) tests are one type, comprising the first level of testing. These tests are performed on any items which are beyond the present state-of-the-art. This is a relatively informal level of testing in order to maximize the flow of technical information. Reviews of the progress of this testing are held regularly with the NASA Project Manager. When any item, in his judgment, is sufficiently demonstrated, the next level of testing is begun.

Verification and Endurance (V&E) tests are the second type, comprising the second and third levels of testing. All but one of the cell tests in Phase III were of this type. The Verification test is a short duration test, consisting of two week-long test cycles, interrupted by a

shutdown. The objective of a Verification test is to demonstrate the ability of the article under test to perform at the conditions in question. The Endurance test is of longer duration; the weekly duty cycle is used for some tests, continuous operation for others. Both Verification and Endurance Tests are more formal and they require written notification to the NASA Project Manager with pertinent descriptions of the test article. Three designs were submitted for NASA approval and were tested in Phase I of the program In carrying out this type of test, the NASA Project manager reviews the results of the Verification test and decides which items shall undergo Endurance testing.

A statistical summary of the single cell testing accomplished during the four phases of the program to date is presented in Table III.

TABLE III

SINGLE CELL OPERATION SUMMARY

Number of cells tested	39
Number of configurations tested	12
Total cell test time	90,927 hours
Longest cell run (100 ASF) (107.6 ma/cm^2)	10,020 hours
Longest cell run (200 ASF) (215.2 ma/cm^2)	6,680 hours

D. Single Cell Design

This section describes the design of the single cell hardware and the single cell design configurations evaluated during the Phase IV effort. The single cell test unit used to evaluate the results of unitization development for performance and endurance testing, and for the formal NASA Verification and Endurance category of testing was that developed in Phase I. It incorporates the novel features of the EMS design, namely:

- Strip cell – 12.0 x 1.375 inches (30.5 x 3.49 cm) cell area
- Edge current collection
- Improved compatibility frame unitization
- Passive Water Removal
- Minimum thickness flow fields and component parts.

Figure 26 shows the working elements of that cell and illustrates that the design represents a significant improvement compared to the existing state-of-the-art as represented by the cell design used in PSD's PC17 Space Shuttle Powerplant. The direct comparison between the PC17 and the EMS cell is not completely fair since the EMS requirement to remove product water by the passive method requires that an additional subassembly, the passive water removal unit, be added to the EMS cell. Nonetheless, the passive water removal cells tested during this program were only 60 percent as thick as PC17 cells.

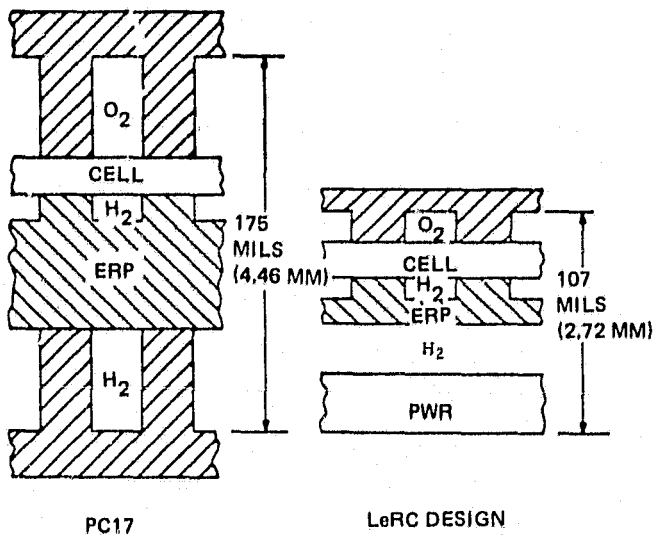

Figure 26 — Size Comparison of Cell Designs Tested

The cell assembly consists of two sections: the unitized electrode assembly (UEA) and a unitized passive water removal unit, shown in Figure 27. These two components can be either bonded together or mated with an elastomer gasket between them to effect the required seal.

The cell test fixtures used during Phase IV were the same as those used in the earlier phases of the program. They are rigid 1/2 inch (1.27 cm) stainless steel plates with provision for sealing and fluid connections. Some of the features of the test fixtures, shown in Figure 28, are:

- Flow field inserts for interchange of field patterns
- O-ring sealing for easy assembly of unitized parts
- Isothermal operation to duplicate EMS Design
- Passive heat rejection for test simplicity
- Nickel plated to avoid corrosion

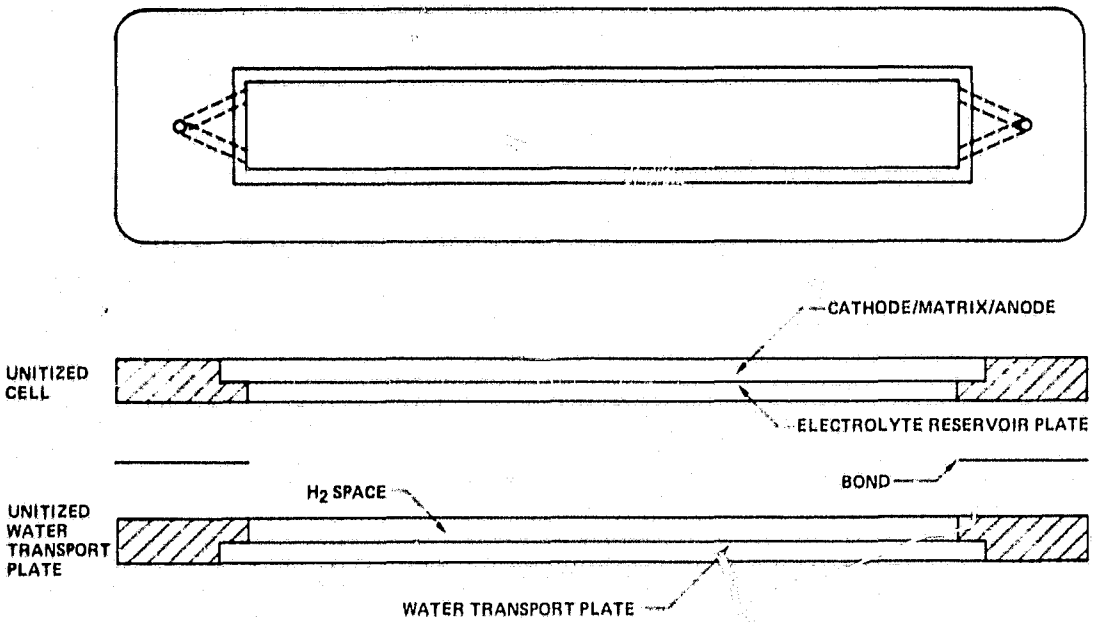

Figure 27 — Single Cell Development Plastic Frame

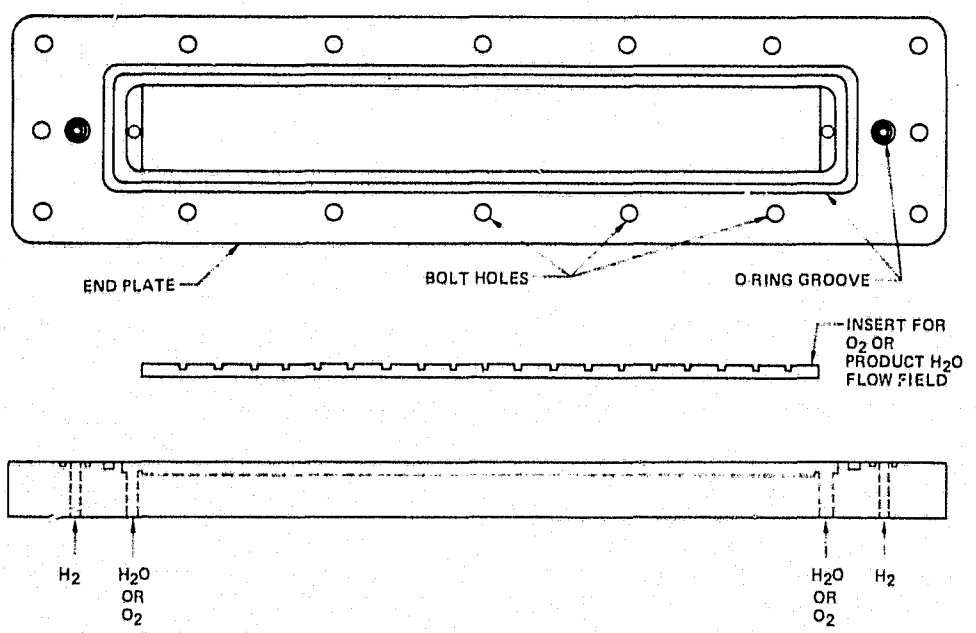

Figure 28 — Single Cell Development Test Fixture

Three thermocouples were installed in each fixture. Readings indicated uniform temperature distribution. Internal thermocouples were placed on electrodes of several cells and the temperature differed from the endplate readings by only 2 or 4°F (1.1 or 2.2°C) at the normal endurance operating conditions of 100 and 200 ASF (107.6 and 215.2 ma/cm^2).

Twelve different NASA-approved designs have undergone development and testing during the program. Their characteristics are summarized in Table IV.

Four of these designs were on test during Phase IV of the program, their configuration is described in detail in Table V.

TABLE IV

SUMMARY OF CELL DESIGNS TESTED

Design No.	UEA Frame	Anode	Cathode	ERP UEA/PWR	Cell #
1	Arylon/Hypon	PPF	PPF	Ni/Ni	12
					13
2	FEP/Teflon	PPF	PPF	Ni/Ni	14
3	Hypon/Matrix	PPF	PPF	Ni/Ni	16
					17
4	TFE/Polypropylene	PPF	PPF	Ni/Ni	21
					22
5	Hypon/Matrix	PPF	90AU-10Pt	Ni/Ni	23
					24
6	Hypon/Matrix	PPF	PPF	Polysulfone/Nickel	25
			90Au-10Pt		27
7	Polysulfone Film	PPF	PPF	Ni/Ni	28
			90Au-10Pt		30
8	Polysulfone/GF Hybrid	PPF 635°F	90Au-10Pt	Ni/Ni	31
					32
9	Polysulfone/GF Hybrid	Supp. Catalyst	90Au-10Pt	Ni/Ni	35
					36
10	Polysulfone/GF Hybrid	Supp. Catalyst	90Au-10Pt	Polysulfone/Polysulfone	38
					39
					39A
11	Polysulfone/GF Hybrid	Supp. Catalyst	80Au-20Pt	Polysulfone/Polysulfone	40
					41
12	Polysulfone/GF Hybrid	PPF	90Au-10Pt	Polysulfone/Polysulfone	42
					43
					44

TABLE V

DESIGN DETAILS OF CELLS TESTED DURING PHASE IV

Cell Number	NASA Design Number	UEA Description	PWR Description	Oxygen Field	Hydrogen Field
35	9	Hybrid Polysulfone/ Epoxy-Glass Fiber Prepreg Frame Construction Supported Catalyst Anode Au-Pt Cathode Ni ERP - 22 mils (0.56 mm)	Hypon-Matrix Frame, 11 mil (0.28-mm) Sintered Ni, 10-mil (0.25-mm) RAM Goretex Membrane	Machined Insert 0.015" (0.38 mm)	Polypropylene Screen 0.033" (0.84 mm)
39A	10	Hybrid Polysulfone/ Epoxy-Glass Fiber Prepreg Frame Construction Supported Catalyst Anode 90 Au-Pt Cathode 30 mil (0.76 mm) Polysulfone ERP	Epoxy-Glass Fiber Frame, 22-mil (0.56-mm) Porous Polysulfone, 20-mil (0.51-mm) RAM Goretex Membrane	Same as 35	Same as 35
40	11	Hybrid Polysulfone/ Epoxy-Glass Fiber Prepreg Supported Catalyst Anode 80 Au-20Pt Cathode 30 mil (0.76 mm) Polysulfone ERP	Same as 39A	Same as 35	Same as 35
41	11	Same as 40	Same as 39A	Same as 35	Same as 35
42	12	Hybrid Polysulfone/ Epoxy-Glass Fiber Prepreg PPF Anode 90Au-10Pt Cathode 30-mil (0.76 mm) Polysulfone ERP Fybex Matrix	Same as 39A	Same as 35	Polypropylene Screen 0.033" (0.84 mm)
43	12	Same as 42	Same as 39A	Same as 35	Teflon Screen 0.028" (0.71 mm)
44	12	Same as 42	Same as 39A except 10-mil (0.25 mm) Matrix at 1323 load hours	Same as 35	Same as 43

E. Single Cell Test Results

This section reviews each of the cell tests conducted during Phase IV. The results of the cell tests are summarized in Table VI.

TABLE VI

FULL SIZE SINGLE CELL TEST SUMMARY

Cell No.	Load Time (Hrs.)	Performance (Volts) Initial	Peak	Final	Initial IR (mv) @ 100 ASF (107.6 ma/cm^2)	Percent Conversion to K_2CO_3	Comments
35	6,500	0.912	0.916	0.820	8	3.9 at 320 hrs. 42 at 6500 hrs.	
39A	2,234	0.846	0.846	0.838	10	3.6 at 304 hrs. 7.2 at 2234 hrs.	Quoted at 200ASF (215.2 ma/cm^2)
40	4,160	0.869	0.880	0.800	8	2.1 at 345 hrs. 18.0 at 4160 hrs.	
41	4,303	0.876	0.880	0.830	13	2.5 at 325 hrs. 15.0 at 4303 hrs.	
42	4,668	0.910	0.911	--	7	9.9 at 342 hrs.	Test Continuing
43	911	0.922	0.922	0.892	9	5.8 at 322 hrs.	Quoted at 27 psia (18.6 n/cm^2), 250°F, (121.1°C) 100ASF (107.6 ma/cm^2)
44	1,757	0.911	0.913	--	9	16.0 at 1323 hrs.	Test Continuing

Cell No. 35

Cell No. 35 featured a hybrid polysulfone – epoxy/glass-fiber frame, nickel ERP, 90Au-10Pt cathode, and supported catalyst anode. The cell was constructed to NASA Verification Design No. 9. The primary test objectives were to evaluate the supported catalyst anodes and to further evaluate hybrid polysulfone frame corrosion resistance. The cell accumulated 6500 hours at 100 ASF, (107.6 ma/cm^2), 180°F, (82.2°C) as shown in Figure 29, before being shut down because of an internal short. Most of the testing of this cell was conducted during Phase III. As reported in the Phase III report, the cell performance was very stable during the initial 5000 hours of testing. The decay rate during this time period was about 8.5 μV/hr., lower than any cell tested up to that time. A summary of cell losses appears in Table VII.

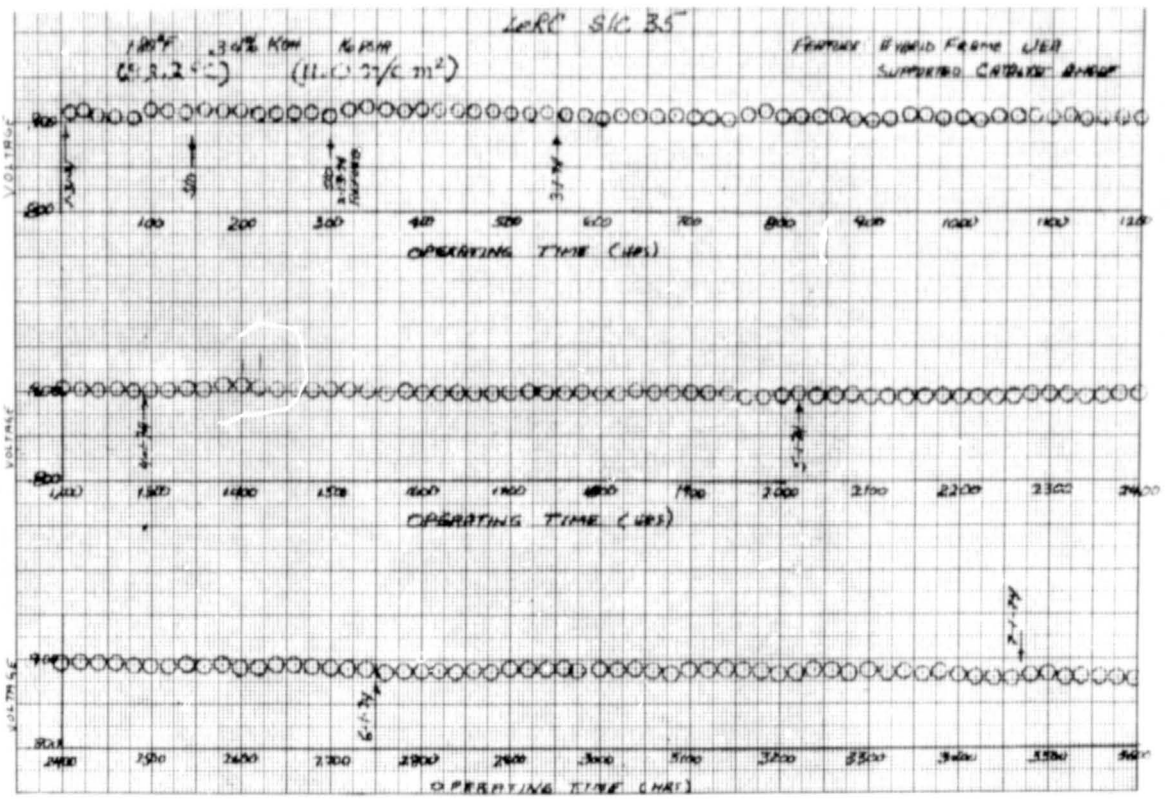

Figure 29 – Cell No. 35 Performance History Sheet 1 of 2

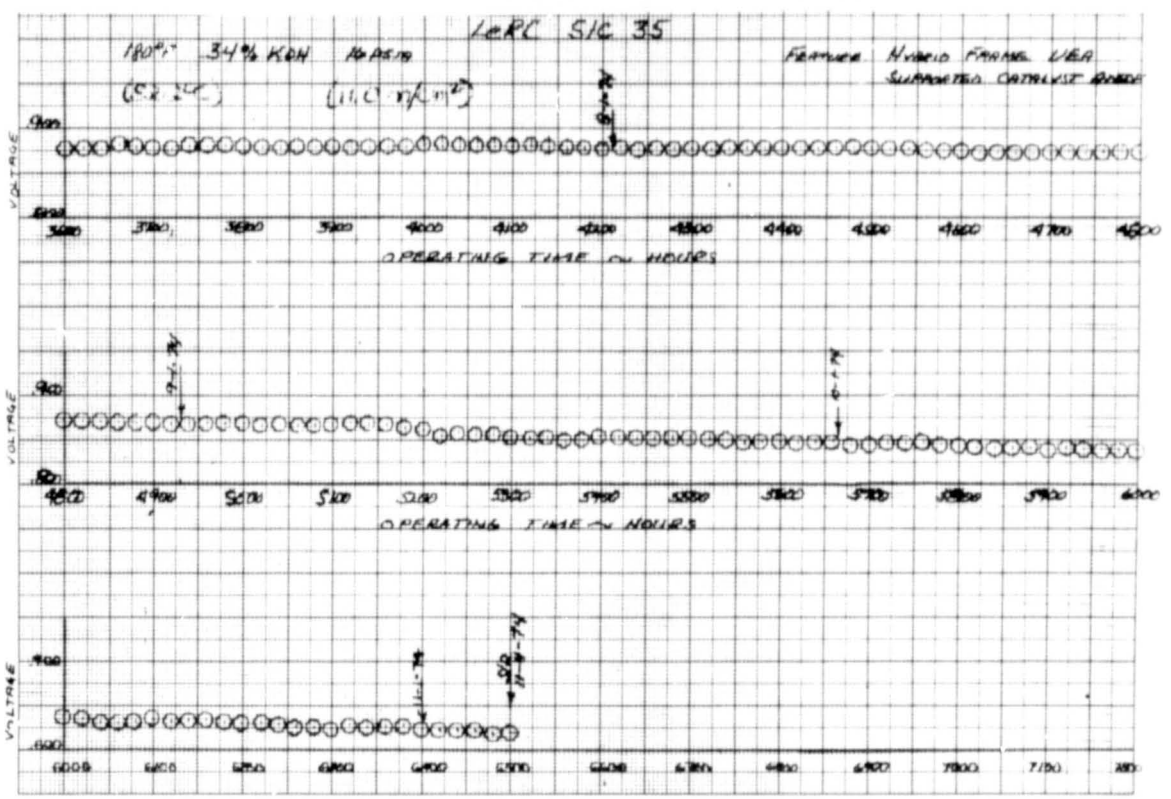

Figure 29 – Cell No. 35 Performance History Sheet 2 of 2

TABLE VII

CELL NO. 35 ACCOUNTABLE LOSSES

Hybrid Polysulfone – Epoxy/Glass Fiber Frame,
90Au-10Pt Cathode,
Supported Catalyst Anode

Rig 38503-35 0.114 Ft^2
180°F(82.2°C)34% KOH/16 psia(11.0 n/cm^2) PWR

	Performance					100 ASF (107.6 ma/cm^2) Diffusion Losses		
Load Time (Hrs.)	1.0 ASF (1.076 ma/cm^2) (Volts)	2.0 ASF (2.152 ma/cm^2) (Volts)	100 ASF (107.6 ma/cm^2) (IR Corr.)	IR Loss 100 ASF (107.6 ma/cm^2) (mv)	Activation Loss (mv)	Total (mv)	Anode (mv)	Cathode (mv)
87	1.035	1.023	0.917	8	–	34	30	4
290	1.038	1.025	0.917	10	–	37	33	4
322	1.041	1.030	0.922	7	–	38	33	5
1020	1.032	1.021	0.913	8	3	35	31	4
1713	1.029	1.017	0.904	8	6	41	37	4
2527	1.027	1.014	0.898	8	8	45	39	6
3360	1.023	1.011	0.887	8	12	48	42	6
4150	1.021	1.008	0.882	8	14	57	49	8
5060	1.013	1.000	0.873	8	22	59	52	7
5697	1.009	0.997	0.854	10	26	72	66	6
6014	1.007	0.994	0.844	8	28	83	77	6
6487	1.005	0.992	0.825	10	30	97	84	13

The low initial performance resulted from higher than normal anode diffusion levels. The bulk of the subsequent cell performance decay was due to increases in anode diffusion and loss of cathode activation. A small but noticeable electrical short appeared at about 4000 hours load time. Diagnostics run at 5697, 6014, and 6487 hours showed substantial increases in anode diffusion losses. In addition, the tolerance excursion at 6008 hours, see Figure 30, showed a characteristic normally associated with an increase in electrolyte carbonate level. The magnitude of the short increased toward the end of testing resulting in deteriorating performance. The results of the final dilute gas diagnostic taken at 6487 hours are presented in Figure 31. The open circuit voltage was depressed as a result of the short to a value of about 0.99V at shutdown.

Post-test analysis of the electrolyte showed 42 percent of the KOH converted to $K_2 CO_3$, see Figure 32. The fact that this level is higher than expected may be the result of the internal short which caused higher local temperatures and corrosion rates. Post-test inspection showed the probable cause of the short to be a misaligned flow field insert which caused excessive pinch at the oxygen inlet.

It was concluded from this test that the supported catalyst anode is a viable electrode for future fuel cell configurations.

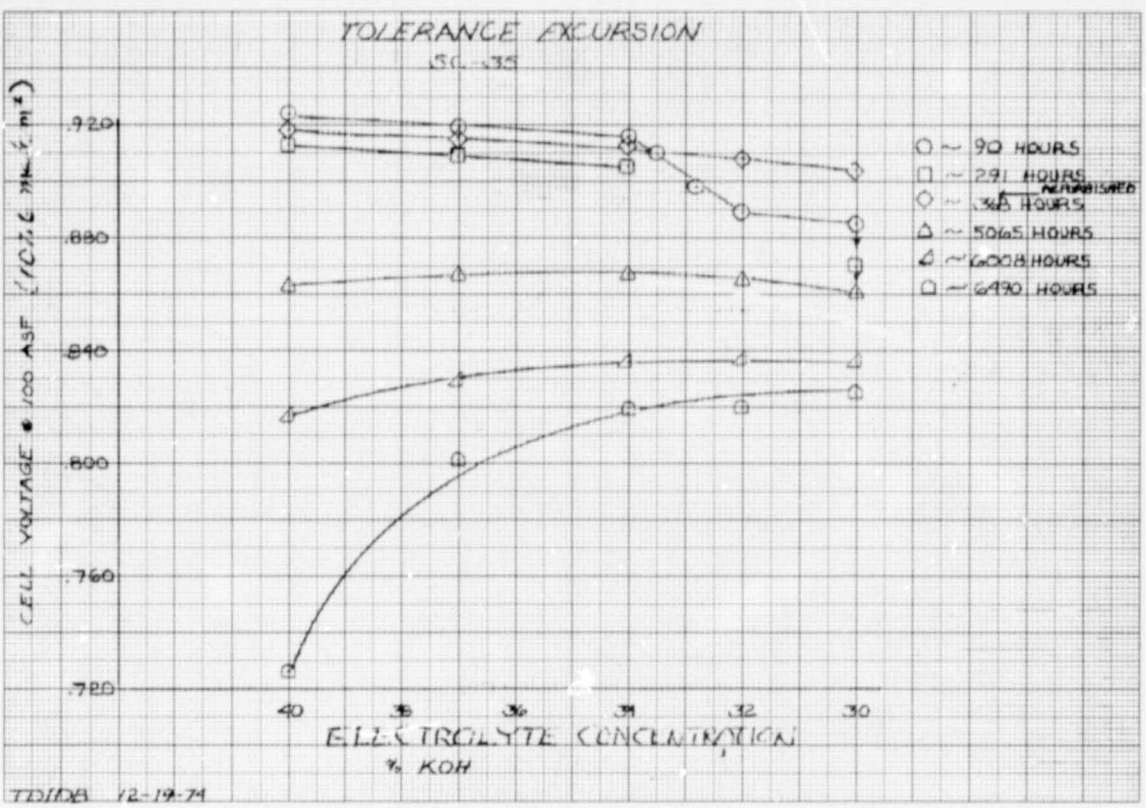

Figure 30 – Cell No 35 Tolerance Excursion Data

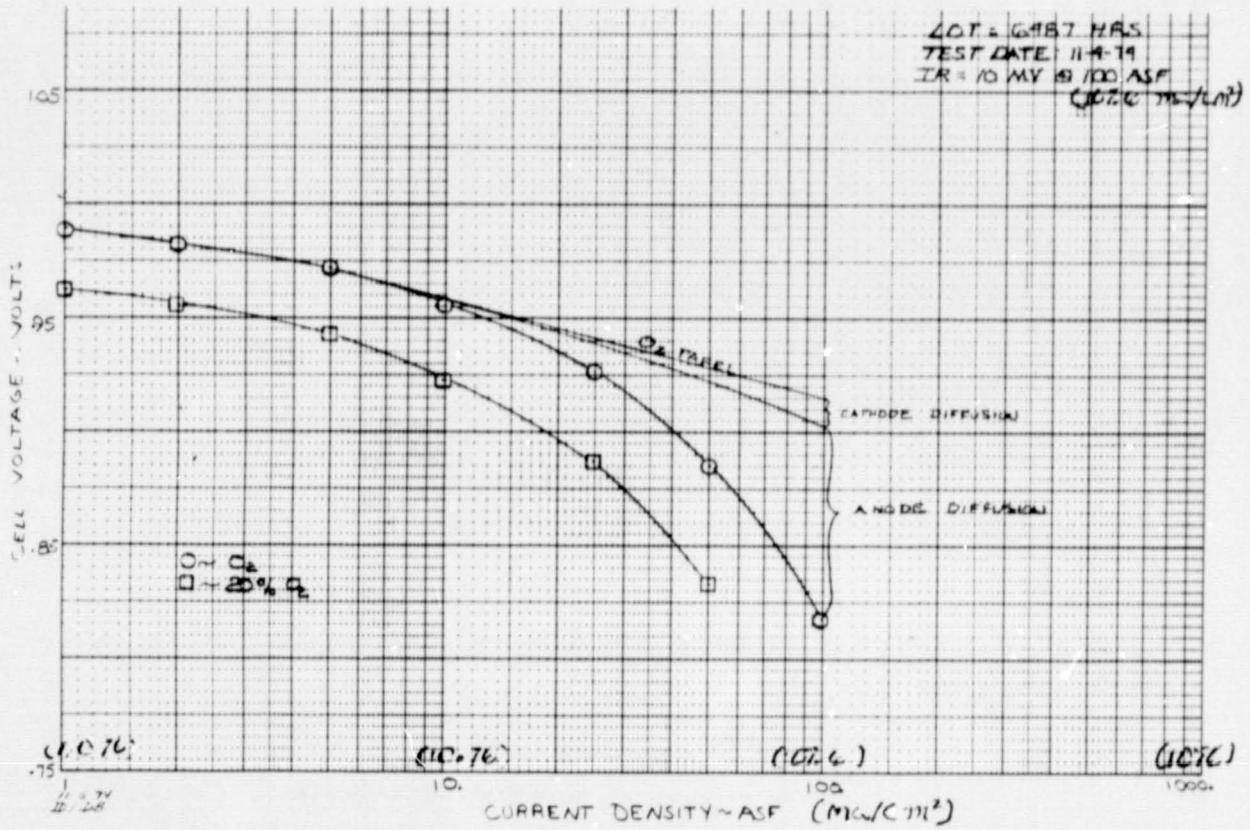

Figure 31 — Cell No. 35 Tafel Characteristics

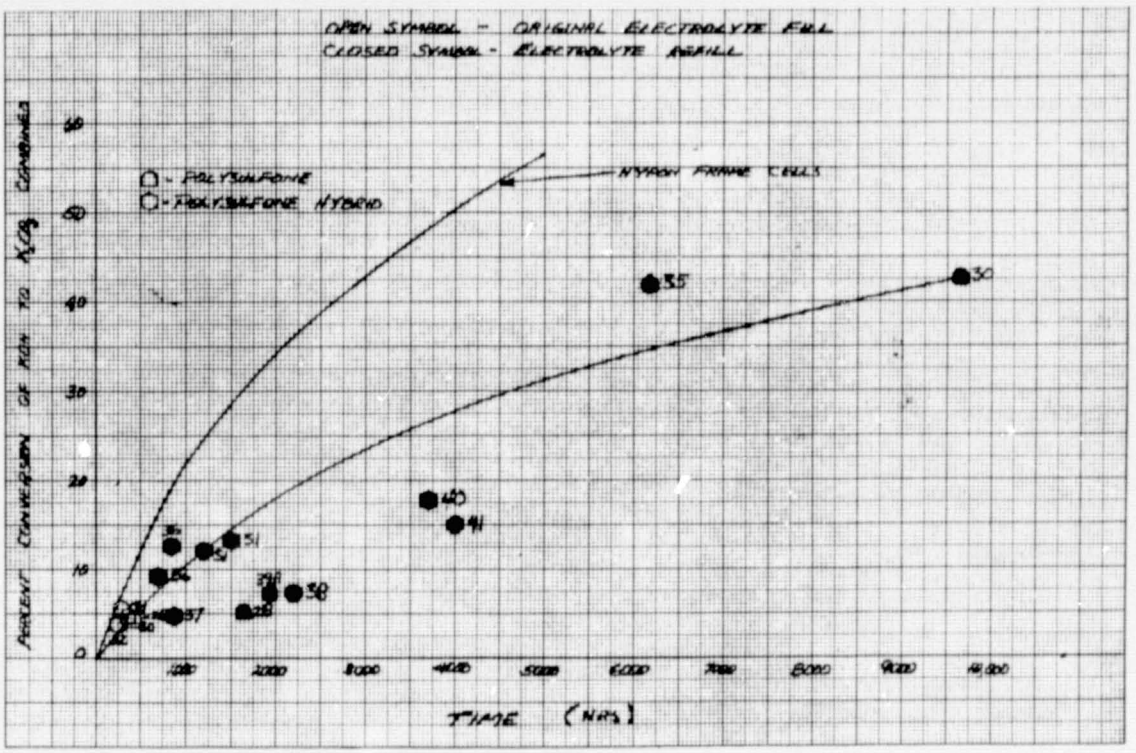

Figure 32 — Electrolyte Carbonation Data

Cell No. 39A

Cell No. 39A featured a 20-mil (0.51-mm) porous polysulfone ERP in the product water removal (PWR) unit and a 30-mil (0.76-mm) polysulfone ERP in the UEA. The UEA frame was of the hybrid polysulfone-epoxy/glass-fiber type and the PWR frame was also made of epoxy/glass fiber. The cathode was 90Au-10Pt and the anode was of the supported catalyst type. The cell was constructed to NASA Verification Design No. 10. which was the first design to incorporate polysulfone ERP's in both the UEA and PWR. Total endurance time on this cell was 2234 hours, 1557 hours of which were accumulated in Phase III. The performance history of this cell is presented in Figure 33. The cell was run at 100 ASF (107.6 ma/cm^2) for its initial 373 hours during which time a refill was required to thoroughly wet the anode. Except for the final 80 hours the remainder of the test was conducted at 200 ASF (215.2 ma/cm^2). Signs of reactant crossover were first noted at 1839 hours during dilute gas diagnostic testing, see Figure 34.

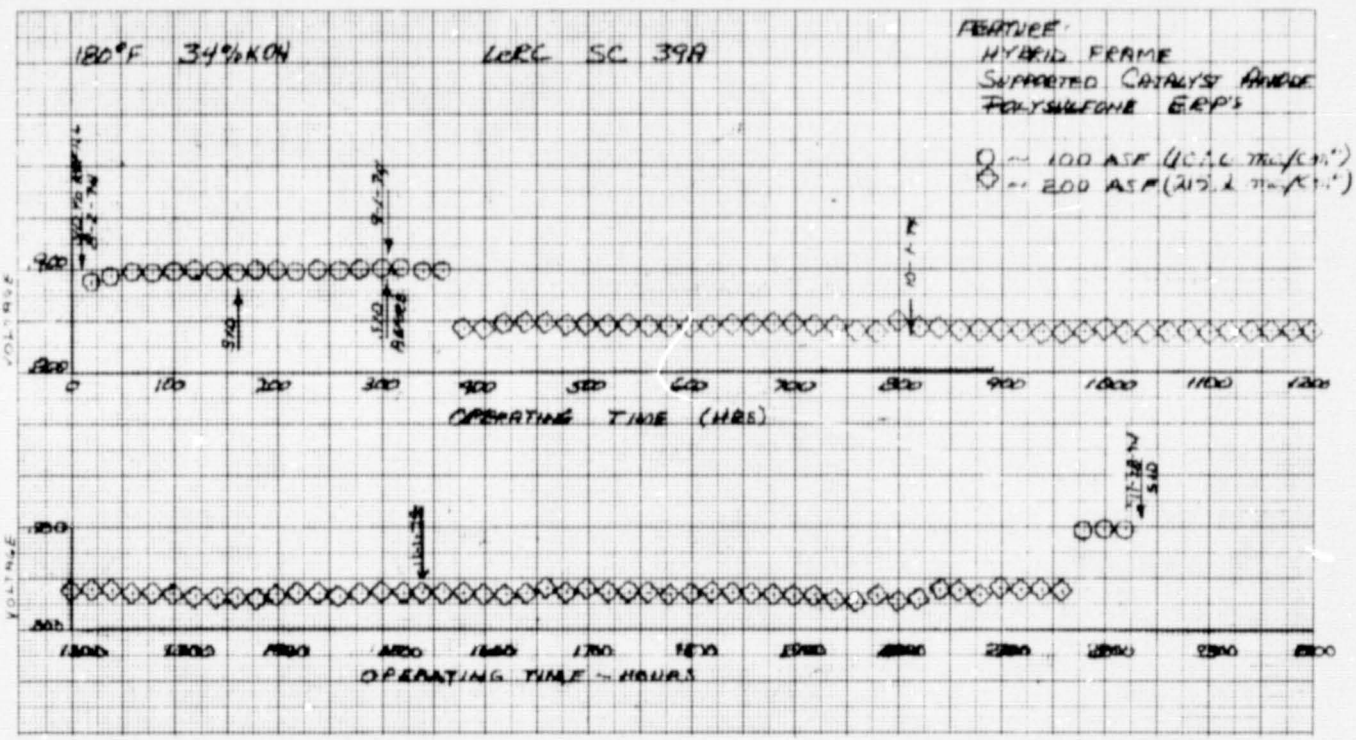

Figure 33 – Cell No. 39A Performance History

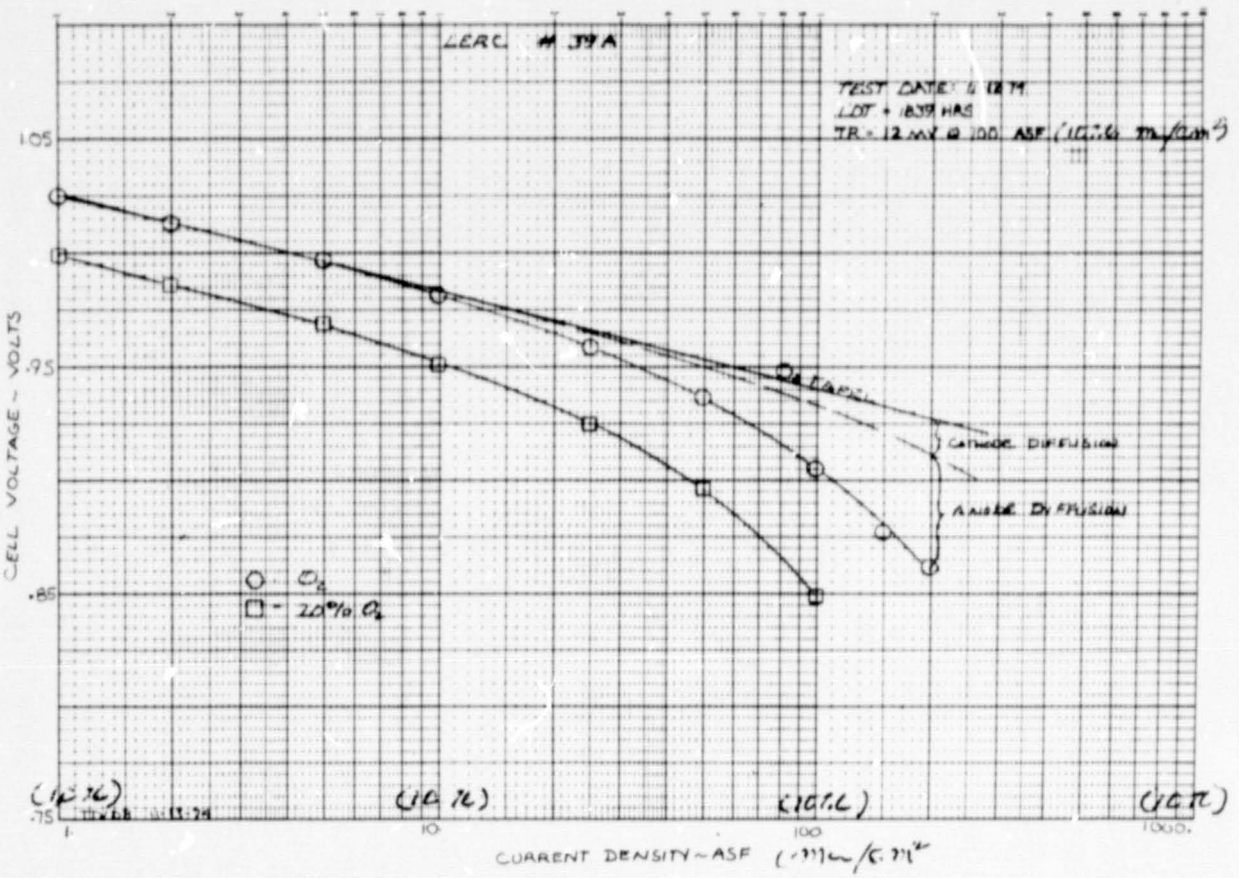

Figure 34 — Cell No. 39A Tafel Characteristics

During the last 300 hours of testing the cell performance became somewhat erratic because of the incipient reactant crossover and the cell load was reduced to 100 ASF (107.6 ma/cm^2) at 2160 hours. At 2234 hours the cell was shut down as the result of reactant crossover. Post-test inspection showed a crack at the matrix-polysulfone – epoxy/glass-fiber interface in the UEA frame near the oxygen inlet port. This was caused by swelling of the triangular epoxy/glass-fiber piece which is part of the oxygen inlet port. The swelling overstessed the frame-matrix bond resulting in the cracking. The problem was resolved in subsequent cells by cutting back the triangular part to eliminate the overlap of the polysulfone area. Accountable losses for this cell are shown in Table VIII. An electrolyte conversion level of 7.2 percent was obtained in post-test analysis and is compared with that of other cells in Figure 32. This level is consistent with other cells of the hybrid frame type.

TABLE VIII

CELL NO. 39A ACCOUNTABLE LOSSES

Hybrid Polysulfone – Epoxy/Glass-Fiber Frame,
90Au-10Pt Cathode,
Supported Catalyst Anode,
Polysulfone ERP's

Rig 38507-39 0.114 Ft^2
180°F(82.2°C)34% KOH/16 psia(11.0n/cm^2)PWR

	Performance					100 ASF (107.6 ma/cm^2) Diffusion Losses			
Load Time (Hrs.)	1.0 ASF (1.076 ma/cm^2) (Volts)	2.0 ASF (2.152 ma/cm^2) (Volts)	100 ASF (107.6 ma/cm^2) (IR Corr.)	IR Loss 100 ASF (107.6 ma/cm^2) (mv)	Activation Loss (mv)	Total (mv)	Anode (mv)	Cathode (mv)	Comments
2	1.023	1.009	0.847	14	–	87	82	5	
118	1.030	1.017	0.914	12	–	25	17	8	After Refill
303	1.031	1.018	0.915	10	–	30	23	7	
324	1.023	1.009	0.906	10	8	30	23	7	After Refurb
1839	1.025	1.013	0.905	12	6	35	28	7	

Cell Nos. 40 and 41

These cells were fabricated with hybrid polysulfone-epoxy/glass fiber frames. Both cells incorporated supported catalyst anodes, 80Au-20Pt cathodes, and polysulfone ERP's. These cathodes, because of higher alloying and surface area characteristics were expected to exhibit the performance and endurance characteristics of 90Au-10Pt cathodes with only half the catalyst loading. This configuration was approved by the NASA Program Manager to be Verification Design No. 11. The objective of the test was to evaluate the stability and performance of 80Au-20Pt cathodes.

Both cells required a refill before good performance was obtained because of the relative hydrophobicity of the anodes. Both cells showed lower 100 ASF (107.6 ma/cm^2) performance levels than previous cells, apparently resulting from the slightly lower cathode activity combined with the higher anode diffusion losses consistent with other supported catalyst anodes.

Cell No. 40

Cell No. 40 accumulated 4160 hours at 100 ASF (107.6 ma/cm^2), 180°F (82.2°C). Operating test results are presented in Figure 35. Anode diffusion losses after the initial refill and subsequent refurbishment were stable but higher than normal through the first 2000 hours of testing, see Table IX. After 3500 hours the diffusion level began to rise, probably because of increasing flooding of the anode. Losses in activation level and cathode and anode diffusion increased after this time, but the largest contributor to cell voltage loss was anode diffusion. Total activation losses of the 80Au-20Pt cathode were comparable to those experienced on the 90Au-10Pt cathode although diffusion losses were somewhat higher. Intermittent problems with a leaking PWR assembly were apparent, especially on days when atmospheric pressure was quite low resulting in dry conditions. An automatic cell shutdown was experienced due to PWR crossover at a cell load time of 4075 hours. Refilling the cell sealed the PWR assembly,

but subsequent testing revealed considerable increase in anode diffusion level, probably caused by increased anode wetting due to the refill. The cell was then shut down at 4160 hours because of poor performance. Teardown inspection revealed no mechanical difficulties with the assembly. However, one portion of the PWR assembly appeared quite dry. Final carbonate analysis showed 18 percent conversion of the electrolyte over a 3735 hour period, see Figure 32.

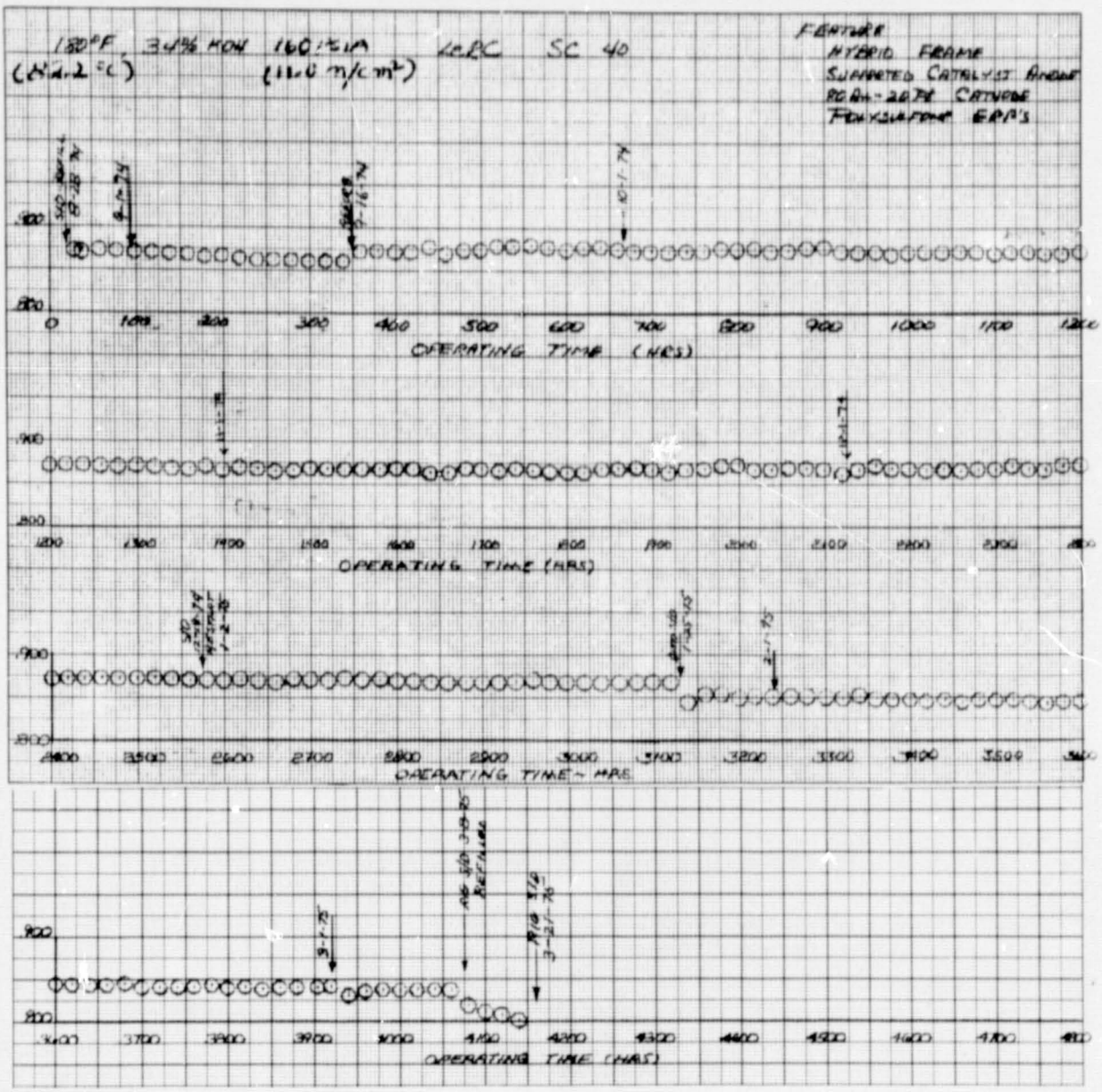

Figure 35 – Cell No. 40 Performance History

TABLE IX

CELL NO. 40 ACCOUNTABLE LOSSES

Hybrid Polysulfone – Epoxy/Glass Fiber Frame,
80Au-20Pt Cathode,
Supported Catalyst Anode,
Polysulfone ERP's

RIG 38740-40 0.114 Ft^2
180°F (82.2°C) 34% KOH/16 PSIA (11.0n/cm^2) PWR

	Performance					100 ASF (107.6 ma/cm^2) Diffusion Losses			
Load Time (Hrs.)	1.0 ASF (1.076 ma/cm^2) (Volts)	2.0 ASF (2.152 ma/cm^2) (Volts)	100 ASF (107.6 ma/cm^2) (IR Corr.)	IR Loss 100 ASF (107.6 ma/cm^2) (mv)	Activation Loss (mv)	Total (mv)	Anode (mv)	Cathode (mv)	Comments
18	1.029	1.015	0.835	8	–	104	93	11	
32	1.029	1.016	0.880	8	–	67	55	12	Refilled
335	1.019	1.007	0.867	9	10	64	55	9	
367	1.018	1.005	0.882	10	11	49	41	8	After Refurb.
1018	1.016	1.004	0.881	10	13	53	45	8	
1930	1.016	1.004	0.877	11	13	54	45	9	
2501	1.020	1.008	0.883	12	9	53	43	10	
3990	1.015	1.002	0.852	16	14	80	63	17	
4100	1.008	0.995	0.816	13	21	107	83	24	After Refill

Cell No. 41

Cell No. 41 was constructed to the same configuration as Cell No. 40, and was the second cell of NASA Verification Design No. 11. The performance characteristics throughout the test were similar to Cell Nos. 39A and 40. All three cells had anodes made with catalyst from the same lot. The cell accumulated 4303 hours before being shut down because of reactant crossover, see Figure 36. The diagnostic tests performed on this cell are summarized in Table X. Anode diffusion losses were at a minimum after cell refurbishment, but increased significantly as the test progressed. Initial testing of the cell indicated as incomplete anode fill and improvement in anode diffusion loss was seen after the initial fill and subsequent refurbishment. The final dilute gas diagnostic at 3870 hours is presented in Figure 37.

TABLE X

CELL NO. 41 ACCOUNTABLE LOSSES

Hybrid Polysulfone – Epoxy/Glass-Fiber Frame,
80Au-20Pt Cathode,
Supported Catalyst Anode,
Polysulfone ERP's

Rig 38750-41 0.114 Ft^2
180°F (82.2°C)/34% KOH/16 PSIA (11.0n/cm^2/PWR

	Performance					100 ASF (107.6 ma/cm^2) Diffusion Losses			
Load Time (Hrs.)	100 ASF (107.6 ma/cm^2) (Volts)	2.0 ASF (2.152 ma/cm^2) (Volts)	100 ASF (107.6 ma/cm^2) (IR Corr.)	IR Loss 100 ASF (107.6 ma/cm^2) (mv)	Activation Loss (mv)	Total (mv)	Anode (mv)	Cathode (mv)	Comments
14	1.027	1.013	0.815	15	–	130	120	10	
62	1.026	1.011	0.889	14	1	49	42	7	After Refill
322	1.022	1.010	0.888	14	5	42	37	5	
347	1.026	1.014	0.901	13	1	40	33	7	After Refurb.
1527	1.029	1.009	0.888	14	5	51	40	11	
2338	1.014	1.002	0.877	15	13	55	45	10	
3870	1.013	1.001	0.862	16	14	73	56	17	

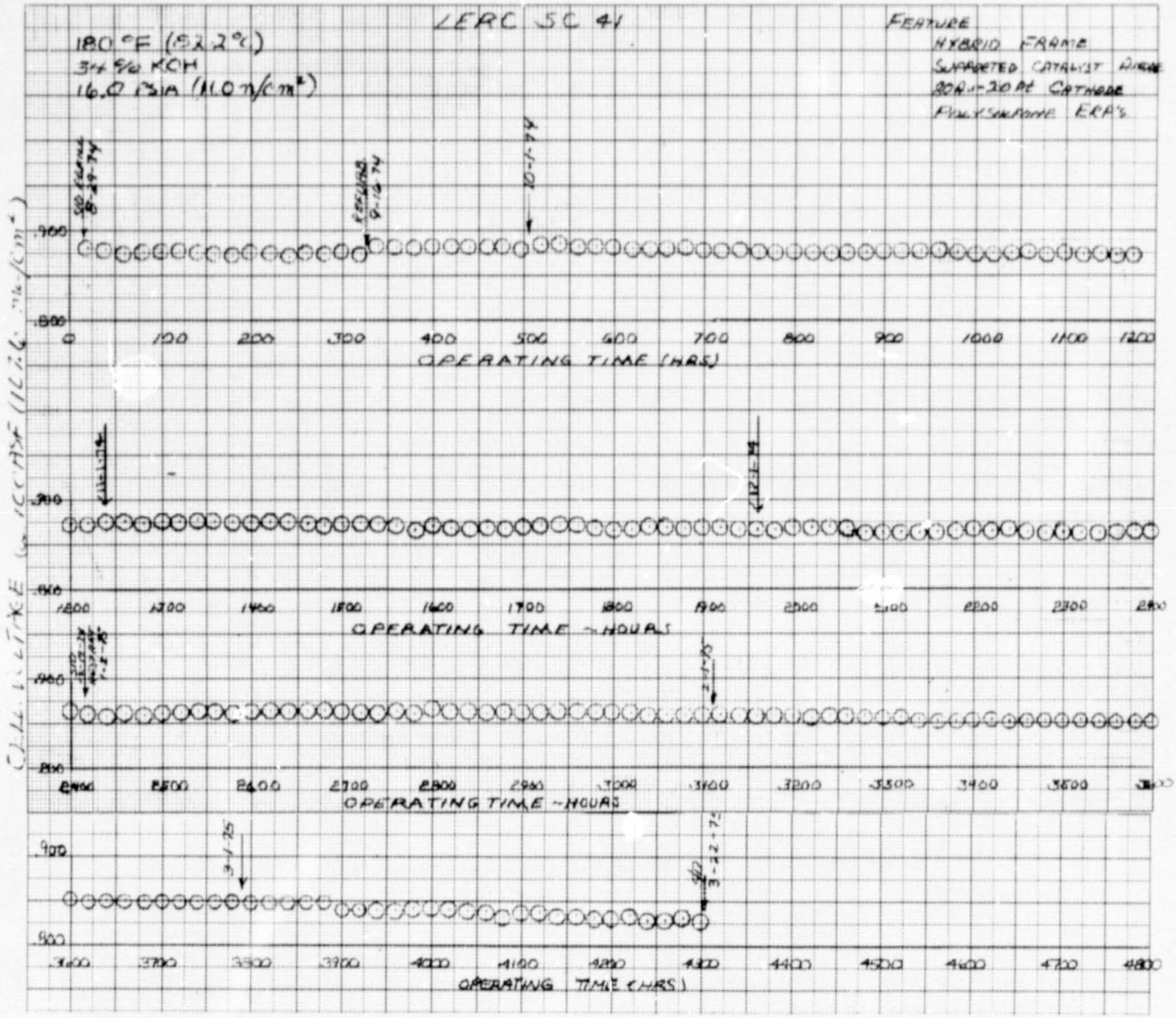

Figure 36 – Cell No. 41 Performance History

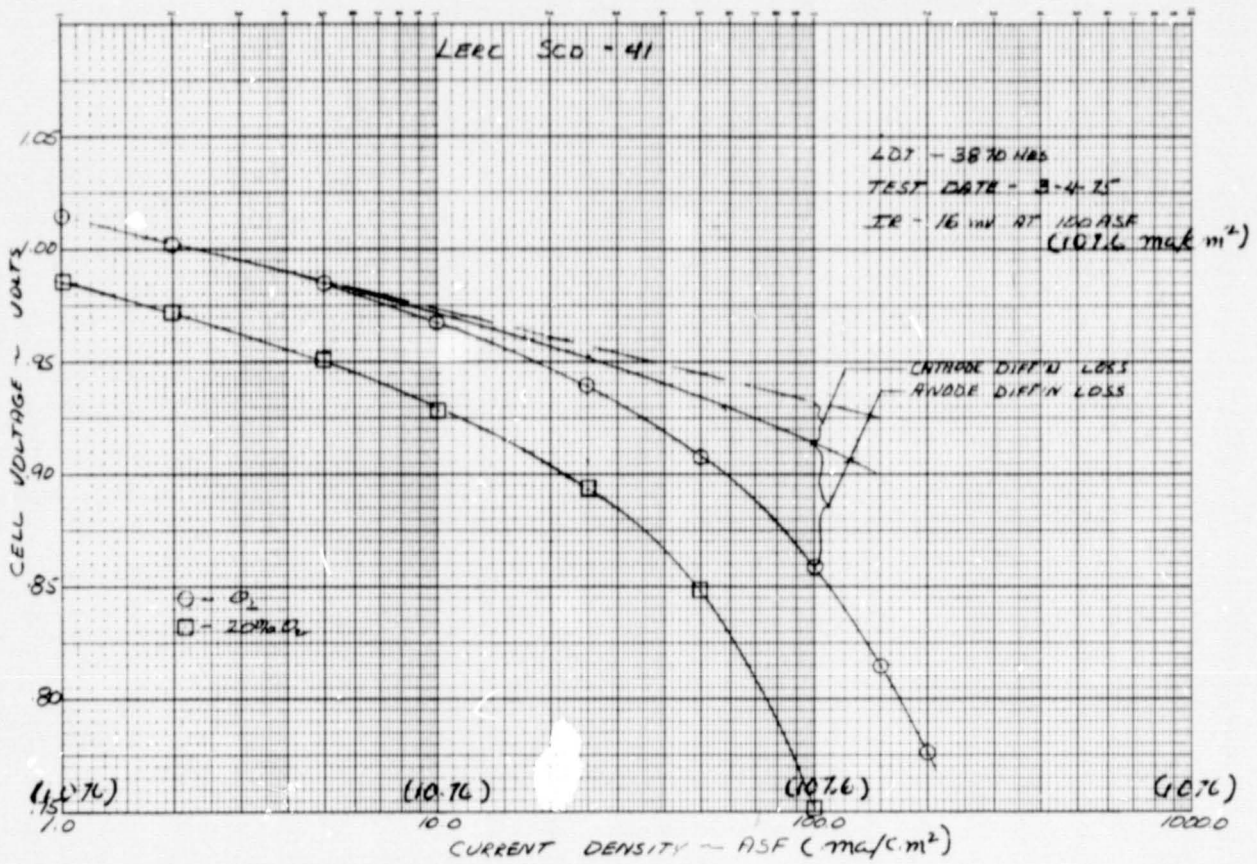

Figure 37 – Cell No. 41 Tafel Characteristics

Again, the activation losses of the 80Au-20Pt cathode compares favorably with the 90Au-10Pt experience.

Teardown of the cell revealed cracking of the polysulfone frame adjacent to the matrix at the hydrogen exit. This was apparently the result of shearing caused by an oversized rubber gasket pressing on this area. Post-test analysis showed a KOH conversion level of 15 percent as shown in Figure 32.

Cell Nos. 42, 43, and 44

These cells were fabricated with hybrid polysulfone – epoxy/glass-fiber frame with standard PPF anodes, 90Au-10Pt cathodes, polysulfone ERP's and Fybex matrices. This configuration was approved by the NASA Program Manager as Verification Design No. 12. The objective of the test was to evaluate the endurance characteristics of Fybex-matrix cells. Use of the Fybex matrix was expected to improve the endurance characteristics of these cells. During Phase III, silicates in asbestos were found to produce, over very long operating periods, silicon containing deposits on the anode which caused anode flooding and performance degradation.

Cell No. 42

During the contract period Cell No. 42 accumulated 4405 hours at 100 ASF (107.6 ma/cm^2), 180°F (82.2°C). The operating test results are shown in Figure 38. During the first 800 hours of testing the cell lost 18 mV at 100 ASF (107.6 ma/cm^2). Review of the cell's activation loss and diffusion losses, see Table XI, showed that compared with earlier cells, the activation losses were high. Since the electrodes were standard and the only difference in ths cell was the Fybex matrix, a poisoning effect was suspected. The laboratory cell tests, see Section III A2). of matrices to confirm this theory. However, after 800 hours the performance stabilized and the decay rate was less than 1μV/hour. The overall decay rate was only 6μV/hour which is the lowest long-term decay rate for any cell in the LeRC series. The stabilization of the anode diffusion losses is the primary difference between this cell and other comparable long-term endurance cells. Its improved stability is apparently due to the absence of silicon in the Fybex matrix. The electrolyte tolerance response shown in Figure 39, remained normal throughout the test. The test is continuing at 100 ASF, (107.6 ma/cm^2) 180°F (82.2°C).

TABLE XI

CELL NO. 42 ACCOUNTABLE LOSSES

Hybrid Polysulfone – Epoxy/Glass-Fiber Frame,
90Au-10Pt Cathode, PPF Anode
Polysulfone ERP's
Fybex Matrix

Rig 38901-42 0.114 Ft^2
180°F (82.2°C)/34% KOH/16 PSIA (11.0n/cm^2)/PWR

	Performance					100 ASF (107.6 ma/cm^2) Diffusion Losses		
Load Time (Hrs.)	1.0 ASF (1.076 ma/cm^2) (Volts)	2.0 ASF (2.152 ma/cm^2) (Volts)	100 ASF (107.6 ma/cm^2) (IR Corr.)	IR Loss 100 ASF (107.6 ma/cm^2) (mv)	Activation Loss (mv)	Total (mv)	Anode (mv)	Cathode (mv)
21	1.024	1.012	0.917	7	–	13	10	3
320	1.019	1.006	0.907	7.5	5	18	11	7
482	1.020	1.007	0.905	6.0	4	19	11	8
846	1.018	1.004	0.898	6.2	6	21	16	5
2018	1.017	1.003	0.894	6.0	7	25	19	6
2524	1.019	1.005	0.895	7.0	5	25	18	7
3767	1.019	1.006	0.896	7.0	5	27	17	10

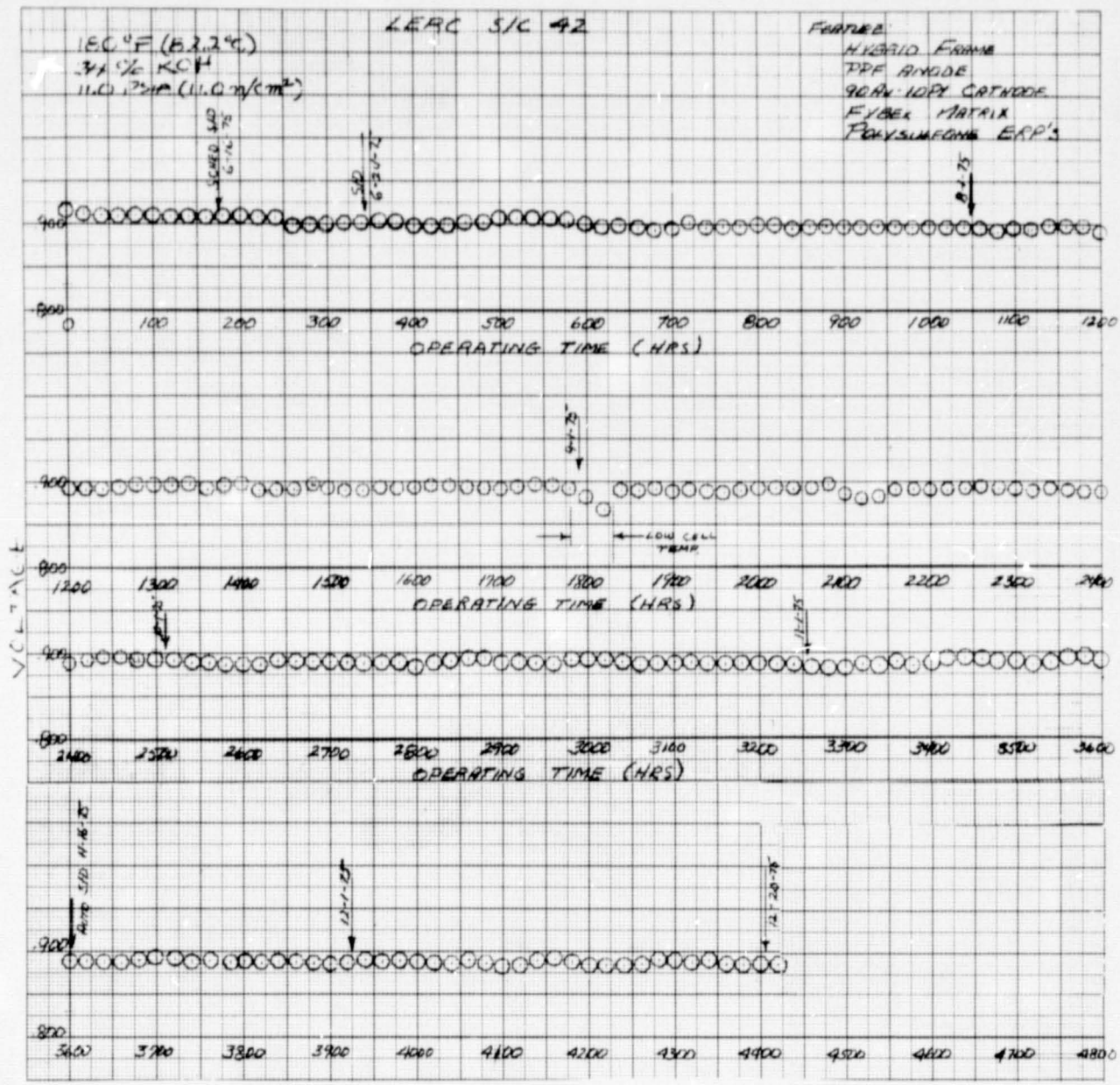

Figure 38 — Cell No. 42 Performance History

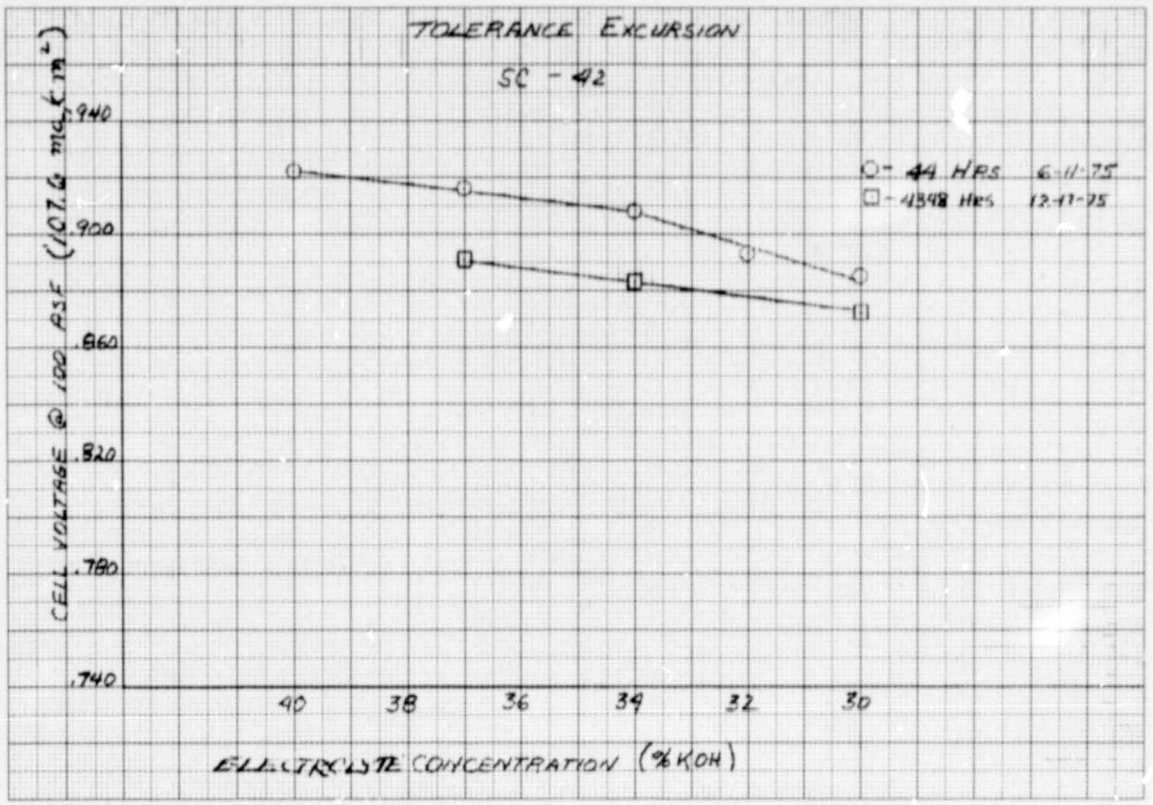

Figure 39 — Cell No. 42 Tolerance Excursion Data

Cell No. 43

Cell No. 43 was run for a total of 911 hours at 100 ASF (107.6 ma/cm^2) during Phase IV program. Of this total, 541 hours of test were accumulated at 250°F (121.1°C) and 27 psia (18.6n/cm^2) with atmospheric product water removal. The remaining load hours were at the standard 180°F (82.2°C) and 16 psia (11.0n/cm) conditions. The cell operating test results are presented in Figure 40.

As in Cell No. 42, the initial cathode activity level was somewhat low and was again attributed to some interaction of Fybex matrix wetting agent and cathode catalyst. During the initial 300 hour verification period, at 180°F (82.2°C) and 16 psia (11.0n/cn^2) full diagnostic tests were performed which showed results similar to those of Cell No. 42, both in electrode activation and diffusion losses, see Table XII, and cell tolerance response, see Figure 41. Following electrolyte refuel, cell conditions of 250°F (121.1°C) and 27 (18.0n/cm^2) psia were set. This resulted in a performance gain of about 5mV at 100 ASF (107.6ma/cm^2), see Figure 42, at the new conditions; however, the cell voltage was quite sensitive to reactant gas flow rates as well as to pressure in the water removal passage. This apparently was a function of the high level of water vapor pressure relative to the reactant pressure at these conditions. Other than this problem, the operation of the water removal unit under these conditions was quite satisfactory. At 664 hours, the cell was shut down because of passive water removal unit crossover. The carbonate level was found to be 7.6 percent, see Figure 43, after the 250°F (121.1°C) testing; this level is somewhat higher than equivalent cells run at 180°F (82.2°C). A check of the PWR, after soaking in water for carbonate analysis, showed no indication of crossover. Teardown of the cell showed excessive pinch on the cell, but, since PWR crossover was eliminated with a water soak, it was concluded that inlet drying may have been responsible for the crossover. The cell was rebuilt with a new PWR assembly and reduced pinch. A thin nickel foil was incorporated into the cell at the hydrogen inlet port to avoid direct impingement of gas and its possible drying effect on the PWR.

The restart of Cell No. 43 showed poor performance response at 180°F (82.2°C) and 16 psia (11.0n/cm^2). Cell diagnostics indicated the major loss to be anode diffusion, see Figure 44 and Table XII. Changing test conditions to 250°F (121.1°C) and 27 psia (18.0n/cm^2) reduced anode diffusion from 131mV to 40mV but this level was still higher than seen before the shutdown at these conditions. Cell testing continued to 911 total load hours when an automatic shutdown caused by PWR crossover terminated testing.

Post-test inspection and analysis of the cell electrode revealed anode flooding and reduced cathode activity, see Section IIIA1. However, the frame areas showed little effect of the prolonged high temperature testing.

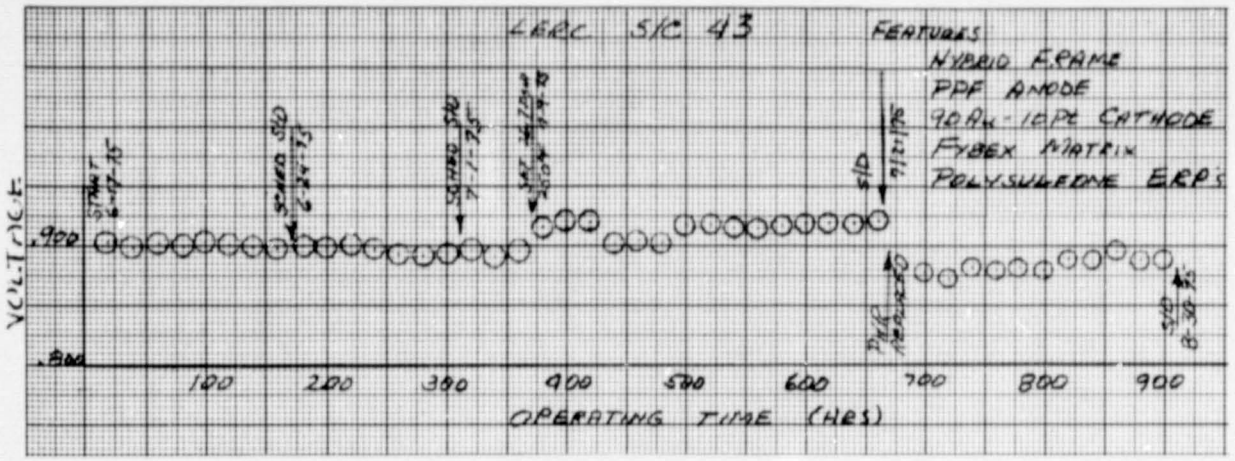

Figure 40 — Cell No. 43 Performance History

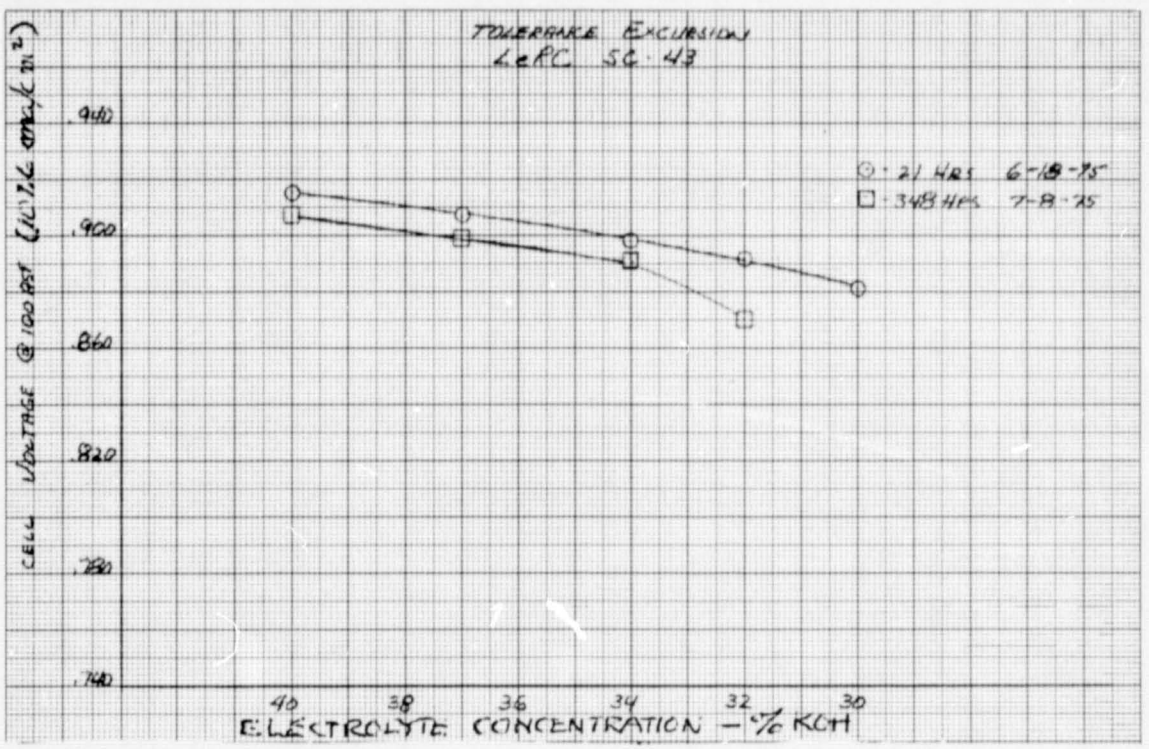

Figure 41 — Cell No. 43 — Tolerance Excursion Data

TABLE XII

CELL NO. 43 ACCOUNTABLE LOSSES

Hybrid Polysulfone – Epoxy/Glass-Fiber Frame,
90Au-10Pt Cathode, PPF Anode
Polysulfone ERP's
Fybex Matrix

Rig 38913-43 0.114 Ft^2
180°F(82.2°C)/34%KOH/16 PSIA(11.0 n/cm^2)/PWR

Load Time (Hrs.)	Performance 1.0 ASF (1.076 ma/cm^2) (Volts)	2.0 ASF (2.152 ma/cm^2) (Volts)	100 ASF (107.6 ma/cm^2) (IR Corr.)	IR Loss 100 ASF (107.6 ma/cm^2) (mv)	Activation Loss (mv)	100 ASF (107.6 ma/cm^2) Diffusion Losses Total (mv)	Anode (mv)	Cathode (mv)
18	1.027	1.015	0.978	9	–	20	14	6
310	1.023	1.010	0.907	8	4	25	18	7
344	1.024	1.011	0.902	9	3	29	25	4
389	1.038	1.024	0.927	7.0	+11	12	5	7*
682	1.013	1.001	0.781	10	14	143	131	12*
800	1.033	1.020	0.877	9	+6	46	40	6**

*250°F(121.1°C), 27 psia (18.0n/cm^2)
**250°F(121.0°C), 29 psia (10.9n/cm^2)

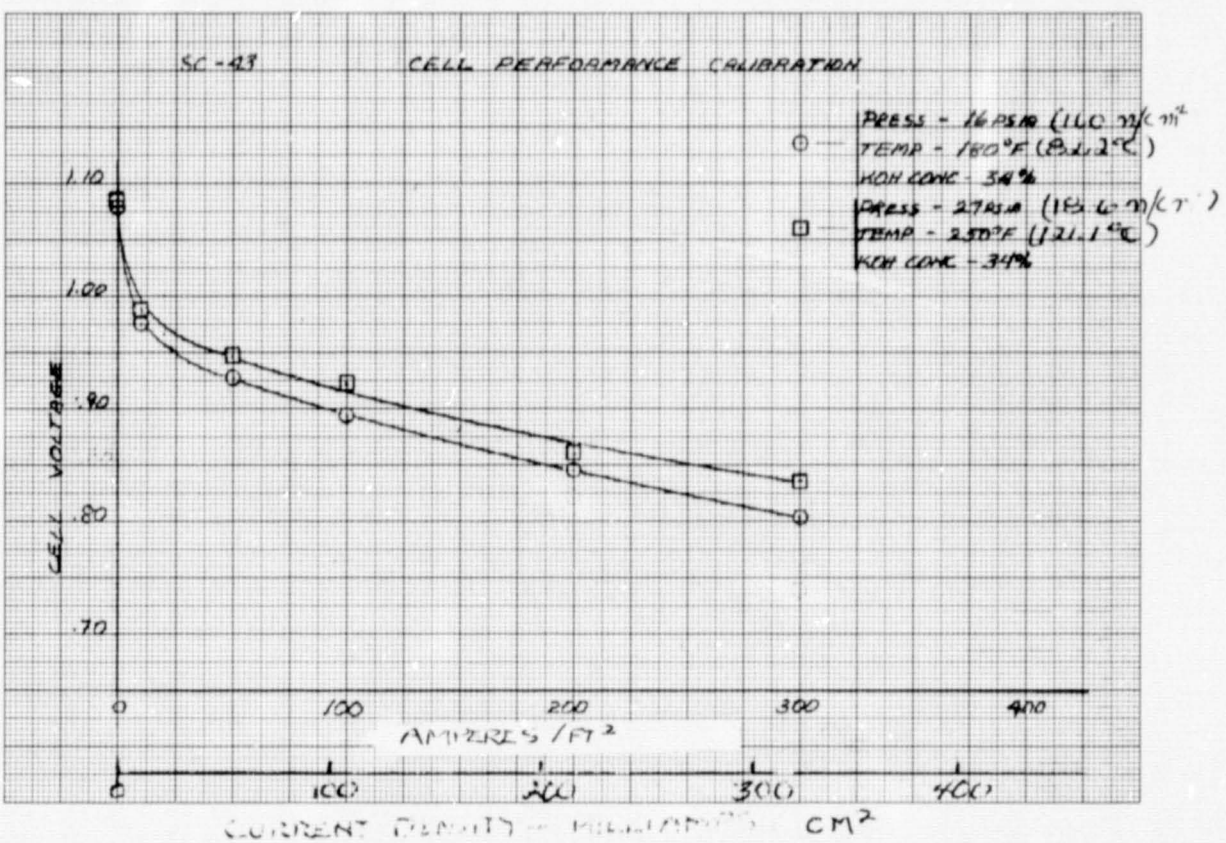

Figure 42 – Cell No. 43 Performance Calibration

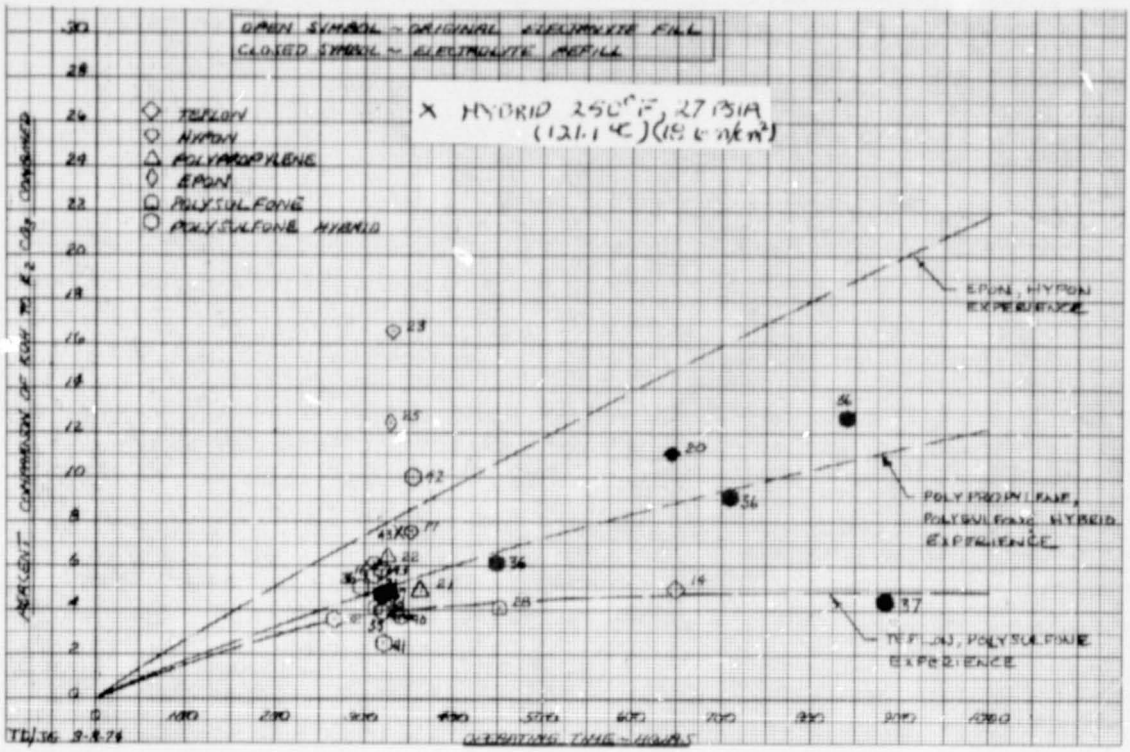

Figure 43 – Electrode Carbonation Data

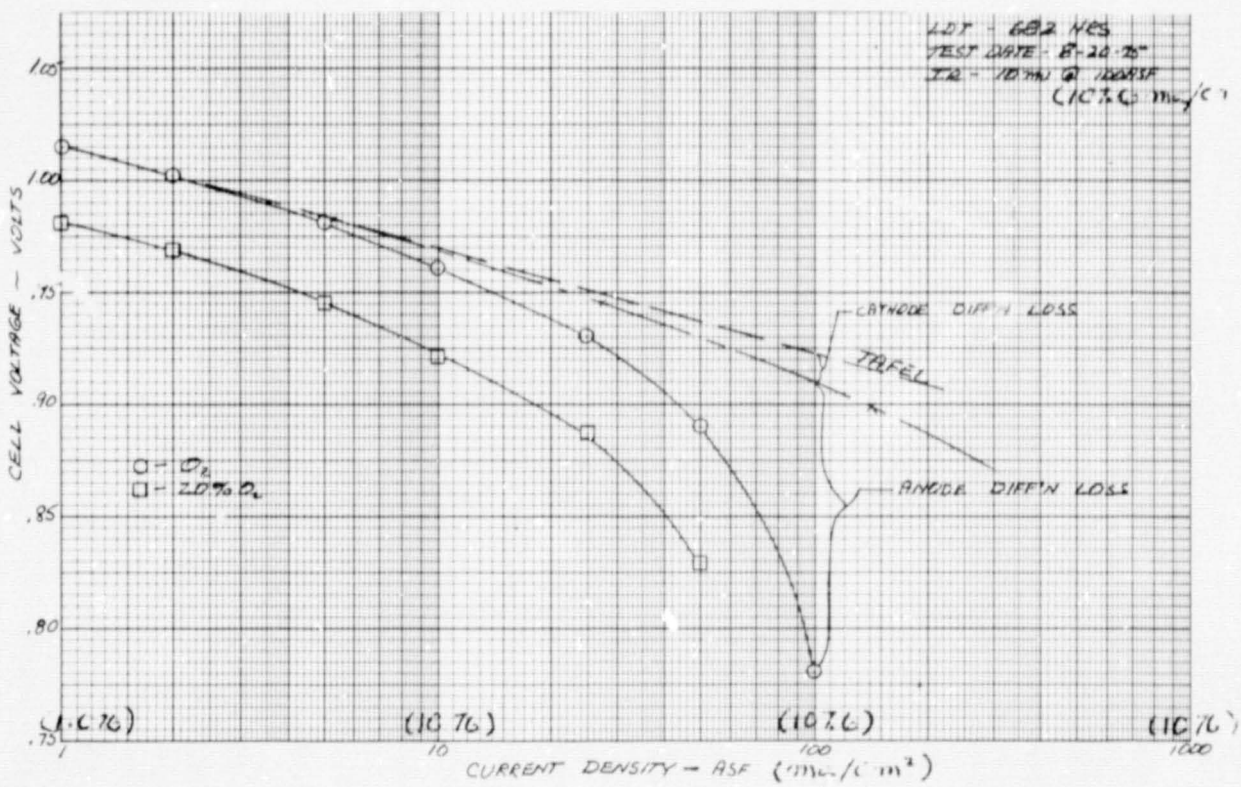

Figure 44 – Cell No. 43 – Tafel Characteristics

Cell No. 44

Cell No. 44 was assembled for testing as a replacement for Cell No. 43. This cell's matrix was fabricated with no Triton wetting agent to eliminate any possibility of electrode poisoning from this source. The operating test results of this cell to date are shown in Figure 45, and a compilation of accountable losses is shown in Table XIII. Complete diagnostics of the cell indicated good tolerance response and normal anode diffusion, see Figure 46. However, the elimination of the use of triton in the Fybex filtering did not result in any significant gain in initial activity level. The initial cell decay characteristic was similar to that of Cell No. 42 although the total decay before stability occurred was reduced by 5 mV, see Figure 47. Most of the loss was in the activation region. As in Cell No. 42, the performance stabilized at about 800 to 1000 hours. At 1322 hours an automatic shutdown occurred and was traced to PWR crossover during a time of low barometric pressure. The electrolyte carbonate analysis showed 16 percent conversion to K_2CO_3, see Figure 48. It should be noted that this cell was not refilled after its Verification Test which accounts for its slightly higher than normal conversion value. As with Cell No. 43, the water soak for the carbonate analysis had the effect of sealing the PWR so that no crossover was evident. A review of past cell shutdown histories showed that PWR crossover occurred only in cells, running under normal conditions, with polysulfone ERP's where the PWR matrix/ERP thickness ratio was 1 to 1. Calculations confirmed that a cell with this combination in the PWR might be marginal on dry-side tolerance with a moderate amount of carbonate in the electrolyte, see Figure 49. To ensure that the PWR ERP remained at least 20 percent filled at all times the cell was rebuilt with a 10-mil (025-mm) matrix and 20-mil (0.51-mm) ERP in the PWR. When returned to test, the cell restarted with no problems and diagnostic testing showed the cell behavior to be normal. Total load time at the end of the contract period was 1719 hours at 100 ASF, (107.6 ma/cm^2) 180°F (82.2°C). The test is continuing.

TABLE XIII

CELL NO. 44 – ACCOUNTABLE LOSSES

Hybrid Polysulfone – Epoxy/Glass-Fiber Frame,
90Au-10Pt Cathode, PPF Anode
Polysulfone ERP's
Fybex Matrix

Rig 38956-44 0.114 Ft^2
180°F (82.2°C/34%KOH/16 PSIA (11.0n/cm^2)/PWR

	Performance					100 ASF (107.6 ma/cm^2) Diffusion Losses			
Load Time (Hrs.)	1.0 ASF (1.076 ma/cm^2) (Volts)	2.0 ASF (2.152 ma/cm^2) (Volts)	100 ASF (107.6 ma/cm^2) (IR Corr.)	IR Loss 100 ASF (107.6 ma/cm^2) (mv)	Activation Loss (mv)	Total (mv)	Anode (mv)	Cathode (mv)	Comments
21	1.026	1.013	0.920	9	–	20	13	7	
515	1.017	1.004	0.907	10	9	23	17	6	
1345	1.026	1.013	0.918	9	–	19	12	7	PWR Replaced

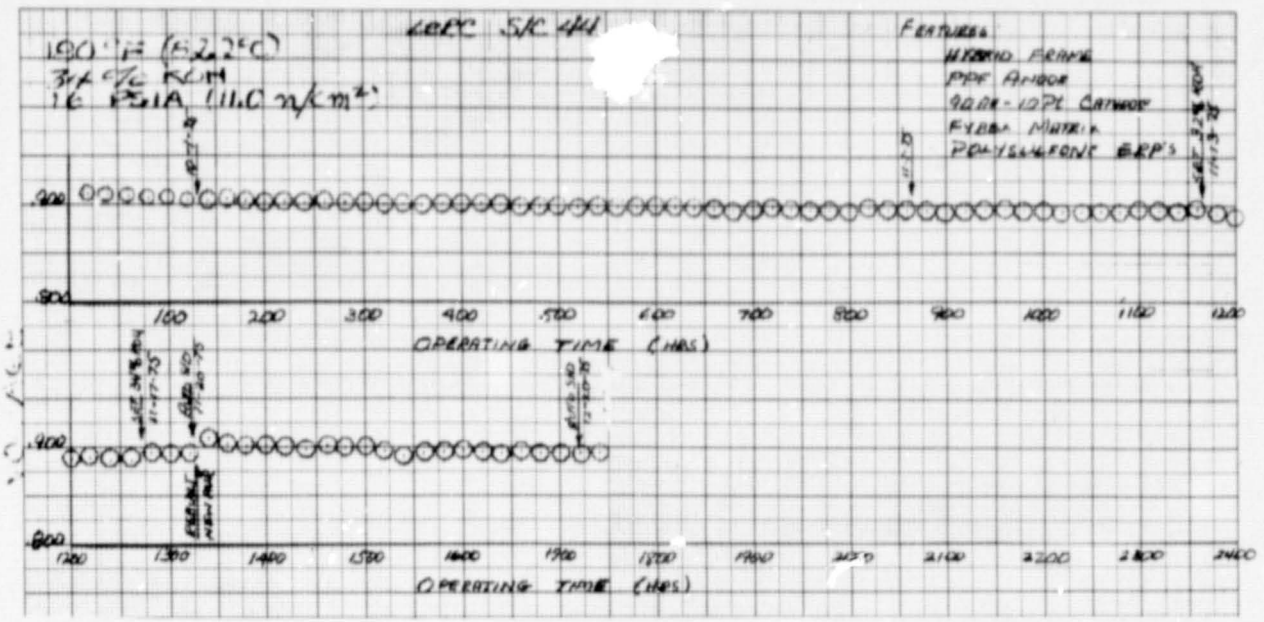

Figure 45 – Cell No. 44 Performance Calibration

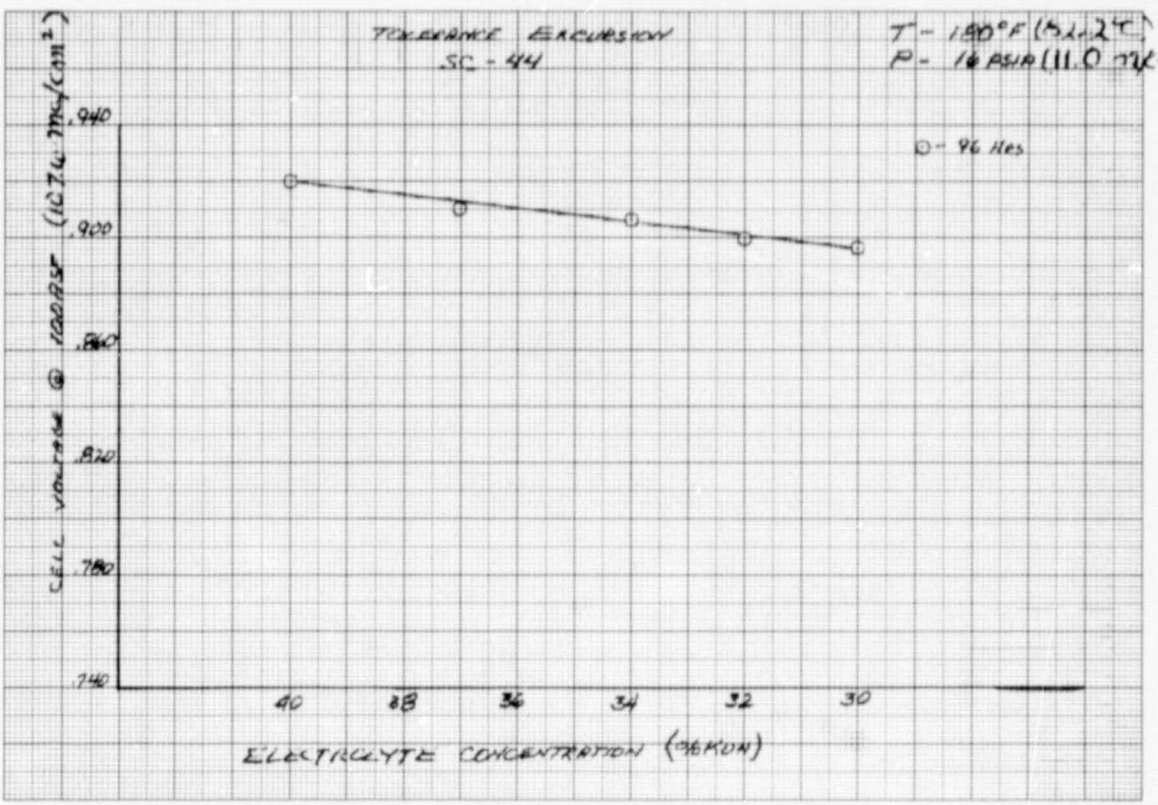

Figure 46 – Cell No. 44 Tolerance Excursion

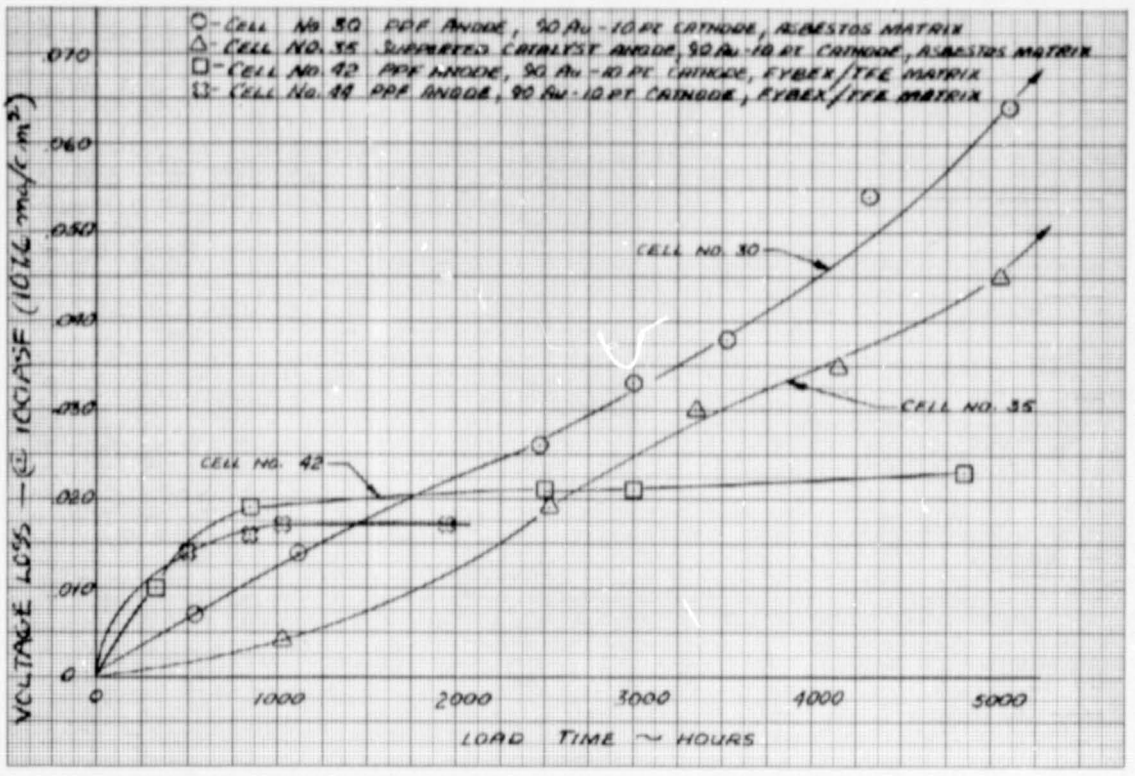

Figure 47 – Single Cell Voltage Loss Comparison

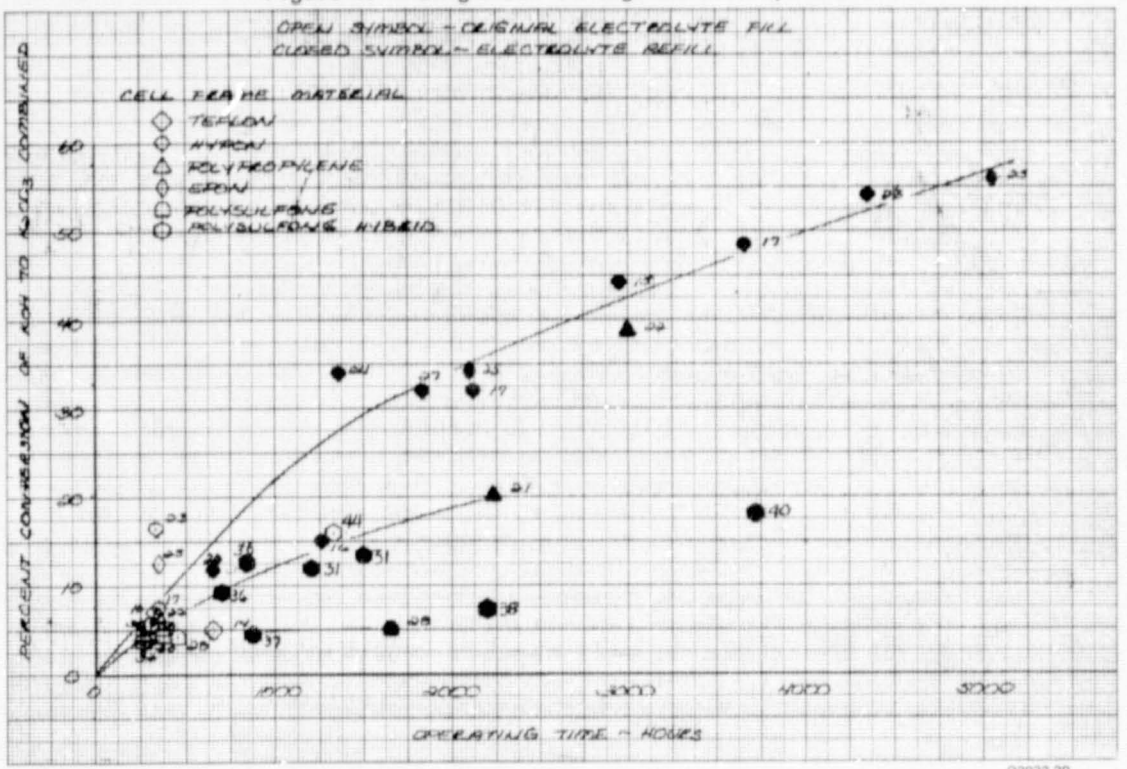

Q2032-20

Figure 48 – Carbonate Conversion Data

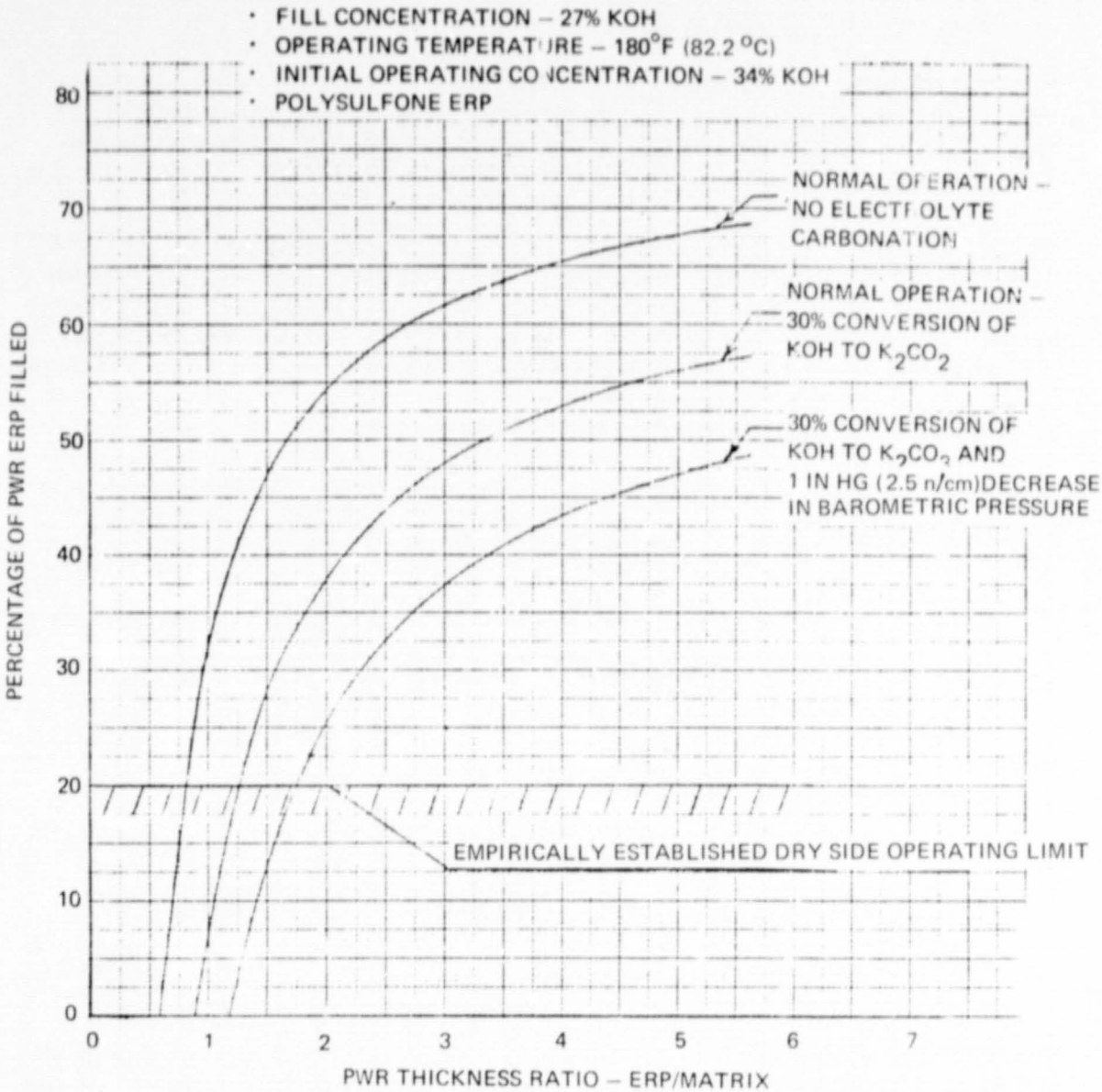

Figure 49 – Passive Water Removal Unit Electrolyte Volume Tolerance Characteristics

F. Summary of Two-Cell Plaque Testing

The overall objectives of the two-cell plaque test program were to: (1) perform short-term performance tests to determine plaque performance and operating characteristics, and , (2) define endurance characteristics and limiting phenomena with extended tests. The testing accomplished during Phase IV is summarized statistically in Table XIV.

The development of the two-cell plaque design, while taking place entirely in Phase IV, was an outgrowth of the six-cell plaque experience of earlier phases. Testing of six-cell plaques showed that their endurance was limited by the transfer of electrolyte from cells of higher to cells of lower potential. The path for cell-to-cell electrolyte transfer was through the gas flow fields common to all six cells of the plaque and across the intercell dividers of the plaque. Therefore, the major thrust of the two-cell plaque development program was to design and fabricate a plaque with a positive electrolyte barrier between the cells.

The design selected was one in which each cell is completely isolated from its neighbor with its own dedicated manifolds and gas supply fields. A discussion of this design and its fabrication is presented in Section V B.

TABLE XIV

TWO CELL PLAQUE TEST SUMMARY

NUMBER OF PLAQUES TESTED	2
NUMBER OF CONFIGURATIONS TESTED	2
TOTAL PLAQUE TEST TIME	2921 hours
LONGEST PLAQUE RUN (100 ASF) (107.6 ma/cm^2)	1931 hours

Tests of the two plaques fabricated to this design showed effective sealing between cells had been achieved and this approach to sealing was suitable for plaques of future design, although that was not clear from the initial results. From the outset, the testing revealed an anomoly which was characterized by:

- Higher-than-normal decay rate in both cells of each plaque.
- Cell No. 1 in each plaque showed an initial decay rate higher than Cell No. 2.
- Cell No. 1 in each plaque indicated loss of dry-side tolerance with time while Cell No. 2 remained virtually normal.
- Initially the internal resistance of Cell No. 1 increased with time.

These results can be interpreted to indicate that any one or a combination of the following conditions or mechanisms are present in the plaque:

(1) Insufficient quantity of electrolyte
(2) Anode performance is substandard
(3) Cell-to-cell electrolyte transfer
(4) Insufficient compressive load on the cell
(5) Loss of electrolyte
    (a) Physical loss from the cell
    (b) Matrix-to-anode ERP electrolyte transfer
    (c) UEA-to-PWR electrolyte transfer

Review of the plaque test data and special tests in support of their operation indicates the first three conditions are not the probable cause of the problem. Repeated refilling of the cells precludes the probability of the first condition. Half-cell tests of electrode samples from the same batch of anodes used to fabricate TCP No. 2 showed their performance to be standard and without suspicion. The third condition is ruled out by a special test in which one cell was filled with the standard potassium hydroxide electrolyte and the other with sodium hydroxide. Following their test the cells were checked for transfer of sodium into the potassium hydroxide. It was concluded that transfer was insignificant. This result is corroborated by the fact the dry-side tolerance excursion characteristic of Cell No. 2 remains unchanged with time, indicating no loss of or transfer of electrolyte from that cell.

To resolve item (4) an attempt to increase the compression on Cell No. 1 was made. Shims were added between the bonded-up plaque assembly and the endplates external to the assembly. It is not certain how much additional compression actually reached the cell since no decrease in IR was noted. Additional pinch could not be added due to the onset of shorting. Thus this item has not been eliminated as a possible cause.

The final item, loss of electrolyte, has been partially investigated. No gross loss of electrolyte from the cell has been identified, but accumulation of electrolyte within the cell, so that it does not participate in the cell function, cannot be ruled out. Although electrochemical mechanisms for removing electrolyte from the cell have been offered, none which satisfies all the data at hand has been defined.

To resolve these last items, test of an especially constructed two-cell plaque is recommended. This unit will incorporate provision to: (1) Vary its pinch, and (2) Permit determination of the potential of its individual cell elements when it is operating. Test of this unit will provide data from a plaque with known pinch and should provide sufficient data to permit construction of an electrochemical model of any electrolyte storage mechanism.

G. Two-Cell Plaque Design

This section describes the design of the two-cell plaque hardware and the design configurations evaluated during the Phase IV effort. Each cell in the plaque incorporates the same EMS design features as the single cells, described in Section VI D, and is completely isolated from the other. Because the cells are isolated the plaque incorporates dedicated fluid manifolding for each cell. To ensure the isolation of each cell, the plaque is assembled and bonded together as one complete unit. This was accomplished by bonding the center divider of each part to the center divider of the adjoining part, thus forming a continuous barrier between cells. The unit has no elastomeric seals which might permit cell-to-cell leakage.

The plaque test fixtures used during Phase IV consisted of 1.0-inch-thick (2.54-cm) stainless steel endplates with provisions for sealing and fluid connections, see Figure 50. The endplates included the same features and instrumentation as those of the single cells.

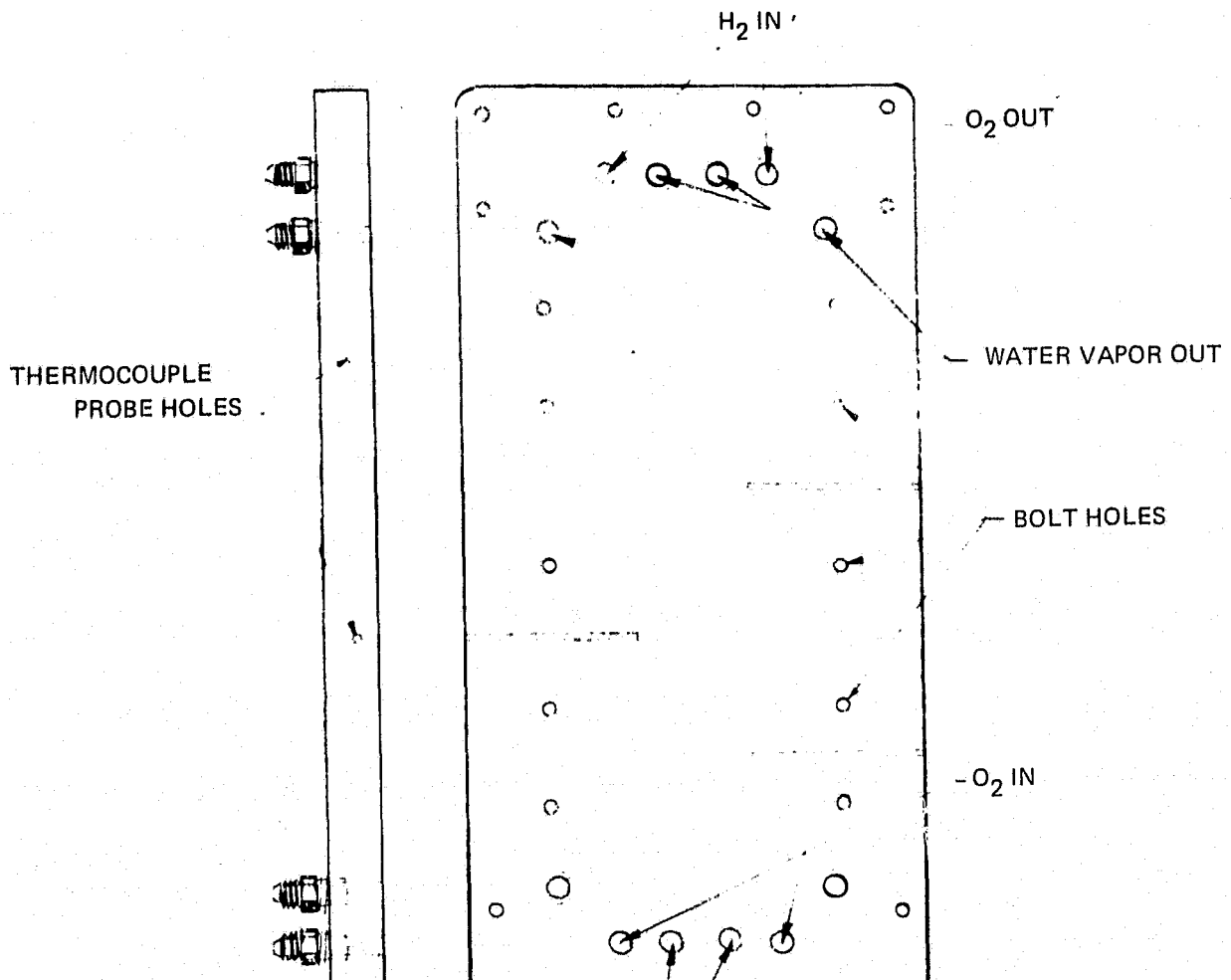

Figure 50 – Two Cell Plaque Test Fixture

Two different designs have undergone development and testing during this contract period. Their characteristics are summarized in Table XV.

TABLE XV

TWO-CELL PLAQUE DESIGNS TESTED DURING PHASE IV

Plaque No.	NASA Design No.	UEA Description	PWR Description	Oxygen Field	Hydrogen Field
1	1	Hybrid Polysulfone-Epoxy/Glass-Fiber Frame, Supported Catalyst Anode, 80Au-20Pt Cathode, 30-mil (0.76 mm) Polysulfone ERP	Epoxy/Glass-Fiber Frame, 20-mil (0.51 mm) RAM, 22-mil (0.56 mm) Polysulfone ERP GORETEX Membrane	28-mil (0.71 mm) TFE Screen 38-mil (0.97 mm) Nickel Kintex	28-mil (0.71 mm) TFE Screen
2	2	Hybrid Polysulfone-Epoxy/Glass-Fiber Frame PPF Anode 90 Au-10Pt Cathode 30 mil (0.76 mm) Polysulfone ERP	Same as No. 1	38-mil (0.90 mm) Nickel Kintex	38-mil (0.05 mm) Nickel Kintex

H. Two-Cell Plaque Test Results

This section reviews the results of the two-cell plaques tested duirng Phase IV.

Two-Cell Plaque No. 1

Two-Cell Plaque No. 1 was constructed using a hybrid frame UEA, supported catalyst anodes and 80Au-20Pt cathodes and is plaque Verification Design No. 1. The anode catalyst was acid leached to reduce the initially high diffusion losses exhibited by earlier supported catalyst anodes. The plaque was designed so that each cell was completely isolated from the other in order to prevent any electrolyte transfer from cell-to-cell. Prior to filling, the plaque was checked with nitrogen for cell-to-cell leakage: No leakage was found in any of the fluid compartments.

This plaque had completed 1644 hours of load time, at 100 ASF (107.6 ma/cm^2), 180°F, 82.2°C) 34% KOH and 16 psia (11.0n/cm) as of the end of the contract period. The operating history is presented in Figure 51. Initial diagnostics showed Cell No. 1 to have a high IR value and poor tolerance characteristics while Cell No. 2 appeared normal, see Figure 52. During the first week of testing, Cell No. 1 showed a decay rate twice that of Cell No. 2 and increasing loss of dry-side tolerance. This trend continued throughout the Verification Test period and until the cell was shut down for electrolyte refill at 560 hours. As can be seen from the Accountable Loss summary, Table XVI, the main mode of decay was anode diffusion losses, although increasing IR was also a contributor. Following refill, the performance and tolerance characteristics of Cell No. 1 returned to their original level. However, the initial trend resumed, after restart. During this period an experiment was conducted to attempt to retard any possible loss of electrolyte via the vent oxygen stream. This was done by closing the oxygen vent and purging only intermittently, at 4-hour intervals. Although the voltage decay of Cell No. 1 did appear to decrease initially, the overall results were inconclusive. No change in the standard intermittent hydrogen purge schedule was made during this period.

The plaque was shut down again for refill at 1058 hours. Before refilling, additional pinch was added to Cell No. 1 in an attempt to improve the anode-to-ERP electrolyte transfer characteristics. Upon restart, the voltage of Cell No. 1 had recovered to within 15mV of its original value and its tolerance characteristic was improved. The IR was not lowered significantly, however. Diagnostics also showed the onset of cell shorting.

The subsequent rate of decay of Cell No. 1 was reduced slightly from the previous two fills. It cannot be concluded that the increased pinch was responsible for this improvement since the decay rate of Cell No. 2 also decreased. The addition of more pinch was ruled out because of the cell shorting. For the remainder of the contract period the plaque was continued on endurance at 100 ASF (107.6 ma/cm^2). Figures 53 and 54 present the tolerance curves which show a continuation of the initial trend following the final refill.

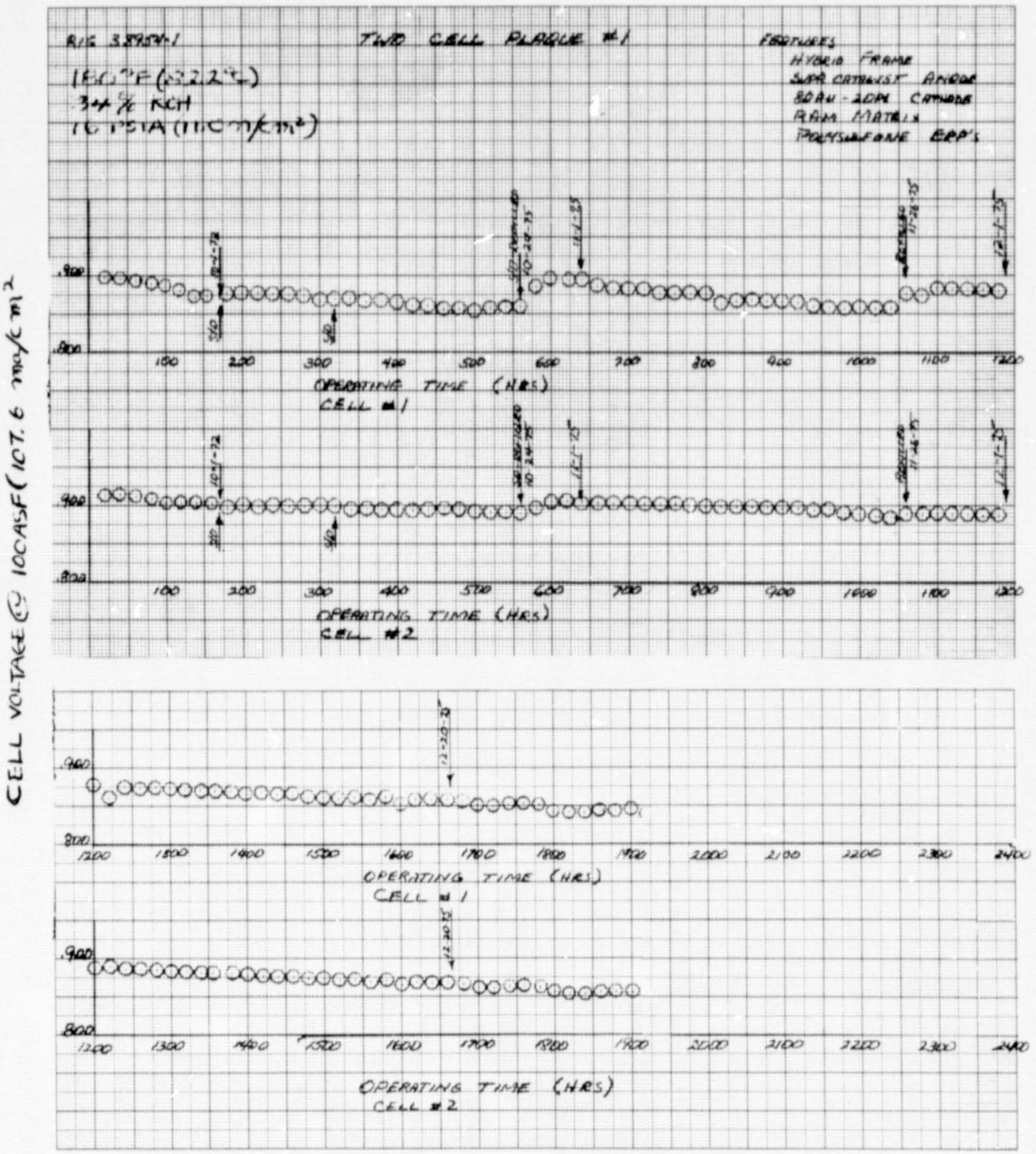

Figure 51 — Two-Cell Plaque No. 1 Performance History

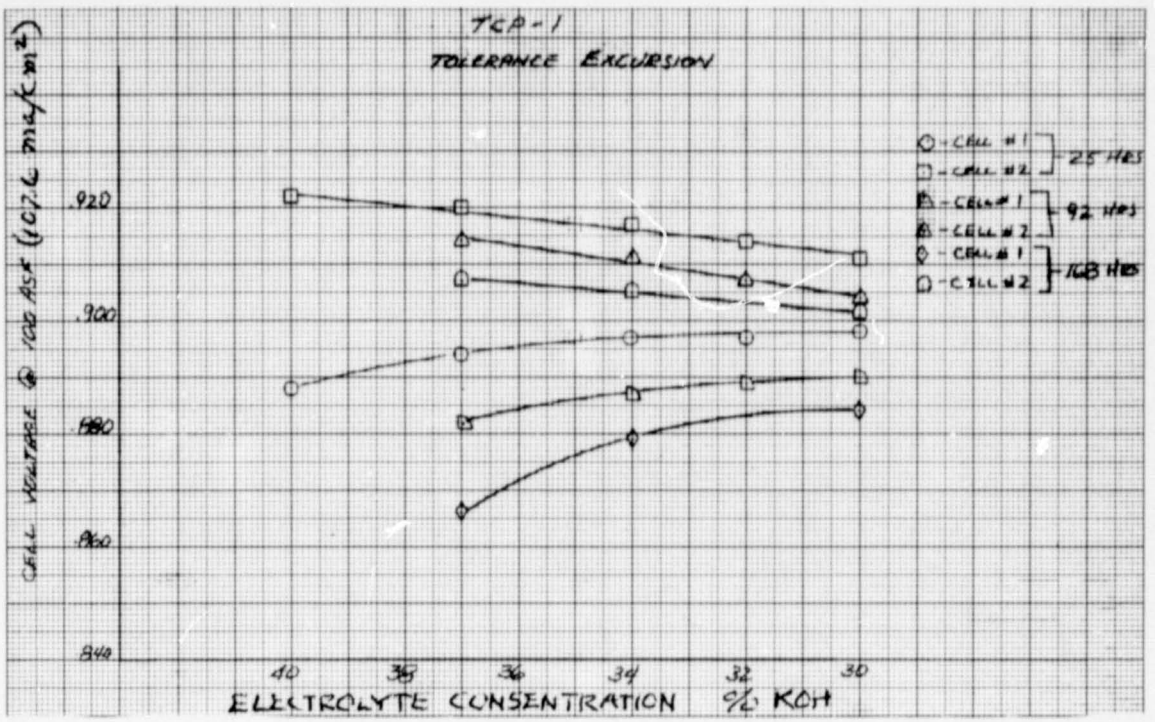

Figure 52 – Two-Cell Plaque No. 1 Tolerance Excursion Data

TABLE XVI

TCP-1 ACCOUNTABLE LOSSES

Hybrid Polysulfone – Epoxy/Glass-Fiber Frame,
80Au-10Pt Cathode, PPF Anode
Polysulfone ERP's
Ram Matrix

Rig 38954-1 0.114 Ft^2
180°F (82.2°C)/34%KOH/ 16 PSIA (11.0n/cm^2) PWR

Cell #	Load Time (Hrs.)	Performance 1.0 ASF (1.076 ma/cm^2) (Volts)	Performance 2.0 ASF (2.152 ma/cm^2) (Volts)	Performance 100 ASF (107.6 ma/cm^2) (IR Corr.)	IR Loss 100 ASF (107.6 ma/cm^2) (mv)	Activation Loss (mv)	100 ASF (107.6 ma/cm^2) Diffusion Losses Total (mv)	Anode (mv)	Cathode (mv)	Comments
1	21	1.032	1.019	0.918	20.0	–	35	27	8	
2	21	1.034	1.022	0.925	10.5	–	24	20	4	
1	320	1.023	1.010	0.890	28.0	9	70	62	8	
2	320	1.026	1.015	0.914	10.0	8	33	24	9	
1	577	1.025	1.015	0.915	17.0	7	35	26	9	After
2	577	1.027	1.015	0.919	9.0	7	26	21	5	Refill
1	1084	1.018*	1.007	0.905	16.0	–	38	–	–	After Adding
2	1084	1.014*	1.002	0.898	9.0	–	34	–	–	Pinch and Refill

*Estimated due to cell shorting

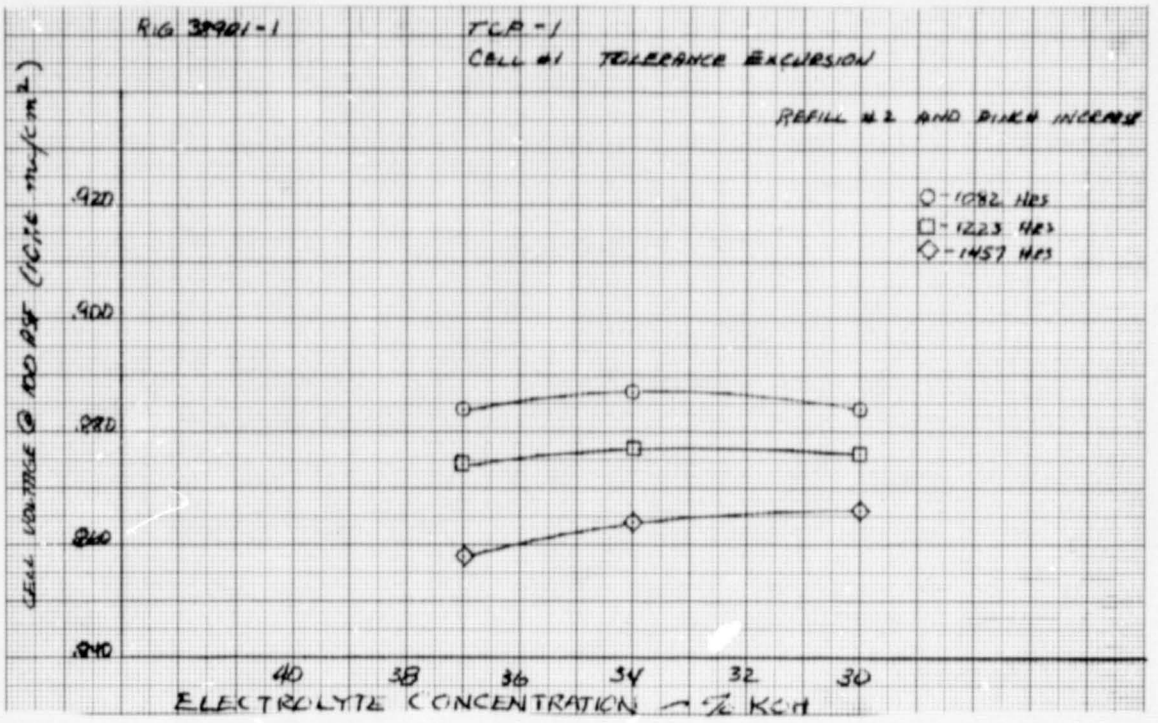

Figure 53 – Two-Cell Plaque No. 1/Cell No. 1 Tolerance Excursion Data

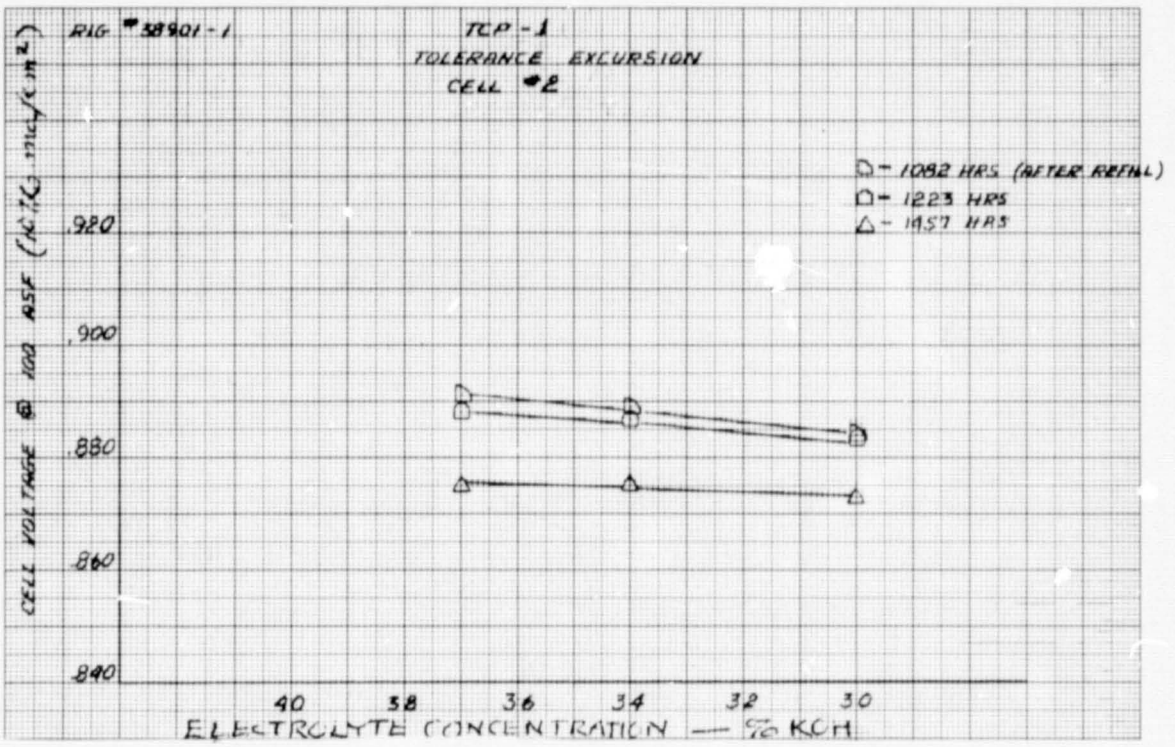

Figure 54 – Two-Cell Plaque No. 1/Cell No. 2 Tolerance Excursion Data

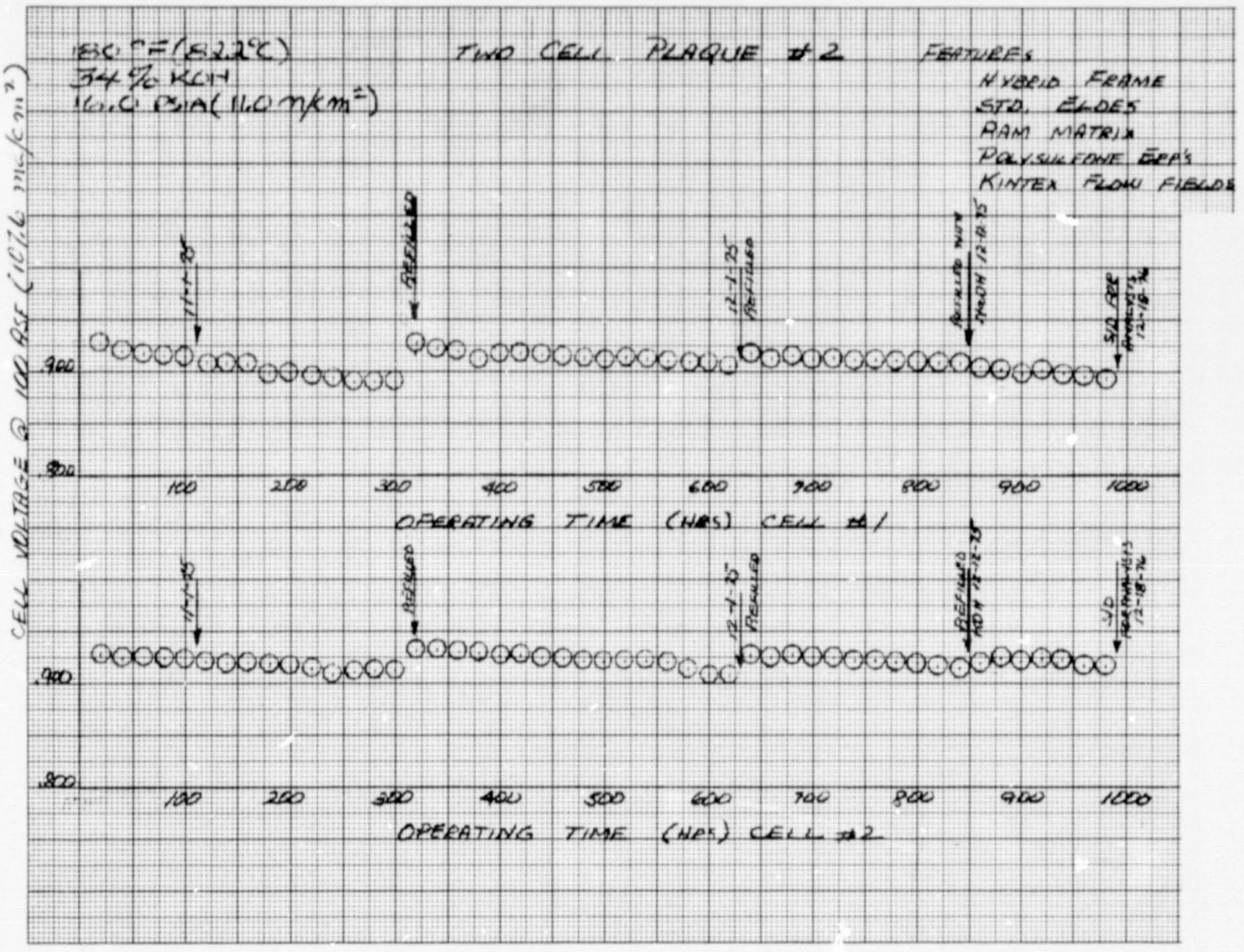

Figure 55 – Two-Cell Plaque No. 2 Performance History

Two-Cell Plaque No. 2

The second two-cell plaque was fabricated in the same manner as Two-Cell Plaque No. 1 with each cell isolated from the other. However, this plaque featured nickel Kintex flow fields in the hydrogen and oxygen cavities along with PPF anodes, 90Au-10Pt cathodes and reconstituted asbestos matrices. The Kintex fields were selected because of their good weight and cost characteristics and low pressure drop. This plaque completed 986 hours of testing at 180°F, (82.2°C); 100 ASF, (107.6 ma/cm^2); 16 psia (11.0n/cm^2); 34% KOH. Figure 55 shows the performance history of this plaque. The initial characteristics of the plaque were much the same as Two-Cell Plaque No. 1, with Cell No. 1 exhibiting a high rate of decay and loss of dry-side tolerance, see Figures 56 and 57. Diagnostics taken at 198 hours showed most of the loss to be divided between anode diffusion and cathode activation, see Table XVII. After completion of the Verification Test period, the cell was refilled. This restored the performance and tolerance characteristics to their initial values. After completion of diagnostics the cell was put on automatic intermittent purging on both electrodes in an attempt to retard any possible electrolyte loss via the vent streams. However, no effect was observed and continuous purging was resumed at 412 hours. The overall decay rate of Cell No. 2 was reduced after the refill but remained within the range of that of the first plaque. At 631 hours an automatic shutdown occurred, apparently due to inert buildup on the hydrogen space and a resultant low voltage. Upon restart, the voltage of both cells was higher than before. The decay rate was not affected however, and at 847 hours the plaque was shut down for refill. Prior to shutdown a tolerance excursion showed a loss of dry-side tolerance on Cell No. 1. Cell No. 2 also showed a slight loss of tolerance. For this refill Cell No. 1 was filled with a sodium hydroxide solution while Cell No. 2 was refilled with the standard potassium hydroxide solution. This was done in order to verify that there was no cell-to-cell electrolyte transfer by analyzing the electrolyte in Cell No. 2 for sodium after the plaque had been operated. Cell No. 1's voltage after restart was some 20 mV lower than after previous refills, reflecting the decreased conductivity of the NaOH solution. Cell No. 2 was also down by 5 to 10 mV. This test was continued for 140 hours before being terminated for electrolyte analysis. During this time the plaque exhibited much the same decay characteristics as it had previously. Cell No. 1 again lost dry-side tolerance while Cell No. 2 remained relatively stable.

Post-test analysis of the electrolyte showed traces of sodium in Cell No. 2. However, the amount of sodium found would not have affected the tolerance or performance characteristics of Cell No. 1. Therefore, it was concluded that cell-to-cell electrolyte transfer was not the primary cause of Cell No. 1 performance loss and that the bonded intercell barrier is effective in preventing electrolyte transfer.

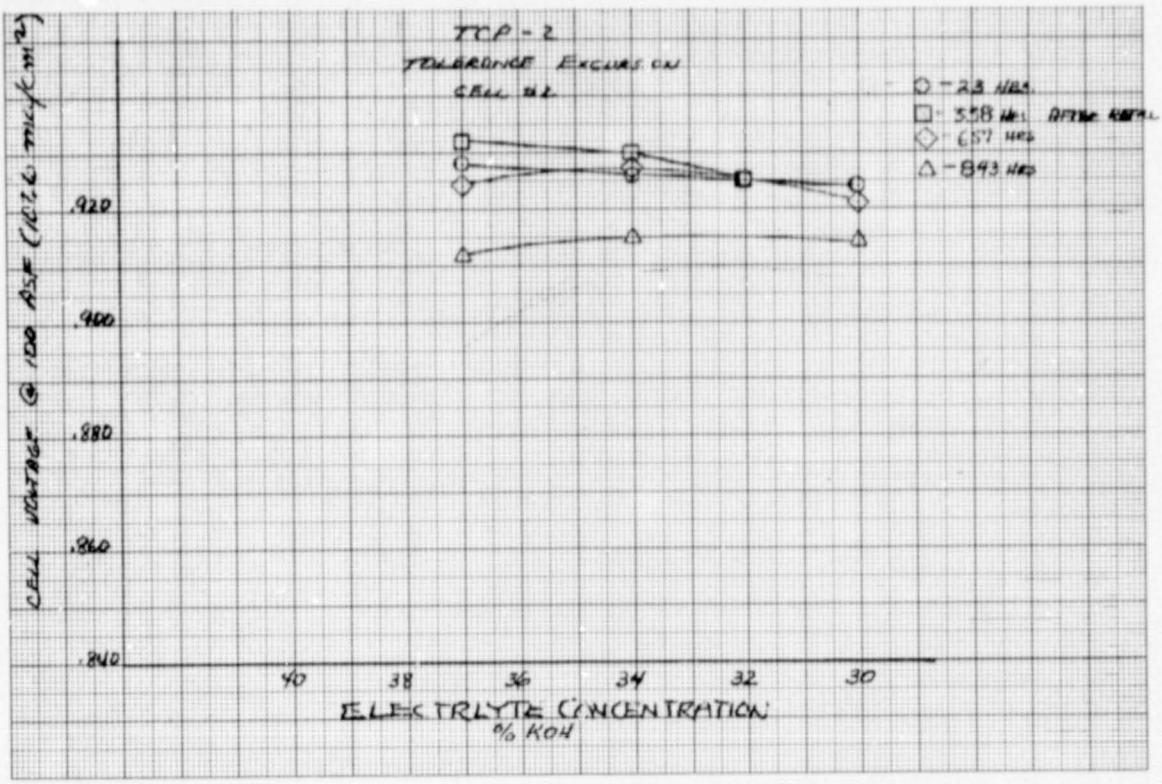

Figure 56 – Two-Cell Plaque No.2/Cell No. 1 Tolerance Excursion Data

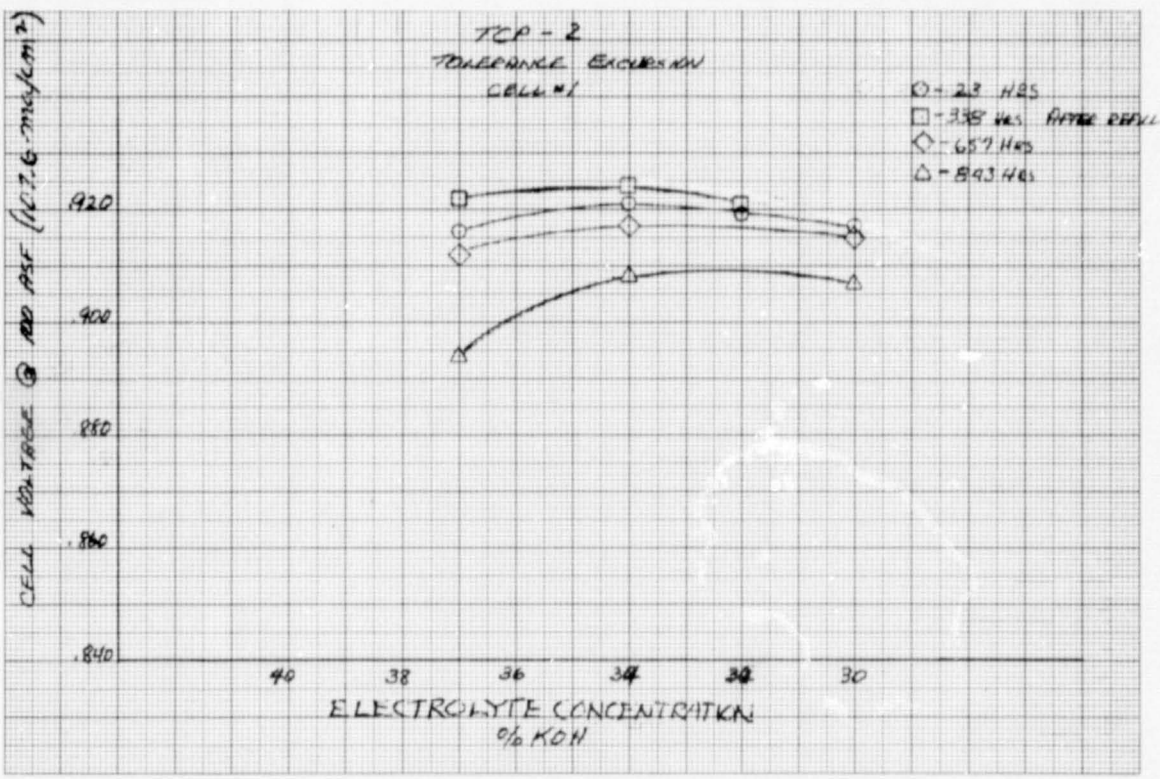

Figure 57 – Two-Cell Plaque No. 2/Cell No. 2 Tolerance Excursion Data

TABLE XVII

TCP-2 ACCOUNTABLE LOSSES

Hybrid Polysulfone – Epoxy/Glass-Fiber Frame
90Au-10Pt Cathode, PPF Anode
Polysulfone ERP's
Ram Matrix – Kintex Flow Fields

Rig 38963-2 0.114 Ft^2
180°F (82.2°C)/34%KOH/16PSIA (11.0n/cm^2) PWR

Cell #	Load Time (Hrs.)	Performance 1.0 ASF (1.076 ma/cm^2) (Volts)	Performance 2.0 ASF (2.152 ma/cm^2) (Volts)	Performance 100 ASF (107.6 ma/cm^2) IIR Corr.)	IR Loss 100 ASF (107.6 ma/cm^2) (mv)	Activation Loss (mv)	100 ASF (107.6 ma/cm^2) Diffusion Losses Total (mv)	Anode (mv)	Cathode (mv)
1	23	1.032	1.020	0.940	14	–	18	14	4
2	23	1.029	1.018	0.936	8	–	19	10	9
1	198	1.024	1.012	0.914	16	8	30	23	7
2	198	1.028	1.016	0.926	8	1	23	17	6
1	337	1.035	1.024	0.939	13	–			
2	337	1.034	1.023	0.937	6	–			

FCR-0165

APPENDIX A

POROUS MATRIX STRUCTURES FOR ALKALINE ELECTROLYTE FUEL CELLS

POROUS MATRIX STRUCTURES FOR ALKALINE ELECTROLYTE FUEL CELLS

by

Raymond W. Vine and Stephen T. Narsavage

Research and development programs have been conducted at P&WA (Pratt & Whitney Aircraft)* for a number of years to produce more chemically stable porous matrix structures with high bubble pressure (crossover resistance) for use as separators in potassium hydroxide (KOH) electrolyte fuel cells. Matrix structures evaluated were freestanding electrolyte-absorbant paper-like structures, or coatings applied directly to electrodes. These structures electronically isolate the electrodes in a cell from each other.

Chrysotile asbestos paper has been the most common separator for matrix-type aqueous KOH electrolyte cells because of its structural characteristics and adequate compatibility for short term, low temperature, 200°F (93°C) and below, cells. Johns-Manville has supplied asbestos paper in continuous rolls or sheets 0.010 and 0.020 inch thick that has been used in cells, but the material exhibits undesirable density variations and will withstand only 15 to 20 pounds per square inch pressure differential before reactant gas crossover occurs. An early development program, proposed by NASA Johnson Space Center, resulted in fabrication of a more uniform density, higher bubble pressure asbestos matrix. The matrix was produced by repulping Johns-Manville paper in water to break up the fiber bundles into smaller bundles or individual fibrils. The repulped slurry was then filtered onto a screen, dewatered by gravity or vacuum, and dried. The improvement in fiber distribution is shown in Figure 1, and the improvements in characteristics are shown in Table I.

Although ideal in structure, corrosion tests to 1000 hours at 250°F in 42 percent KOH show the lack of long term stability of asbestos. A sample lost 30 percent of its original weight, changed in physical structure as shown in Figure 2 and was partially converted to magnesium hydroxide, $Mg(OH)_2$, during exposure to the electrolyte.

The next approach pursued was to convert asbestos to $Mg(OH)_2$ by leaching in hot KOH or to acquire naturally occurring $Mg(OH)_2$ fibers, brucite. Materials leached both by P&WA and IIT Research Institute were evaluated. Low bubble pressures were measured with the P&WA-leached material. The IITRI material, 83 percent by weight $Mg(OH)_2$ and 17 percent unconverted asbestos, further deteriorated during compatibility testing as shown in Figure 3, and low bubble pressures were also measured with this material. Fabrication trials with brucite fibers supplied by Johns-Manville were also unsuccessful. No technique could be found for breaking down the material to achieve individual fibers without drastically fracturing fibers; bubble pressures of matrix structures were low, and no readily available supply of the material could be located.

* *The P&WA Fuel Cell Operation has recently become part of the Power Systems Division of United Technologies Corporation.*

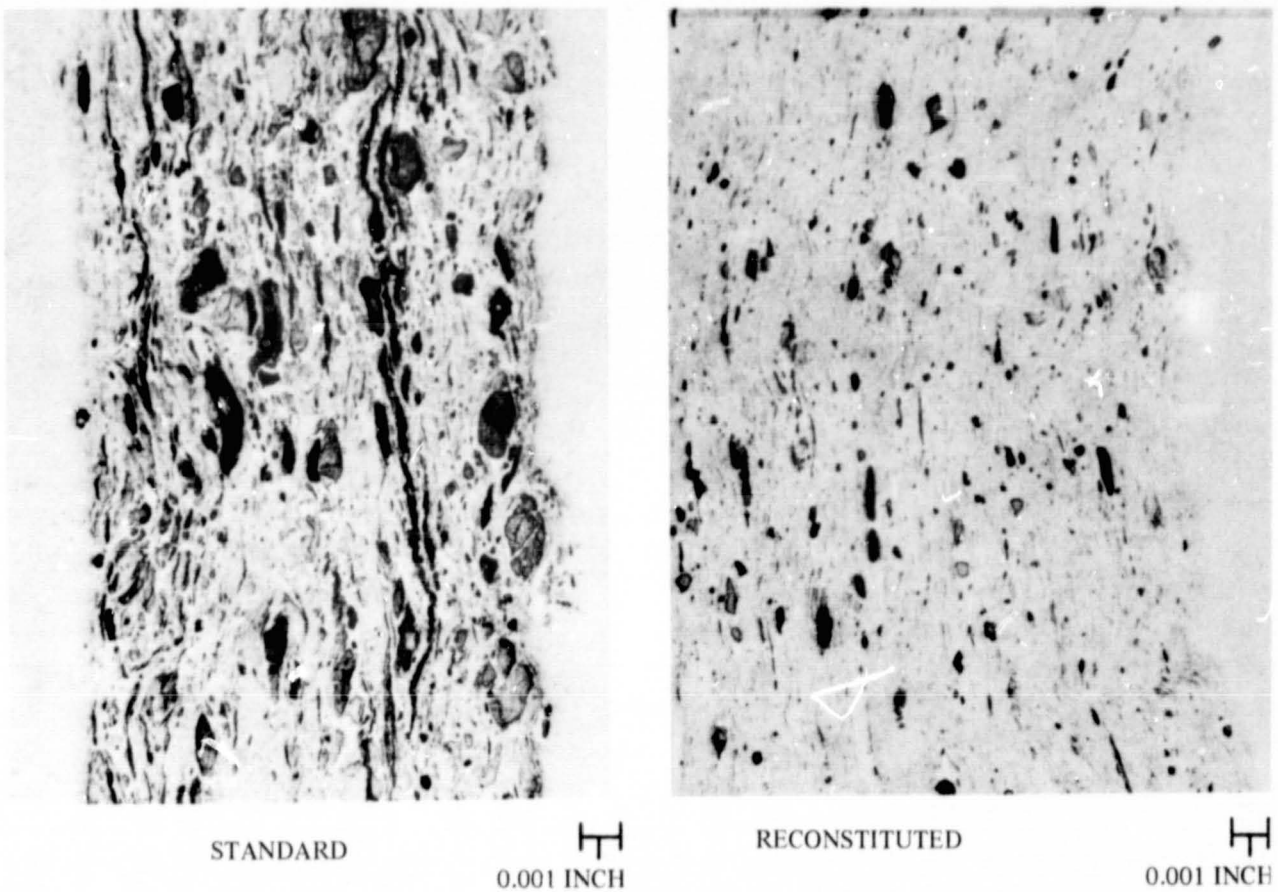

Figure 1 – Asbestos Matrix Materials

TABLE I

CHARACTERISTICS OF ASBESTOS MATRIX MATERIALS

	Thickness (Inch)	Porosity (Percent)	Bubble Pressure (Psi)	Mean Pore Size (μm)	80% Pore Size Range (μm)
Johns-Manville	0.010	70	16-22	1.1	0.1-60
P&WA Reconstituted	0.010	70	50-70	0.7	0.1-30

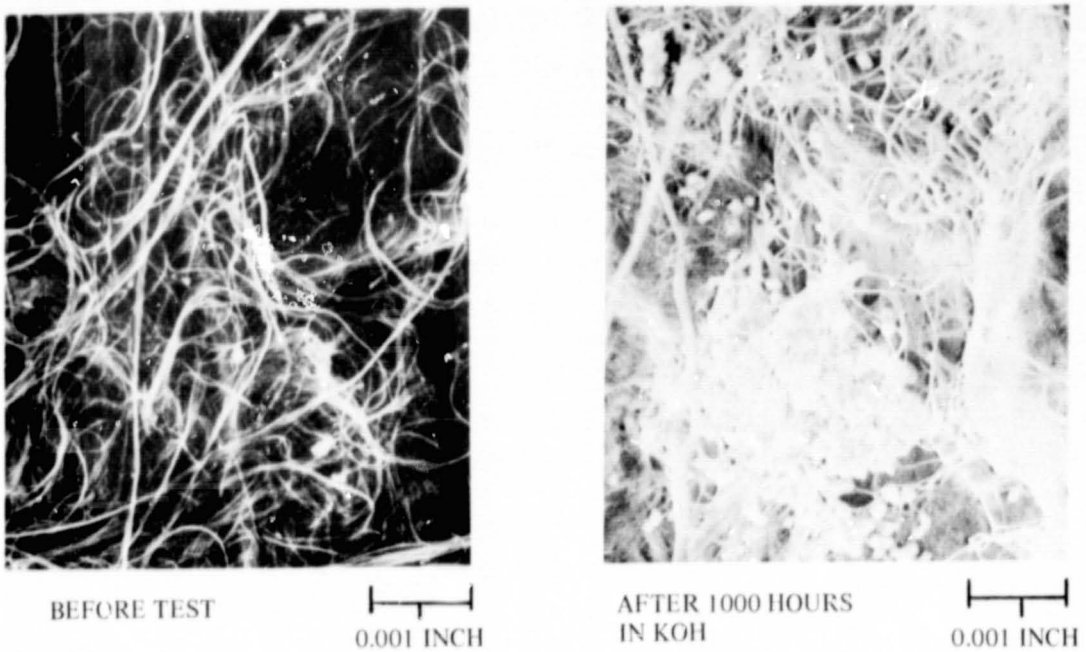

Figure 2 – Asbestos Corrosion Samples

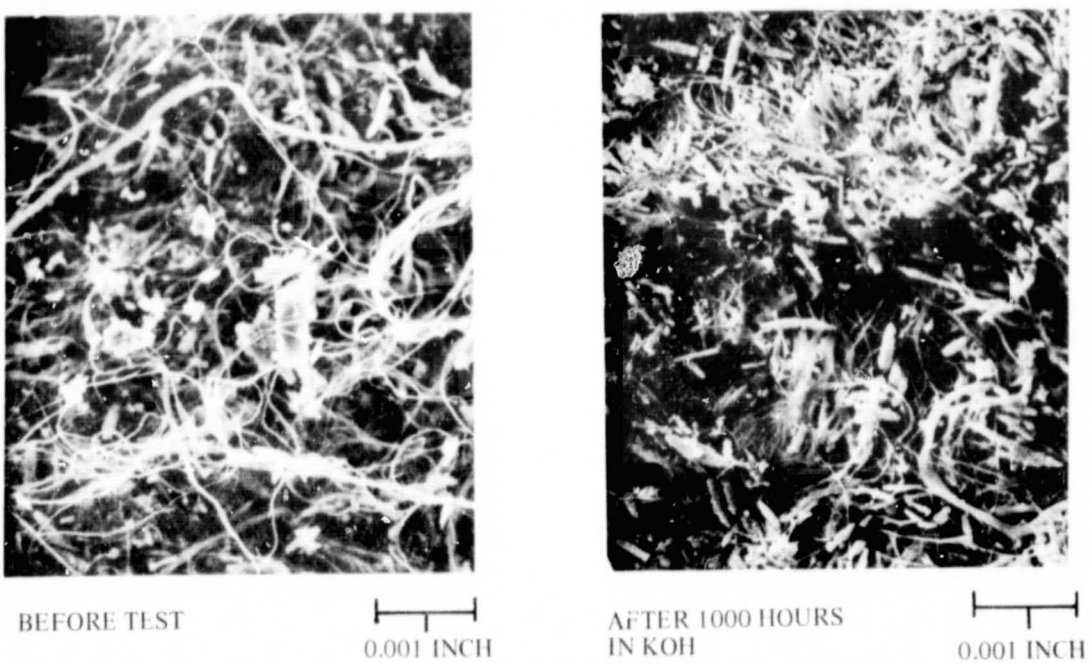

Figure 3 – HTRI Leached Asbestos Corrosion Samples

Some potassium titanate materials, by comparison, have improved compatibility with high temperature KOH; E. I. duPont de Nemours & Co. PKT®, Tipersul® and Fybex D® have been evaluated and used as matrix materials at different periods of time. Fybex has been commercially available for the past three years; thus Fybex-related work has been emphasized recently. The Fybex material is $(K_2O)_X(TiO_2)_Z$ with Z/X about 8 and a 0.10 to 0.15 micrometer fiber diameter; scanning electron microscopy shows a typical fiber length of 4 micrometers with a range from 2 to 22 micrometers. Compatibility testing of 96 weight percent Fybex plus 4 percent Teflon®-3170 has shown no evidence of corrosion through 3000 hours at 250°F in 42 percent KOH. In addition, gas chromatography shows less carbonate forming species present in the Fybex-Teflon matrix than in asbestos. Initially, freestanding Fybex matrix structures were produced by filtration, similar to the method used for producing reconstituted asbestos described above. Papers 13 inches by 13 inches were fabricated that exhibited the characteristics described in Table II. Strengths of the matrix structures improved with an increase in asbestos content; but they were all very fragile, and cell assembly unitizing trials were unsuccessful.

TABLE II

FYBEX PAPER CHARACTERISTICS

Fybex(Weight Percent)	100	95	90	85
Asbestos (Weight Percent)	0	5	10	15
Average Thickness (Inch)	0.020	0.027	0.023	0.023
Thickness Range (Inch)	0.019-0.022	0.021-0.032	0.020-0.025	0.017-0.029
Porosity (Percent)	86	89	88	86
Average Bubble Pressure (Psi)	26	18	32	38
Bubble Pressure Range (Psi)	10-40	6-28	30-36	30-43

Next, experiments were focused on methods of applying Fybex matrix material directly onto electrodes, relying on the electrode for physical support. Fybex compositions bonded with TFE-3170 Teflon were screen printed onto different types of electrodes with several different variations in printing techniques. Bubble pressures to 10 pounds per square inch were achieved with the Fybex material, but the results were disappointing with respect to the 30 to 40 pound per square inch structures produced earlier.

In view of the low bubble pressures measured with screen-printed structures, an analytical study was conducted to determine theoretical bubble pressures possible with Fybex. The approach used was to consider pore structure in a matrix to be a regular arrangement of small capillaries, where the capillary force, which would equal the expulsion force or bubble pressure, can be calculated. Relationships between the forces to expel the fluid from a capillary and the size of the capillary are well known. The basic relationships used were:

$$F = 2\pi r S_{sl} \tag{1}$$

$$S_{sl} = S_{lv}\cos\theta \tag{2}$$

$$P = \frac{F}{A} = \frac{2\pi r S_{lv}\cos\theta}{\pi r^2} = \frac{2S_{lv}\cos\theta}{r} \tag{3}$$

$$P = \frac{4S_{lv}\cos\theta}{d} \tag{4}$$

Where:

- F = force,
- r = radius of capillary,
- S_{sl} = solid-liquid surface tension,
- S_{lv} = liquid-vapor surface tension,
- θ = contact angle between the liquid and solid,
- P = pressure (bubble pressure),
- A = cross sectional area of the capillary,
- d = diameter of capillary.

Inserting mean pore size data into Equation 4 disclosed the potential for much higher bubble pressures and suggested either a wettability or a structural problem. The ease of filling the matrix coatings did not support a wettability problem; thus, it was hypothesized that screen printing might produce imperfections which are not apparent from porosimetry measurements but contribute to lower bubble pressures. It was anticipated that greater bubble pressures could be achieved by filtering, as material is always being deposited in the largest pore during the process.

Excellent results were achieved by filtering 96 percent Fybex plus 4 percent TFE-3170 water base compositions directly onto fuel cell electrodes, followed by drying and partial curing of the matrix binder. Bubble pressures between 30 and 33 pounds per square inch were achieved with matrix coatings 0.030 inch thick and 90 percent porous, which is the same matrix solids content as 0.010 inch thick asbestos. Table III compares bubble pressures of matrix structures prepared either by direct filtration or by screen printing.

TABLE III

CALCULATED AND EXPERIMENTAL BUBBLE PRESSURES

Matrix Material	Fabrication Technique	Mean Pore Size (μm)	Assumed Wetting Angle (Degrees)	Bubble Pressure (Psi)	
				Calculated	Experimental
P&WA Reconstituted Asbestos	Filtered	0.7	0	60	60
96% Fybex + 4% Teflon	Screen Printed	1	0	42	7-10
96% Fybex + 4% Teflon	Screen Printed	1	86	4	7-10
96% Fybex + 4% Teflon	Filtered	1	0	42	30-33

A number of 2-inch by 2-inch electrodes have been coated with filtered Fybex plus 4 percent TFE-3170. Performances with Fybex or asbestos matrix fuel cells were comparable at 190°F, and the increased performance anticipated at 250°F was measured. The most significant test to date has been an endurance cell that was operated for 2325 hours at 250°F. Electron microprobe analyses showed no migration of titanium present in Fybex; reduced performance caused by anode flooding due to silicon or silica migration occurs with long term and/or higher temperature asbestos matrix cells. X-ray diffraction showed no change in crystallography, and scanning electron photomicrographs, Figure 4, showed no evidence of corrosion at the end of the test.

DuPont has reported that Fybex will no longer be available after April of this year; thus a replacement material will have to be found if the production of Fybex or a Fybex-type material is not initiated by another company. It has been determined, however, that excellent high bubble pressure matrix structures can be produced by direct filtration of small inert particle-Teflon mixtures onto fuel cell electrodes. In addition, the potential level of bubble pressures achievable with certain particle size materials can be predicted from the mean pore size of such structures.

Two other materials were compatibility tested at 250°F. They include Teflon bonded beta silicon nitride, Si_3N_4, supplied by Cerac, Incorporated and polybenzimadazole, PBI, fiber supplied by Celanese Corporation. The Si_3N_4 material lost 11 percent by weight after 1000 hours at 250°F in KOH, and it was considered unacceptable for alkaline fuel cell applications. PBI, a polymer material, showed only a 3 percent weight loss and no change in fiber diameter or surface morphology after 5000 hours at 250°F in KOH. Gas chromatography results show the PBI contains approximately the same level of carbonate forming species as asbestos after pre-treating the material 1 hour at 400°F. Current technology permits fabrication of PBI fibers with a minimum average diameter of approximately 15 micrometers, too big for high bubble pressure matrix

structures. Since Celanese would require a development program and additional incentive to determine the feasibility of fabricating PBI fibers with diameters similar to asbestos, evaluation of this material was suspended.

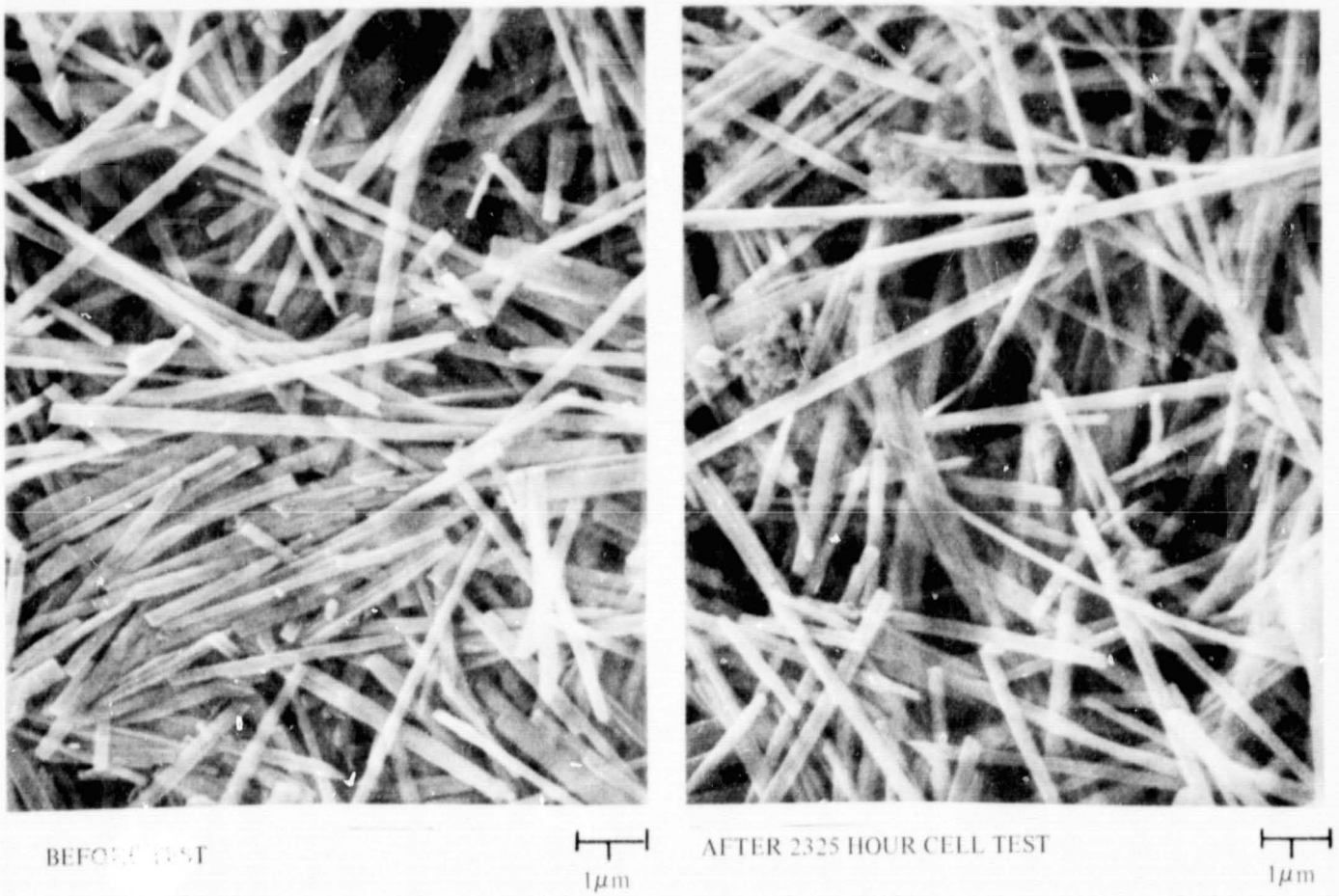

Figure 4 – Fybex Matrix

In summary, the following advancements and results have been realized through a continuing program to develop higher bubble pressure, more chemically stable porous matrix structures for use in KOH electrolyte fuel cells.

1. More uniform, higher bubble pressure (60 pounds per square inch) asbestos matrix structures were produced by reconstituting Johns-Manville asbestos paper.

2. High bubble pressure, stable matrix structures could not be produced by using $Mg(OH)_2$, leached asbestos, or brucite, either by themselves or in combination with asbestos.

3. The excellent compatibility of Fybex potassium titanate with 42 percent KOH at 250°F was measured up to 3000 hours.

4. Screen-printed structures do not exhibit the bubble pressures predicted by analytical studies.

5. Good agreement was found between bubble pressures predicted by an analytical study and those measured with filtered structures.

6. Teflon-bonded Fybex matrix structures with bubble pressures in excess of 30 pounds per square inch have been produced by filtering a water slurry of the mixture directly onto fuel cell electrodes. The structures have performed satisfactorily in laboratory fuel cells.

7. PBI fibers have satisfactory compatibility with 42 percent KOH at 250°F, but beta silicon nitride was unacceptable.

The authors wish to acknowledge the support of the NASA Lewis Research Center for a portion of this work and especially Dr. L. H. Thaller, Project Manager.